

**EVALUATION OF AN ADVANCED FINE COAL CLEANING CIRCUIT**

by

Parthasarathy Venkatraman

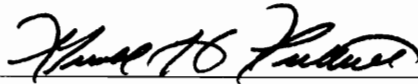
Dissertation submitted to the Faculty of the  
Virginia Polytechnic Institute and State University  
in partial fulfillment of the requirements for the degree of

**DOCTOR OF PHILOSOPHY**

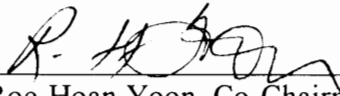
in

Mining and Minerals Engineering

APPROVED:



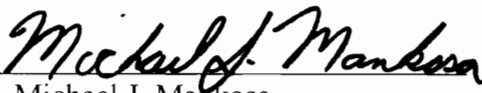
Gerald H. Luttrell, Chairman



Roe-Hoan Yoon, Co-Chairman



Gregory T. Adel



Michael J. Mankosa



Hugh W. Rimmer

May, 1996

Blacksburg, Virginia

Key Words: Desulfurization, Column Flotation, Enhanced Gravity Separation

c.2

LD  
5655  
V856  
1996  
V465  
c.2

# EVALUATION OF AN ADVANCED FINE COAL CLEANING CIRCUIT

by

Parthasarathy Venkatraman

**Chairman: Gerald H. Luttrell**

**Co-Chairman: Roe-Hoan Yoon**

**Mining and Minerals Engineering**

## ABSTRACT

A new fine-coal cleaning circuit, with potential near-term applications, has been evaluated for treating fine coal (i.e., 28 mesh x 0). This circuit combines a surface-based separator known as Microcel™ column flotation with an enhanced gravity separator known as the Multi-Gravity Separator (MGS). The synergistic effect of combining both processes in a single circuit resulted in improved ash and pyritic sulfur rejection with minimal losses in energy recovery. In addition, technical and economic analyses of this processing scheme suggest it compares favorably with existing post-combustion desulfurization techniques.

A detailed study of the MGS included the development of a model based on fundamental principles of fluid mechanics and mineral processing. The theoretical analyses identified drum speed as the most important MGS operating parameter. To

validate these findings, a detailed parametric test program was conducted using coal samples from the Pittsburgh No. 8 and Illinois No. 6 seams. A statistical analysis of the test data also showed that drum speed was the most important variable in controlling the performance of the MGS. The other controlling parameters, i.e., feed percent solids, feed rate and wash-water addition rate, were found to be of lesser importance. The experimental test results were found to be in good agreement with the theoretical predictions obtained using the model.

## ACKNOWLEDGMENTS

I express my deep sense of gratitude to my advisors Dr. Gerald Harvey Luttrell and Dr. Roe-Hoan Yoon for their valuable guidance, supervision of work, immense encouragement and confidence generated throughout the course of this research work.

I am deeply grateful to Dr. Greg T. Adel and Dr. Michael J. Mankosa for their suggestions and criticisms, constant inspiration and support throughout this work. I would like to thank my other committee members Dr. John D. Novak and Dr. Hugh Rimmer for their constructive comments.

I wish to express my indebtedness to Lisa, Steve Stewart, Jerry Rose, Roy Hill and Jeff Phillips for their cooperation in carrying out the experimental work.

The financial support of the U.S. Department of Energy (Contract No.: DE-AC22-92PC92205) is gratefully acknowledged.

I heartily express my sincere thanks to all my friends at Pittsburgh Energy Technology Center (PETC), Carpc Inc., Roberts and Schaefer Co., CONSOL, and Kerr-McGee coal company for their cooperation.

I am thankful to my friends at Plantation Road Jason Pyecha, Eva Cruz, David Hill, Eric Yan and Peter Dunn for their assistance, friendship and support. Very special thanks to Ravishankar, Vivek Subramanian, Rajesh Pazhianur, Neeraj Mendiratta, Suha

Aksoy and all other graduate students at Plantation Road and Holden Hall. Special appreciation to Keith Kutz, Alisa Alls, Wayne Slusser for their support.

Last, but not the least, I dedicate this dissertation to my parents and family members for their encouragement and unconditional support.

## TABLE OF CONTENTS

	Page
TITLE PAGE	i
ABSTRACT	ii
ACKNOWLEDGMENTS	iv
TABLE OF CONTENTS	vi
LIST OF FIGURES	xi
LIST OF TABLES	xvi
<b>CHAPTER 1 INTRODUCTION</b>	<b>1</b>
1.1 Preamble	1
1.2 Literature Review	7
1.2.1 Fine Coal Processing	7
1.2.2 Froth Flotation	7
1.2.3 Fine Particle Gravity Concentrators	14
1.2.3.1 YT Centrifugal Separator	19
1.2.3.2 Kelsey Jig	19
1.2.3.3 Knelson Concentrator	22
1.2.3.4 Falcon Concentrator	22
1.2.3.5 Multi-Gravity Concentrator	25





2.7 Summary and Conclusions	65
2.8 References	66
<b>CHAPTER 3 EXPERIMENTAL SETUP AND PROCEDURE</b>	<b>70</b>
3.1 Introduction	70
3.2 Coal Sample Characterization	72
3.2.1 Size Distribution	72
3.2.2 Washability Characterization	73
3.2.3 Image Analysis Characterization	76
3.2.4 Release Analysis Characterization	84
3.3 Experimental Setup	90
3.3.1 Preparation of Feed	90
3.3.2 Flowsheet Design	90
3.3.3 Circuit Layout	94
3.3.4 Piping	94
3.3.5 Instrumentation	94
3.4 Test Plan	97
3.5 Sampling Procedure	99
3.6 References	100
<b>CHAPTER 4 MULTI-GRAVITY SEPARATOR PARAMETRIC STUDY</b>	<b>101</b>

4.1	Introduction	101
4.2	Objectives	103
4.3	Parametric Design and Procedures	104
4.4	Results	111
4.4.1	Pilot-Plant MGS Testing	111
4.5	Discussion	113
4.5.1	Separation Performance	113
4.5.2	Effect of Particle Size	120
4.5.3	Partition Curves	124
4.5.3.1	Variation in Separation Density ( $SG_{50}$ ) and Probable Error ( $E_p$ ) with Particle Size	124
4.5.4	Statistical Analyses of the Parametric Data	130
4.5.4.1	Model Development	131
4.5.4.2	Interpretation of the Statistical Analyses	131
4.5.4.3	Parametric Testing Summary	138
4.6	Summary and Conclusions	140
4.7	References	143
<b>CHAPTER 5 TESTING OF THE COMBINED FLOTATION/DENSITY CIRCUIT</b>		145
5.1	Introduction	145

5.2 Objectives	147
5.3 Results and Discussion	148
5.3.1 Separation Performance	148
5.3.2 Long-Duration Testing	158
5.3.3 Economic Evaluation	161
5.4 Summary and Conclusions	169
5.5 References	171
<b>CHAPTER 6 CONCLUSIONS</b>	<b>172</b>
<b>CHAPTER 8 RECOMMENDATIONS FOR FURTHER STUDY</b>	<b>174</b>

## LIST OF FIGURES

		Page
Figure 1.1	Flotation time rate of coal as a function of particle size.	4
Figure 1.2	Schematic drawing of the Microcel Column Flotation.	10
Figure 1.3	Product grade as a function of the column bias factor for the flotation of fine coal.	13
Figure 1.4	Theoretical effect of particle diameter on the free-settling velocity of coal (SG=1.3), shale (SG=2.5) and pyrite (SG=4.8) under gravitational fields of 1 and 200 g's.	18
Figure 1.5	Schematic drawing of YT centrifugal separators.	20
Figure 1.6	Schematic drawing of Kelsey Jig.	21
Figure 1.7	Schematic drawing of Knelson concentrator.	23
Figure 1.8	Schematic drawing of Falcon concentrator.	24
Figure 1.9	Schematic drawings of the MGS showing (a) a cross-section through the rotating drum and (b) flow patterns along the drum surface.	26
Figure 2.1	Velocity profile of a thin film on an oscillating surface.	42
Figure 2.2	A schematic diagram of a side-view of the MGS showing the particle trajectory in the fluid.	44
Figure 2.3	A schematic diagram illustrating the forces experienced by a particle a) while it is settling and b) while it is rolling or sliding on the surface of the drum.	45
Figure 2.4	Effect of particle size on the performance of the MGS using liberated coal particles at different drum speeds.	55
Figure 2.5	Effect of particle size on the performance of the MGS using liberated ash particles at different drum speeds.	56
Figure 2.6	Effect of particle size on the performance of the MGS using liberated pyrite particles at different drum speeds.	57

Figure 2.7	Effect of drum speed on the cut gravity and probable error in the MGS.	58
Figure 2.8	Effect of drum speed on the partition curves for the MGS.	59
Figure 2.9	Effect of flow rate on the performance of the MGS using liberated coal particles at a drum speed of 320 rpm.	61
Figure 2.10	Effect of flow rate on the performance of the MGS using liberated ash particles at a drum speed of 320 rpm.	62
Figure 2.11	Effect of flow rate on the performance of the MGS using liberated pyrite particles at a drum speed of 320 rpm.	63
Figure 3.1	Comparison of release analysis and image analysis separation curves for pyrite obtained using a -28 mesh Pittsburgh No. 8 seam coal.	78
Figure 3.2	Comparison of release analysis and image analysis separation curves for mineral matter obtained using a -28 mesh Pittsburgh No. 8 seam coal.	79
Figure 3.3	Comparison of release analysis and image analysis separation curves for pyrite obtained using a -28 mesh Illinois No. 6 seam coal.	80
Figure 3.4	Comparison of release analysis and image analysis separation curves for mineral matter obtained using a -28 mesh Illinois No. 6 seam coal.	81
Figure 3.5	Weight percent pyrite containing carbonaceous inclusions finer than a given size obtained using a -28 mesh Pittsburgh No. 8 seam coal.	82
Figure 3.6	Weight percent pyrite containing carbonaceous inclusions finer than a given size obtained using a -28 mesh Illinois No. 6 seam coal.	83
Figure 3.7	The effect of grind size on the ash release curve obtained for R-O-M Pittsburgh No. 8 seam coal.	85

Figure 3.8	The effect of grind size on the sulfur release curve obtained for R-O-M Pittsburgh No. 8 seam coal.	86
Figure 3.9	The effect of grind size on the ash release curve obtained for R-O-M Illinois No. 6 coal.	87
Figure 3.10	The effect of grind size on the sulfur release curve obtained for R-O-M Illinois No. 6 coal.	88
Figure 3.11	A schematic diagram of the Microcel, MGS and combined Microcel/MGS circuits.	91
Figure 4.1	Comparison of measured and material balanced data obtained for a Pittsburgh No. 8 seam coal.	112
Figure 4.2	Combustible recovery as a function of feed ash rejection obtained for a Pittsburgh No. 8 coal.	114
Figure 4.3	Combustible recovery versus rejection plots obtained during the parametric testing of the MGS using the Pittsburgh No. 8 coal.	115
Figure 4.4	Combustible recovery versus rejection plots obtained during the parametric testing of the MGS using the Illinois No. 6 coal.	116
Figure 4.5	Separation efficiency as a function of rejections of ash, total sulfur and pyritic sulfur for Pittsburgh No. 8 coal.	118
Figure 4.6	Separation efficiency as a function of rejections of ash, total sulfur and pyritic sulfur for Illinois No. 6 coal.	119
Figure 4.7	Effect of particle size on the performance of MGS.	122
Figure 4.8	Effect of particle size on the performance of Falcon concentrator.	123
Figure 4.9	Effect of particle size on the partition curve for the MGS using Pittsburgh No. 8 seam coal.	125

Figure 4.10	Effect of particle size on the partition curve for the MGS using Illinois No. 6 seam coal.	126
Figure 4.11	Effect of particle size on reduced probable error for commonly used separators treating fine coal [14,15,16,].	128
Figure 4.12	Effect of particle size on relative cut specific gravity for commonly used separators treating fine coal [14,15,16].	129
Figure 5.1	Combustible recovery versus rejection plots obtained for the Microcel unit during the parametric testing of the combined Microcel/MGS using the Pittsburgh No. 8 coal.	150
Figure 5.2	Combustible recovery versus rejection plots obtained for the MGS unit during the parametric testing of the combined Microcel/MGS using the Pittsburgh No. 8 coal.	151
Figure 5.3	Combustible recovery versus rejection plots obtained during the parametric testing of the combined Microcel/MGS using the Pittsburgh No. 8 coal.	152
Figure 5.4	Combustible recovery versus rejection plots obtained for the Microcel during the parametric testing of the combined Microcel/MGS using the Illinois No. 6 coal.	153
Figure 5.5	Combustible recovery versus rejection plots obtained for the MGS during the parametric testing of the combined Microcel/MGS using the Illinois No. 6 coal.	154
Figure 5.6	Combustible recovery versus rejection plots obtained during the parametric testing of the combined Microcel/MGS using the Illinois No. 6 coal.	155
Figure 5.7	Concentrate sulfur versus ash content obtained during the parametric testing of the Pittsburgh No. 8 coal.	156
Figure 5.8	Concentrate sulfur versus ash content obtained during the parametric testing of the Illinois No. 6 coal.	157

Figure 5.9	Combustible recovery versus rejection plots obtained during the long-duration testing of the combined Microcel/MGS using the Pittsburgh No. 8 coal.	159
Figure 5.10	Combustible recovery versus rejection plots obtained during the long-duration testing of the combined Microcel/MGS using the Illinois No. 6 coal.	160
Figure 5.11	Cost of SO <sub>2</sub> removed versus pyrite rejection for several traditional and advanced circuits.	168



## LIST OF TABLES

		Page
Table 1.1	Forms of sulfur in various coals.	15
Table 1.2	Range of 'Fines' gravity concentration equipment.	16
Table 2.1	Nomenclature.	40
Table 3.1	Size-by-size ash and sulfur contents for the Pittsburgh No. 8 seam coal.	74
Table 3.2	Size-by-size ash and sulfur contents for the Illinois No. 6 seam coal.	75
Table 3.3	Numbering systems used for the detailed testing program.	98
Table 4.1	A balanced incomplete block design for four variables in the six blocks.	105
Table 4.2	A 2 <sup>2</sup> factorial design.	106
Table 4.3	A three-level design for four variables in three blocks.	108
Table 4.4	Parametric test matrix used to investigate the performance of the MGS unit for the Pittsburgh No. 8 seam coal.	109
Table 4.5	Parametric test matrix used to investigate the performance of the MGS unit for the Illinois No. 6 seam coal.	110
Table 4.6	Performance data for the MGS.	121
Table 4.7	Correlation matrix for the testing of the Pittsburgh No. 8 seam coal using the MGS.	133
Table 4.8	Correlation matrix for the testing of the Illinois No. 6 seam coal using the MGS.	134
Table 5.1	Parametric test matrix used to investigate the performance of the combined Microcel/ MGS circuit for the Pittsburgh No. 8 seam coal.	163

Table 5.2	Parametric test matrix used to investigate the performance of the combined Microcel/ MGS circuit for the Illinois No. 6 seam coal.	164
Table 5.3	Cost-benefit analysis for the Pittsburgh No. 8 seam coal.	165
Table 5.4	Cost-benefit analysis for the Illinois No. 6 seam coal.	166

## CHAPTER 1 - INTRODUCTION

### 1.1 Preamble

Fossil fuels, coal and petroleum constitute more than 80% of the world's energy resources. Due to the wider geographical distribution of coal and its low cost, coal-fired utilities are a major source of power generation. According to a survey conducted in 1993, total world coal reserves were estimated to be 1,039 billion tons, with 23.1% of these reserves in the United States. World annual production in the same time period was 4,357 million tons, of which 886 million tons were produced by the United States. At the present rate of consumption, current coal reserves are expected to last for nearly 250 years [1]. Yet, despite the abundance of coal, increasing international competition for existing coal markets and stricter environmental regulations are starting to restrict the grades of coal that can be easily marketed.

Over the past few decades, considerable research work has been conducted to understand the impact of coal-fired utilities on the environment. It has been shown that almost all fossil fuels contain sulfur. When sulfur is burned, it combines with oxygen in the air to create a colorless gas called sulfur dioxide ( $\text{SO}_2$ ).  $\text{SO}_2$  is a powerful lung irritant that can cause lung seizures in asthmatics and other sensitive groups. The  $\text{SO}_2$  emitted into the atmosphere can further combine with oxygen to form sulfates, when

washed out of the air by fog, clouds, mist or rain forms “acid rain”, as it is popularly called today.

Increasing environmental awareness in the United States recently led to the passage of the 1990 Clean Air Act Amendment (CAAA). This act mandates that electric utilities reduce SO<sub>2</sub> emissions from 17.5 MM tons/year to 8.9 MM tons/year. This is to be accomplished in two phases. In Phase I, 111 plants representing about 261 units will be required to reduce their emissions to 2.5 lb SO<sub>2</sub>/MM Btu by 1995. In Phase II, these plants and almost all others must reduce their emission levels to below 1.2 lb SO<sub>2</sub>/MM Btu by year 2000. With the passage of the CAAA, utilities can either switch to a low sulfur coal or install wet-scrubbers to reduce the SO<sub>2</sub> emissions. At present, coal switching is generally considered to be the more attractive option because of the high capital and operation and maintenance costs associated with wet scrubbers [2]. If the utilities choose to switch coals, it would be a boom for low-sulfur coal producers in the west at the expense of coal producers in the Illinois Basin and central Appalachian regions. It should be noted, however, that most of the upgrading technologies for the western low-rank coals are presently uneconomical without the Oil Barrel Equivalent Tax Credit. The better alternative would be to develop economically viable pre-combustion or post-combustion technologies that could address this problem.

In anticipation of this trend, high-sulfur coal producers have started taking steps to make their coals more cost competitive. Audits have been carried out in different

plants to identify efficiencies and optimize plant performance. Based on these audits, many coal producers have concluded that the largest performance gains can be realized by improving the efficiencies of their fine coal cleaning circuits.

In the past, untreated fines were either blended back with the clean coal from coarser size fractions or discarded, depending on their ash content. Since the 1970's, the cleaning of finer fractions has increased considerably due to the increasing costs of mining and waste disposal [3]. Among the technologies available during the past several decades, conventional flotation has proved to be the most efficient means of recovering fine coal. According to one estimate, almost 40 million tons of coal are treated each year by this method [4]. In spite of its wide acceptance, conventional flotation has many shortcomings. Earlier research work has shown that the separation efficiency of conventional flotation decreases with particle size [5,6,7]. As can be seen in Figure 1.1, the flotation rate constant decreases sharply when the particle size falls below 200 mesh [8]. Also, a significant amount of -400 mesh particles in the feed report to the concentrate non-selectively due to hydraulic entrainment.

Since 1970, extensive research work has been carried out to identify the causes for the low flotation rate and poor selectivity of -200 mesh coal [7,8,9,10]. Hydrodynamic analyses of the bubble-particle interaction suggested that smaller air bubbles could be used to improve the recovery of micron-sized particles. This study also

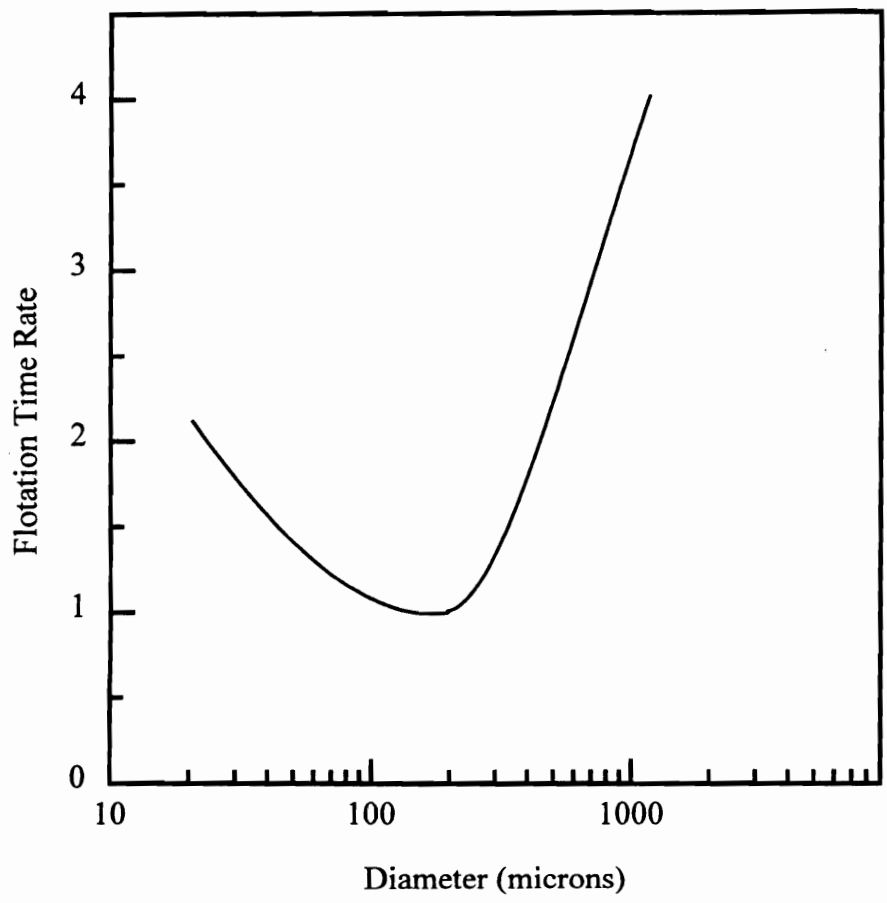


Figure 1.1 Flotation time rate of coal as a function of particle size [8].

indicated that bubble-particle contact can be enhanced using a countercurrent feeding arrangement. It was also realized that fine mineral matter which non-selectively reported to the froth concentrate by entrainment could be effectively reduced by washing the froth with a countercurrent flow of rinse water. Unfortunately, none of these improvements could be easily incorporated as part of the design of conventional flotation systems.

During the past two decades, extensive research work has been carried out at the Center for Coal and Minerals Processing (CCMP) and other research institutes in order to develop new cell designs capable of overcoming the shortcomings of conventional flotation [11,12]. This research work culminated in the development of a host of flotation column designs with unique air spargers and wash water systems. Of these designs, the Microcel™ column cell developed at Virginia Tech has been the most successful in gaining commercial acceptance in the coal industry.

Because of the superior performance of columns in treating fine particles, there has been a growing interest in column flotation in the coal industry. In many applications, column flotation is capable of producing a near perfect separation in terms of ash rejection [13]. However, studies suggest that flotation is less effective in rejecting pyrite. The main reasons for the poor rejection include: (a) the formation of superficial oxidation products (e.g., elemental sulfur) on the surface of pyrite which make it hydrophobic and (b) the incomplete liberation of pyrite from coal which results in coal-

pyrite composites [14]. In either case, it is difficult to separate coal from pyrite using surface-based separation techniques under these conditions.

Recent studies involving centrifugal float-sink tests and image analysis suggest that efficient density-based separations should achieve higher rejections of pyritic sulfur than surface-based processes such as froth flotation [15]. Unfortunately, traditional density-based separation processes are very inefficient when treating fine particles due to their low settling rates. However, the settling rates can be significantly increased by subjecting the particles to higher g-forces. This realization has led to the recent development of a variety of new fine particle concentrators which utilize centrifugal force to enhance the settling and separating rate of the coal fines [16]. The development of these “enhanced” gravity separators may pose a serious challenge to the monopoly of flotation for treating fine coals.

It is the purpose of this work to develop and evaluate an efficient fine coal cleaning circuit capable of treating flotation feed that is nominally 28 mesh x 0. The test work will include performance evaluation of column flotation (Microcel), enhanced gravity separation (MGS) [17], and combined flotation and enhanced gravity separation circuits.



## **1.2 Literature Review**

### **1.2.1 Fine Coal Processing**

The processing of fine coal (-28 mesh) has been a long-standing problem in the coal industry. Conventional coal preparation, namely, dense-media separation and gravity concentration, is highly successful in separating coarse mineral matter, but is not effective in treating fine particles. Until recently, coal fines were either incorporated into the clean coal or simply discarded. As a result, nearly 2 billion tons of coal fines presently reside in abandoned U.S. waste impoundment and an additional 40 million tons are added annually [3]. This practice is becoming less attractive, however, due to growing economic pressures to increase coal production and reduce waste disposal costs.

### **1.2.2 Froth Flotation**

Although several physical coal cleaning processes are available, froth flotation is generally recognized as the best method for beneficiating fine coal [18]. Coal is particularly well suited to separation from hydrophilic gangue using flotation because of its inherent floatability. However, in spite of its preeminent position in treating fine coal, studies have shown that the efficiency of froth flotation drops rapidly when treating -200 mesh particles [19,20,21].

In conventional flotation, the final stage of upgrading occurs by differential drainage of hydraulically entrained pulp away from the bubbles. The non-selective entrainment is a result of material being carried into the froth by the wake of a rising bubble and being trapped between the bubble lamella. Vanangamudi *et.al.* [22] showed that a linear relationship exists between water recovery and the amount of mineral matter recovered to the concentrate. To further complicate the separation process, the finer size fractions generally contain a disproportionate percentage of mineral matter (mainly clays). Therefore, hydraulic entrainment brings an increased amount of clay particles into the concentrate. Researchers have identified that an increase in bubble coalescence and pulp drainage could minimize the hydraulic entrainment problem [23]. Unfortunately, this also results in a loss of froth carrying capacity and coal recovery.

The development of column flotation in the 1960's by Boutin and Wheeler heralded a new era in fine particle processing [24]. The flotation column is a radical departure from conventional flotation in terms of its physical dimensions and basic operating principles. The initial test results exemplified the advantages of this system over conventional flotation, however, industrial acceptance was slow to come.

Concerted efforts by several research groups around the world over the last two decades helped in understanding the fundamental operating principles of column flotation [25]. Fundamental studies aided in identifying the reasons for its superior performance over conventional flotation. The basic areas where column differs from

conventional flotation are bubble generation, particle capture and froth stability. Based on these fundamental studies several column designs have been developed by different research groups around the world. Some of the popular designs are the Cominco [26], Flotaire [27], Hydrochem [28], Jameson [29], Leeds [30], Microcel [31] and the Packed columns [32].

Since the Microcel was used in the present investigation, a detailed description of the development of the Microcel column, followed by a brief description of this process, is provided in the following paragraphs. The Microcel flotation column was developed in the early 1980's to take advantage of the benefits of using smaller air bubbles for flotation. Small air bubbles increase the rate of flotation and allow a higher throughput to be achieved at a given coal recovery. Like most other column flotation cells, the Microcel column is also equipped with a wash water system that minimizes the entrainment of ultrafine mineral matter (such as clay) into the froth product. Thus, the Microcel is capable of achieving a better rejection of mineral matter than conventional flotation cells.

A schematic representation of a typical Microcel unit is shown in Figure 1.2. In this device, air bubbles in the range of 0.1 to 0.4 mm diameter are generated by passing air and a portion of the flotation pulp through one or more in-line static mixers. The high-shear agitation provided by the in-line mixers generate smaller bubbles.

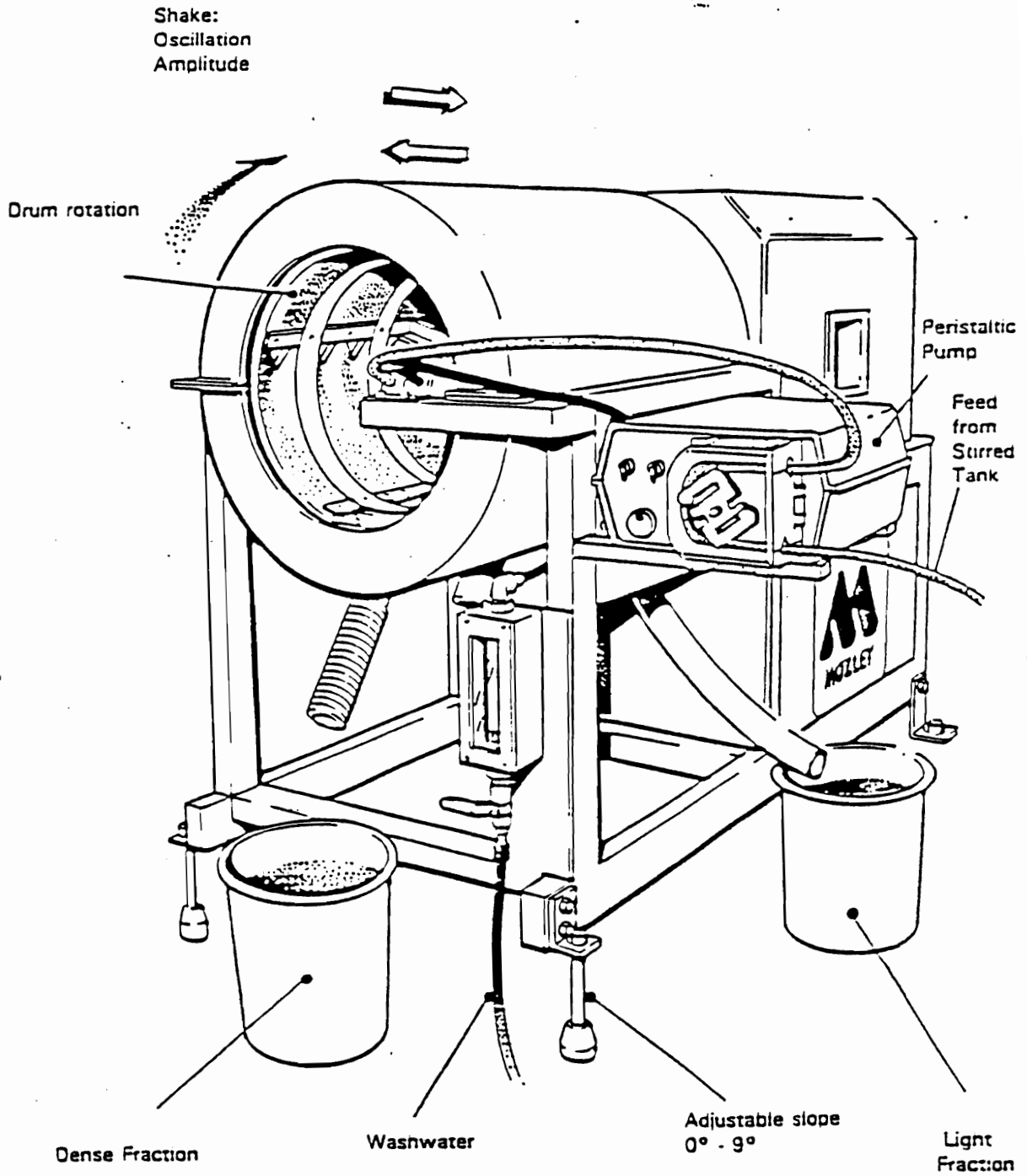


Figure 1.2 A schematic representation of a typical microcel unit.

In column flotation, the feed slurry descends through a long, cylindrical tube against a countercurrent stream of pneumatically generated bubbles. The column geometry is such that length-to-diameter ratios usually vary from 5:1 to 30:1. As the bubbles rise into the base of the froth they are washed by a countercurrent stream of freshwater which is injected into the froth zone. This rinsing action prevents the physical entrainment of fine mineral matter, thus providing a higher degree of separation (Figure 1.3). Additionally, the removal of an impeller system provides for more quiescent conditions in the column recovery zone. This is advantageous in terms of collection rates due to improved bubble/particle hydrodynamics as well as reduced axial dispersion [33].

In the field of coal preparation, washability analysis has been widely used to predict and evaluate the performance of gravity separators. In contrast, there was no acceptable test procedure to generate an ideal separation curve for coal fines (-28 mesh). In the last decade, research efforts at CSIRO Australia, CCMP and other groups has helped in developing acceptable procedures to evaluate flotation performance [34,35,36]. Most of these techniques are some variation on the “release analysis” procedure developed by C.C. Dell [37].

Several researchers have evaluated the performance of conventional flotation versus column flotation [38]. In these studies, the performance of column and conventional flotation were compared with the ideal separation curve generated by release analysis. These experiments clearly demonstrated that the column is capable of

producing cleaner products with higher recoveries. As discussed earlier, the superior performance of a column can be attributed to reduction in hydraulic entrainment and an increase in the probability of bubble-particle attachment. However, sulfur rejection capabilities are limited due to superficial oxidation and/or incomplete liberation of pyrite.

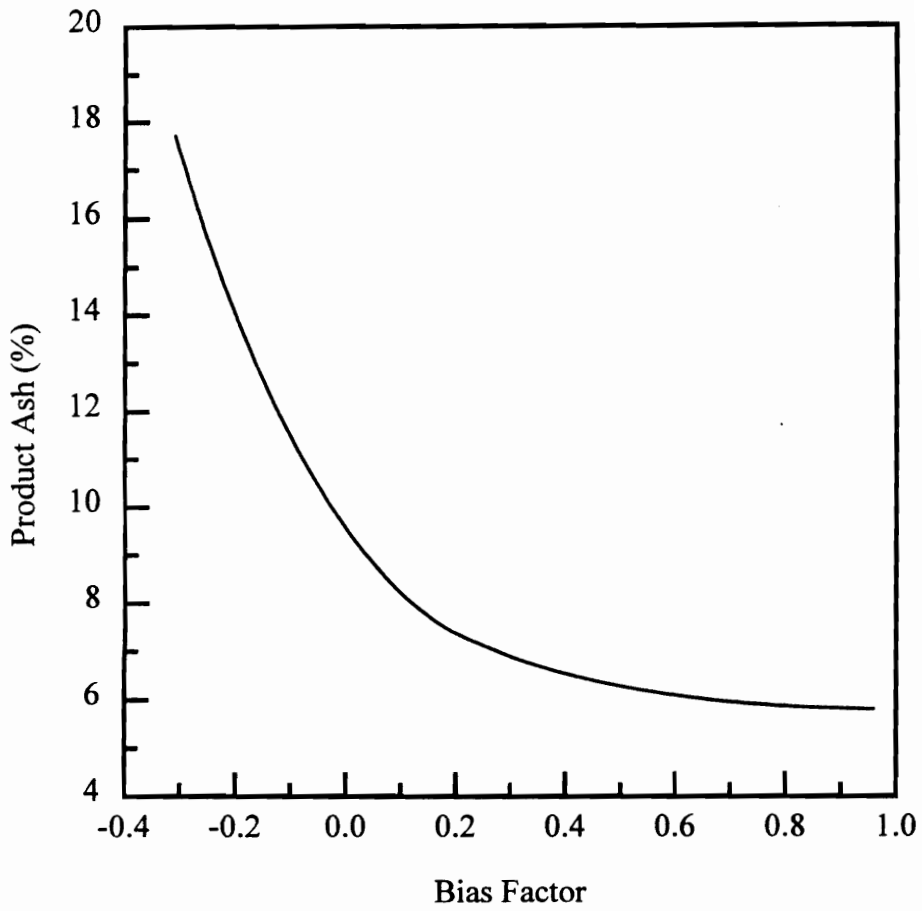


Figure 1.3. Product grade as a function of the column bias factor for the flotation of fine coal [13].

### 1.2.3 Fine Particle Gravity Concentrators

In the past, coal producers were concerned primarily with the ash content and heating value of the clean coal. However, with the passage of the Clean Air Act, sulfur content in the product also became an important consideration. In coal, the main forms of sulfur are organic, sulfate and pyritic. Studies have shown that organic sulfur as percentage of total sulfur can be as high as 80% in U.S. coals. However, in some coal seams, pyritic sulfur as a percentage of total sulfur can be as high as 70% (see Table 1.1) [39]. In general, sulfates are a very minor contributor to sulfur, which is generally of only academic importance. Therefore, the reduction in the organic or pyritic sulfur content of coal is important to meet the new emission standards. Since organic sulfur is chemically bound to coal, conventional coal cleaning methods are not practical. Therefore, there is a growing need to reject pyritic sulfur. Fortunately, there exists a significant specific gravity difference between coal ( $SG \approx 1.5$ ) and pyrite ( $SG \approx 4.8$ ). Separation techniques that can exploit this difference are likely to be able to achieve higher sulfur rejections.

Table 1.2 highlights the range of gravity concentration equipment operating under normal gravity that are, or have been, of commercial importance [16]. Most of these are some form of flowing film separators. In the early days of mineral processing, stationary deck concentrators were used. Because of its low capacity and lower performance, these unit operations have become obsolete. In order to increase the



**Table 1.1****Forms of Sulfur in various coals [39].**

Location of Mine	Coal Seam	Total Sulfur	Pyritic Sulfur	Organic Sulfur
Washington Co., PA	Pittsburgh	1.13	0.35	0.78
Clearfield Co., PA	Upper Freeport	3.56	2.82	0.74
Allegheny Co., PA	Thick Freeport	0.92	0.46	0.45
Somerset Co., PA	B	0.78	0.19	0.57
Somerset Co., PA	C prime	2.00	1.43	0.54
Clearfield Co., PA	B	1.90	1.12	0.75
Cambaria Co., PA	Miller	1.25	0.56	0.65
Franklin Co., IL	No. 6	2.52	1.50	1.02
Franklin Co., IL	No. 6	1.50	0.81	0.69
Montgomery Co., IL	No. 6	4.97	2.53	2.40
Williamson Co., IL	No. 6	4.01	2.17	1.80
Union Co., KY	No. 9	3.28	1.05	2.23
Webster Co., KY	No. 12	1.48	0.70	0.78
Pike Co., KY	Freeburn	0.46	0.13	0.33
Letcher Co., KY	Elkhorn	0.68	0.13	0.51
McDowell Co., WV	Pocahontas No. 3	0.55	0.08	0.46
Boone Co., WV	Eagle	2.48	1.47	1.01
Walker Co., AL	Pratt	1.62	0.81	0.82
Clay Co., IL	No. 3	3.92	2.13	1.79
Cumnock Co., NC	Deep River	2.32	1.52	0.80
Meigs Co., OH	8 - A	2.51	1.61	0.86
Allegany Co., MD	Big Vein	0.86	0.18	0.67

NOTE: Sulfur forms are reported in % Moisture free basis. Sulfate sulfur values are not recorded in this table. Where the sum of pyritic and organic sulfur is not equal to total sulfur, the difference is sulfate sulfur. In other cases, sulfate sulfur is included with the pyritic sulfur.

**Table 1.2**

**Range of 'Fines' gravity concentration equipment [19].**

Stationary Deck Equipment	Stirred Bed Devices
Buddle Round Table Strake Corduoy Table McKelvey Concentrator Denver Buckman Tilting Frame Spiral Sluice	<u>Discontinuous Shear</u> Vanners Shaking Table Kieve Rocking Shaking Vanner GEC Duplex Concentrator  <u>Unidirectional Shear</u> Endless Belt Concentrator Johnson Barrel Hodgson Separator Rotating Cone Separator  <u>Orbital Shear</u> Shaken Helicoid Bartles-Mozley Separator Bartles Crossbelt Concentrator

effectiveness of flowing film separators, it is necessary to impart additional shear by the movement of the deck relative to the film. There are mainly three different methods of deck shear namely, discontinuous shear, unidirectional shear and orbital shear.

The shaking table, which employs a discontinuous shear mechanism, is one of the workhorses of the mineral processing industry. It is interesting to note that there are applications where shaking tables are capable of effectively treating material as coarse as 15 mm (coal) or as fine as 15 microns (tin). But, in general, separation efficiency is generally poor when treating particles finer than 200 microns.

It has been clearly understood that the difference in the settling velocity between the valuable and waste minerals is key to achieve effective separations. In a recent review paper on enhanced fine gravity separators, Luttrell *et. al.* [40] have discussed the problems of treating very fine particles by density-based separation processes. It was shown that the settling velocity of particles subjected to the normal gravitational field rises very rapidly above 1 mm. Since the gravitational force is proportional to particle mass, the settling velocity difference between particles finer than 1 mm is considerably smaller, resulting in poor separation. However, by applying an artificial gravitational field, particle settling velocities can be greatly enhanced and the effective size range over which efficient separations can be achieved can be extended to much finer sizes. As shown in Figure 1.4, high settling velocities can be maintained down to 0.1 mm by

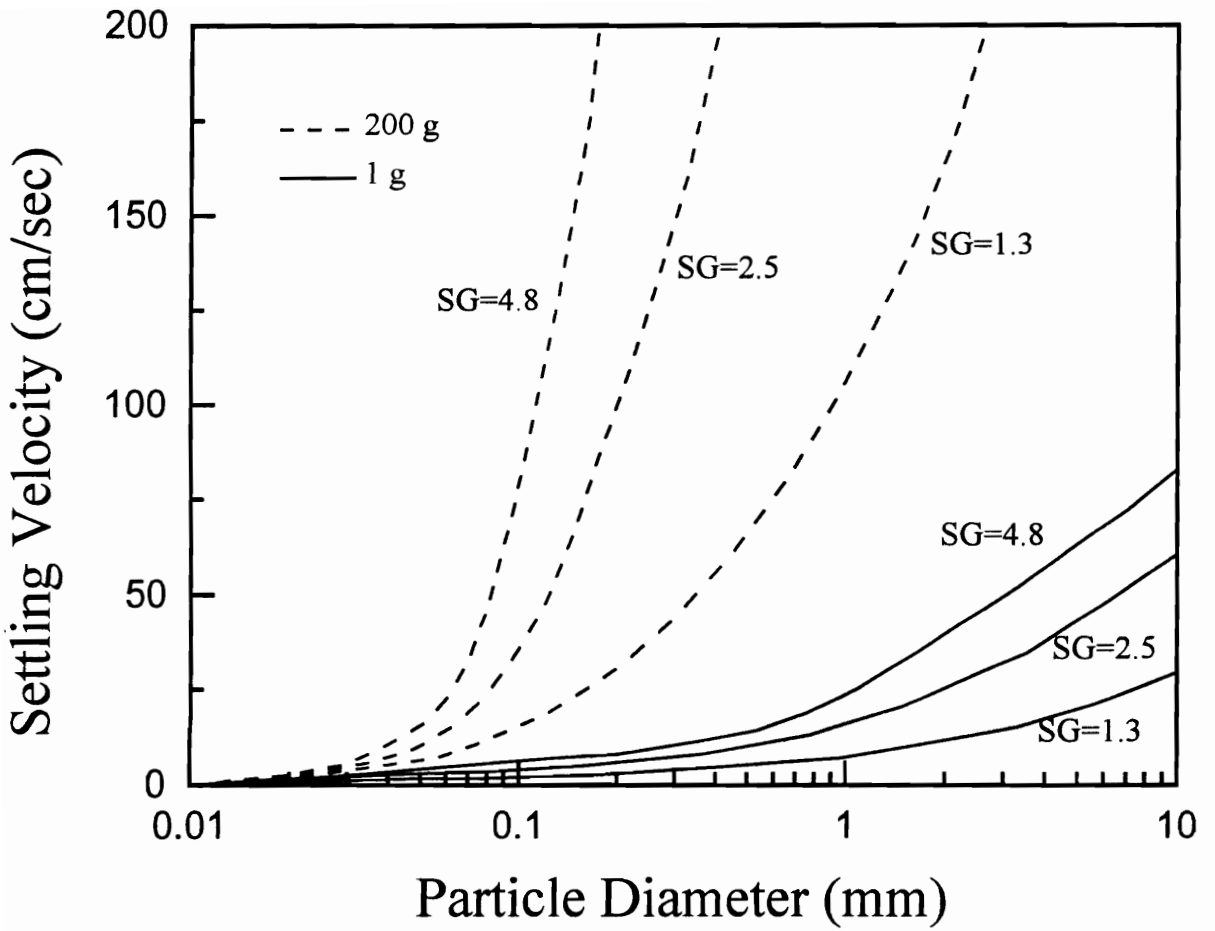


Figure 1.4 Theoretical effect of particle diameter on the free-settling velocity of coal (SG=1.3), Shale (SG=2.5) and pyrite (SG=4.8) under gravitational fields of 1 and 200 g's.

applying an artificial gravitational field of 200 g's. The additional force permits efficient separations to be achieved at very fine particle sizes.

The use of centrifugal force, or elevated gravity constant, to increase the settling rate of particles has been commercially applied for many years in classification. However, apart from some isolated work by Ferrara [41], most of the development work utilizing centrifugal force to enhance gravity concentration was carried out in the Soviet Union and China.

#### 1.2.3.1 *YT Centrifugal Separators*

In China, the YT Centrifugal Separator was first introduced at the Yunan tin operations and are now widely applied to a variety of minerals, including iron [42]. This unit consists of a drum with a small included cone angle, rotating on a horizontal axis. In this process, concentration is by preferential settling of heavier minerals which are then washed from the unit at predetermined intervals (Figure 1.5).

#### 1.2.3.2 *Kelsey Jig*

The operating principle of the Kelsey jig is similar to that of a conventional jig, except that a normal jig is effectively wrapped in a circle and spun on a vertical axis at high speed [43]. The unit is capable of generating centrifugal fields up to 100 g's. As shown in Figure 1.6, a cylindrical screen is mounted across the top of the hutch to retain ragging material. Feed slurry enters the unit through the central feed pipe and flows outward across the bed of ragging. Mechanical pulsators located within each hutch

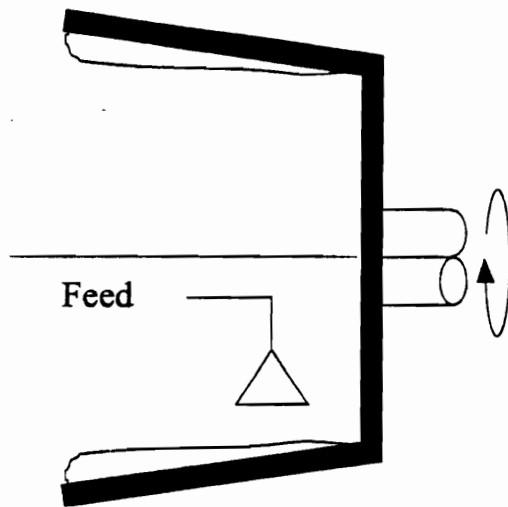


Figure 1.5. Schematic drawing of YT centrifugal separator.

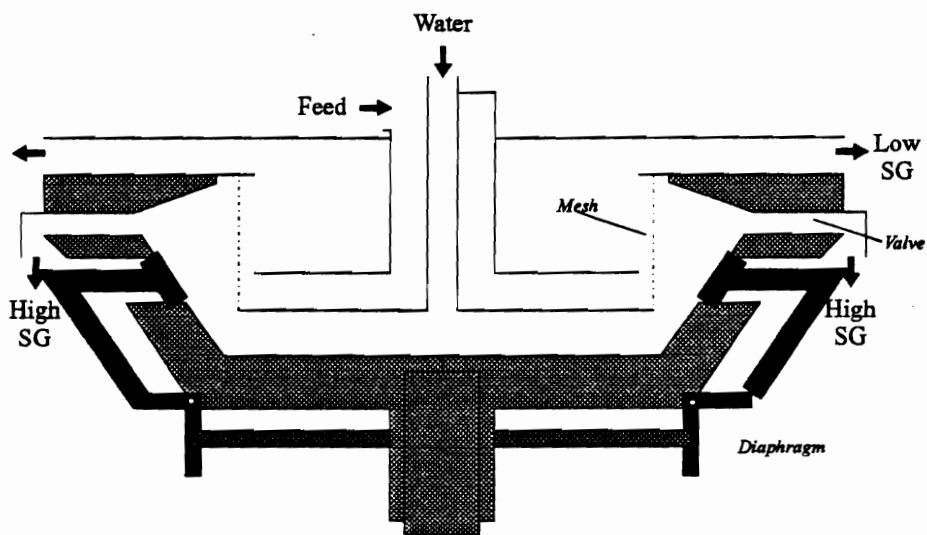


Figure 1.6. Schematic drawing of Kelsey jig.

create oscillations in the bed that differentially accelerate particles based on differences in density. Low-density particles flow across the raggng material and overflow the top of the unit, while high-density particles pass downward through the raggng/screen and are discharged through actuated valves. In most cases the unit forms its own raggng material from coarser and heavier feed particles.

#### 1.2.3.3 *Knelson Concentrator*

The Knelson separator consists of a rotating truncated cone which is stair-stepped by several ring type partitions [44]. The unit is capable of generating centrifugal fields up to 60 g's. As shown in Figure 1.7, feed slurry is introduced through a center pipe at the base of the bowl where it is immediately propelled towards the wall. The slurry rises in a countercurrent fashion from partition to partition until it overflows the top of the rotating bowl. Centrifugal forces that would cause packing of material between the partitions is offset by the injection of water through the partitions from the surrounding pressurized water jacket. This creates a fluidized bed of particles between each partition whose density is that of the pulp. Particles which have a density higher than that of the fluidized bed are collected behind the partitions, while the lighter ones are flushed out over the partitions.

#### 1.2.3.4 *Falcon Concentrator*

The Falcon Concentrator is essentially a centrifugal sluice. The unit consists of a smooth-surface truncated cone which rotates at a very high speed (Figure 1.8) [45]. Feed



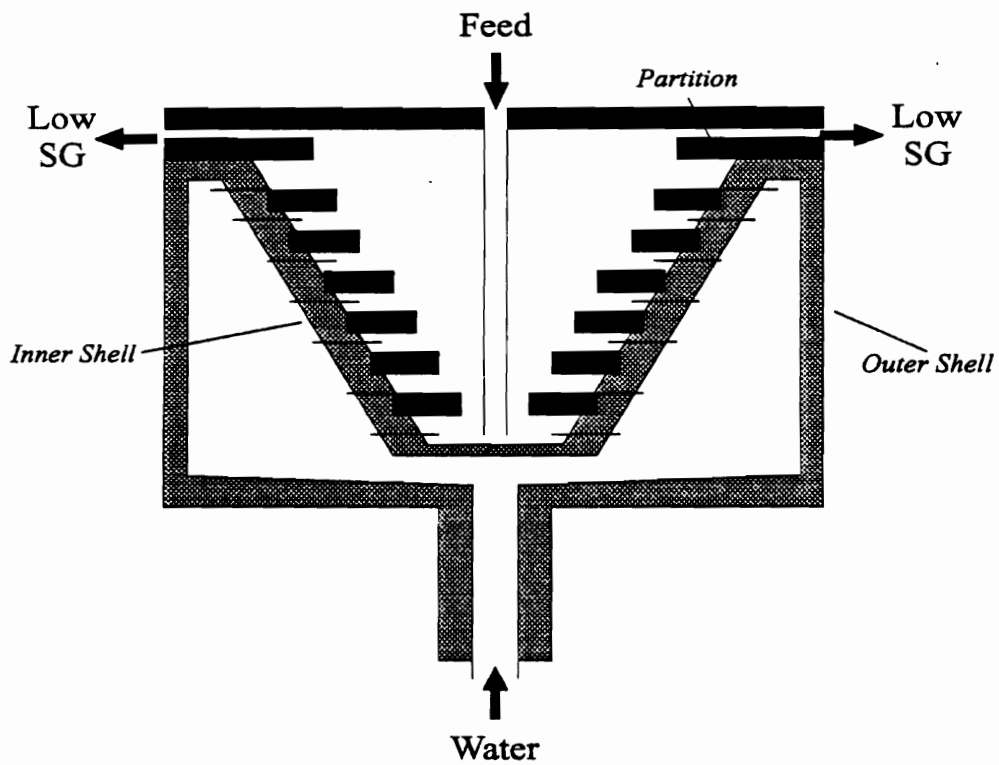


Figure 1.7. Schematic drawing of Knelson concentrator [44].

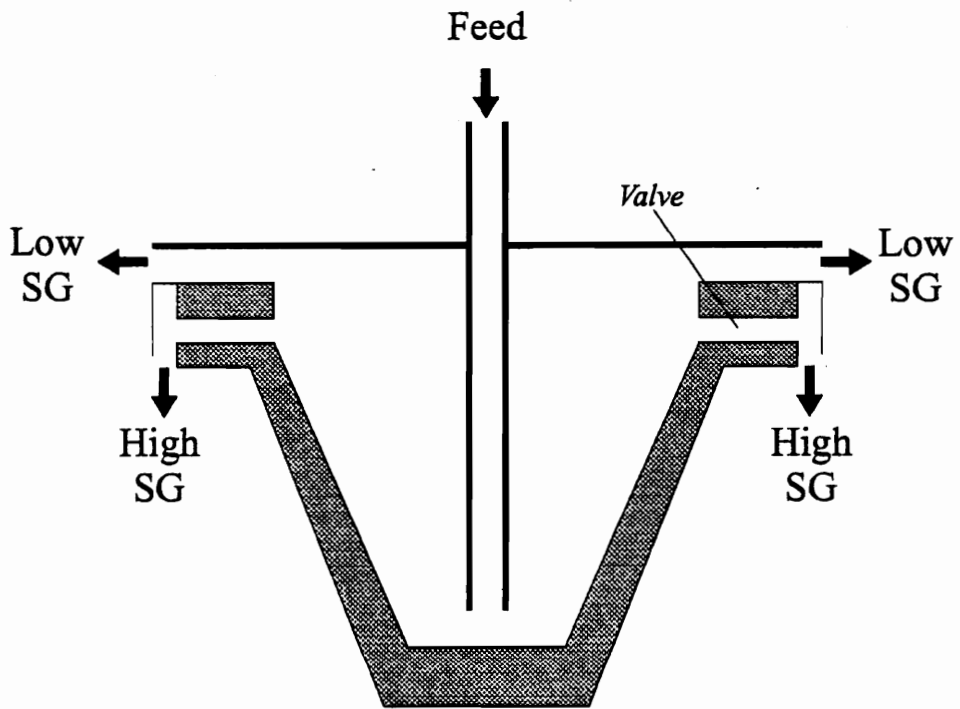
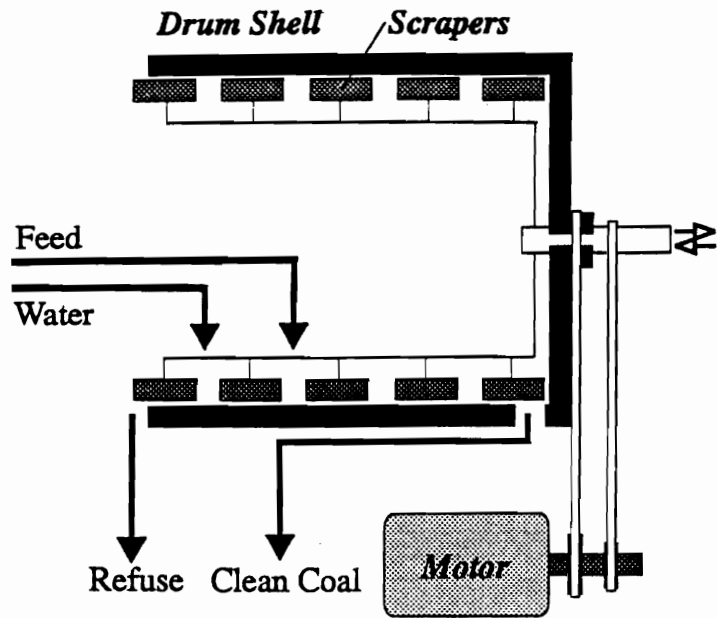


Figure 1.8. Schematic drawing of Falcon concentrator [45].

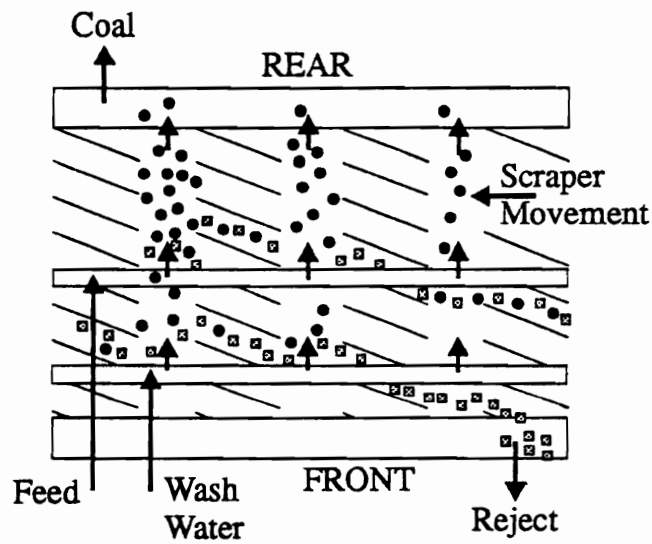
slurry is injected near the bottom of the cone and is accelerated up the cone wall by the centrifugal field (up to 300 g's). The slurry forms a thin flowing film in which particles become stratified based on differences in density. Light particles atop the stratified layer are discharged over the lip at the end of the cone, while high density particles which move along the cone wall are discharged via small reject ports.

#### 1.2.3.6 Multi-Gravity Separator (MGS)

The mechanical operation of the MGS can be best visualised from the schematics shown in Figure 1.9 [46]. Figure 1.9a shows a cross-section through the rotating drum, while 1.9b shows the flow patterns along the “unrolled” internal surface of the drum. During operation, feed slurry is passed through the front end of the unit and distributed onto the drum surface near its midpoint. The drum has a smooth surface and is slightly tapered so that the feed slurry naturally flows toward the rear end of the drum. The drum is rotated at a speed sufficient to pin high-density particles to the surface of the drum wall. The pinned particles are dragged in stepwise fashion toward the narrow end of the drum using a series of parallel scrapers. The rotation speed of the scraper is slightly offset from that of the drum in order to achieve the desired scraping action. A small flow of wash water is also introduced onto the drum surface at a point inside the drum. The countercurrent flow of water ensures that the high-density product is thoroughly washed prior to being discharged. Lighter particles, which remain in suspension, are carried along in the flowing-film and are discharged at the opposite end of the drum.



(a)



(b)

Figure 1.9 Schematic drawings of the MGS showing (a) a cross-section through the rotating drum and (b) flow patterns along the drum surface.

### **1.3 Research Objectives**

The primary objective of the present investigation was to evaluate the performance of an advanced two-stage coal cleaning circuit which combines froth flotation with an enhanced gravity concentrator. Literature studies indicate that froth flotation is an effective process for rejecting common ash-forming minerals such as clay, while enhanced gravity concentrators are superior for removing particles containing a high-density component such as pyrite. These studies suggest that the highest rejections of mineral matter can be achieved by combining both surface- and density-based separation processes into a single fine-coal cleaning circuit.

In order to meet the project objectives, a systematic study was conducted to evaluate the performance of the proposed two-stage circuit for treating coal samples from the Illinois No. 6 and Pittsburgh No. 8 seams. Studies were also carried out to determine trace element removal capabilities of the combined circuit. Since very little information was available in the literature concerning the operation of the MGS, an effort was also made to develop a first-principles model to understand the fundamental operating mechanisms of the MGS.

## **1.4 Organization of this Report**

An overview of recent developments in the field of fine particle processing is included in Chapter 1. This chapter also contains a comprehensive review of column flotation and enhanced gravity separators, and their potential for treating fine coal.

Chapter 2 discusses the development of a theoretical model to analyze the response of the Multi-Gravity separator (MGS) to various operating and feed conditions. Sample preparation and characterization, and experimental setup and procedure are presented in Chapter 3. Discussions on the experimental procedures include the test circuit layout and test plan.

To determine the important operating parameters of the MGS and evaluate its potential as a stand-alone unit operation that is capable of producing compliance coal, a detailed parametric study was conducted. Chapter 4 discusses the experimental design and the results of the parametric study. The experimental results are then compared with the predictions obtained using the theoretical model described in Chapter 2.

Chapter 5 contains the detailed evaluation of a combined Microcel/MGS circuit. Technical and economic analyses of this circuit, in terms of its potential for near-term application in the coal industry, are included in this chapter.

Conclusions derived from this investigation and recommendations for future study are presented in Chapters 6 and 7, respectively.

## 1.5 References

1. Kawatra, K., High Efficiency Coal Preparation: An International Symposium, Littleton, Colorado (1995).
2. Coal and Synfuels Technology, November, 11 (1991).
3. Schimmoller, B.K., Jacobsen, P.S., and Hucko, R.E., Proc. 19th Int. Tech. Conf. on Coal Utilization and Fuel Systems, Clearwater, Florida, U.S.A, May 21-24, p. 805, (1994).
4. Aplan, F.F., and Arnold, B.J., Coal Preparation, J.W. Leonard (Ed.), 5th Edition, p. 450, (1991).
5. Trahar, W.J., and Warren, L.J., Int. J. Min. Process., Vol. 3, p. 289, (1981).
6. Fuerstenau, D.W., "Fine Particle Flotation," Fine Particle Process., Somasundaram, P., (Ed.), AIME, New York, N.Y., (1980).
7. Vanangamudi, M., and Rao, T.C., Minerals Engineering, Vol. 2, No.2, p. 185, (1989).
8. Zimmerman, D.E., and Sun, S.C., Coal Preparation, J.W. Leonard (Ed.), 4th edition, p. 10, (1979).
9. Flint, L.R., and Howarth, W.J., Chem. Eng. Sci., Vol. 26, p. 1155, (1971).
10. Collins, G.L., and Jameson, G.J., Chem. Eng. Sci., Vol. 31, p 985, (1976).
11. Yoon, R.H., Adel, G.T., and Luttrell, G.H., Proc. 2nd Int. Conf. on Process. and Utilization of High Sulfur Coals, Carbondale, Illinois, Sept. 27 - Oct. 1, 1987).

12. Espinosa-Gomez, R., Yianatos, J.B., Finch, J.A., and Johnson, N.W., Column Flotation '88, K.V.S. Sastry (Ed.), SME Inc., Littleton, CO, p. 143, 1988).
13. Luttrell, G.H., and Yoon, R.H., Beneficiation of Phosphate: Theory and Practice, p. 361, (1993).
14. Heyes, G.W., and Trahar, W.J., Int. J. Min. Process., Vol. 4, p. 317, (1977).
15. Adel, G.T., Wang, D., and Yoon, R.H., Proc. Eighth Annual Int. Pittsburgh Coal Conf., p. 204, (1991).
16. Burt, R.O., Prod. and Process. of Fine Particles, Plumpton (Ed.), CIMM, p. 375, (1988).
17. Chan, S.K., Mozley, R.H., and Childs, G.J.C., Symp. Min. Proc. in the U.K., IMM Leeds, U.K., (1989).
18. Aplan, F.F., Flotation A.M. Gaudin Memorial Volume, Fuerstenau, D.W., (Ed.), SME, Littleton, Colorado, p. 1235, (1976).
19. Warren, L.J., Int. J. Min. Process., Vol. 114, p. 33, (1985).
20. Luttrell, G.H., Hydrodynamic Studies and Mathematical Modeling of Fine Coal Flotation, Ph. D., Dissertation, Virginia Tech, (1986).
21. Panapoulous, G., King, R.P., and Juckes, A.H., J. S. Afr. Inst. Min. Metall., p. 141, (1986).
22. Vanangamudi, M., and Rao, T.C., Minerals Engineering., Vol. 2, No. 2, p. 185, (1989).



23. Gaudin, A.M., Flotation, 2nd, ed., McGraw-Hill, New York, (1957).
24. Boutin, P., and Wheeler, D.A., Canadian Mining J., Vol. 88, p. 94, (1967).
25. Luttrell, G.H., Weber, A.T., Adel, G.T., and Yoon, R.H., Column Flotation'88, (K.V.S. Sastry, Ed.), SME, Littleton, Colorado, p. 205, (1988).
26. Cominco Column Flotation Application Sheet.
27. Zipperian, D.E., and Svensson, U., Column Flotation'88, (K.V.S. Sastry, Ed.), SME, Littleton, Colorado, p. 43, (1988).
28. Schneider, J.C., and Van Weert, G., Column Flotation'88, (K.V.S. Sastry, Ed.), SME, Littleton, Colorado, p. 287, (1988).
29. Jameson, G.J., Column Flotation'88, (K.V.S. Sastry, Ed.), SME, Littleton, Colorado, p. 281, (1988).
30. Dell, C.C., and Jenkins, W.W., VII Int. Coal Prep. Cong., Sydney, Australia, (1976).
31. Yoon, R.H., and Luttrell, G.H., Coal Preparation., Vol. 2, p. 179, (1986).
32. Yang, D.C., Column Flotation'88, (K.V.S. Sastry, Ed.), SME, Littleton, Colorado, p. 257, (1988).
33. Finch, J.A., and Dobby, G.S., Column Flotation, Pergamon Press, New York, (1990).
34. Pratten, S.J., Bensley, C.N., and Nicol, S.K., Int. J. Min. Process., Vol. 27, p. 243, (1989).

35. Forrest, W.R., Processing of High-Sulfur Coals using Microbubble Column Flotation, M.S. Thesis, Virginia Tech, (1990).
36. Vanangamudi, M., and Rao, T.C., Coal Preparation, Vol. 2, (1989).
37. Dell, C.C., J. Inst. Fuel, Vol. 37, p. 149, (1964).
38. Mankosa, M.J., Scale-up of Column Flotation, Ph. D., Dissertation, Virginia Tech, (1990).
39. Hower, J.C., and Parekh, B.K., Coal Preparation, Leonard, J.W. (Ed.), 5th Edition, p. 1, (1991).
40. Luttrell, G.H, Honaker, R.Q., and Phillips, D.I., 12th Int. Coal Prep. Exhibition and Conf., May 2-4, (1995).
41. Ferrarra, G., 5th IMPC, The Inst. of Mining and Metall. London, p. 173, (1960).
42. Luo, Q., Non-Ferrous Metals, Vol. 33, p. 48, (1981).
43. Fosserberg, E., and Nordquist, T., Minl. and Metall. Process., May, (1987).
44. Knelson, B., Minerals Engg., Vol. 5, No. 10-12, p. 1091, (1992).
45. Honaker, R.H., Proc. SME, February, 14 - 17, (1994).
46. U.K. Patent Application No. 8712031, Enhanced Gravity Separator.

## **CHAPTER 2 - MODELING OF THE MGS**

### **2.1 Introduction**

Traditionally, flotation is widely used to beneficiate the finer size fractions (below 200 microns). Earlier research work clearly indicates that the separation efficiency of the flotation process deteriorates with increase in the percentage of composite grains (middlings) in the feed [1-3]. It has been observed that the response to flotation of these middlings particles is similar to that of the desired mineral, resulting in a poor flotation performance. But with the depletion of good ore reserves, mining of low grade deposits with higher middlings content has increased. Therefore, in order to achieve a desired final product, it has become necessary to find an efficient processing scheme that could remove both the middlings and gangue particles. Recent research work carried out at CCMP (Center for Coal and Minerals Processing) and other research groups has shown that density-based separation processes can effectively remove middlings from valuable minerals [4-5]. Hence, there is a growing interest in using fine particle gravity concentrators to upgrade flotation size particles.

The MGS is one of the fine particle gravity concentrator developed in the 1980's, that uses centrifugal force to enhance the separation of fine particles. The operating principle of this device is similar to that of a shaking table. However, by rolling the

horizontal surface of the conventional table, then rotating it, it is possible to achieve many times the gravitational pull on the particles as they move in the flowing film along the internal surface of the drum.

Over the last decade considerable research effort has gone into the development of several gravity concentrators to upgrade fine particles based on their density difference [6-8]. Most of the improvements in the unit operations performance have come about only through trial-and-error approaches [9-11]. More recently, there is a growing interest in the development of process type models which can be used to predetermine the separators response. An accurate model helps in understanding the fundamental processes taking place in the concentrator, which eventually helps in optimizing the performance of the unit operation.

## 2.2 Literature Review

The primary purpose of modeling is to predict the performance of any unit operation and also to evaluate the response to various operating parameters. In addition, models provide an excellent tool for developing a clearer understanding of the fundamental processes of a given unit operation. Furthermore, an appropriate model can be used for equipment design, scale-up, process control and optimization.

Since the MGS was developed only in the 1980's, the amount of literature available is limited. Most of the previous work deals with the performance studies or descriptions of the equipment [12-15]. Presently, little research work is focused on the development of an empirical model for the MGS [16]. These models are based on a mathematical description of the relationships between the recovery to concentrate and the size and SG of the material. Empirical models are useful for predicting the performance of the MGS between the limits of previously obtained experimental data. Even though, empirical models are easy to develop, they cannot be used beyond the experimental data base and yield little information regarding the fundamental mechanisms of the process.

In order to gain an insight into the underlying principles of the MGS, it is logical to understand the fundamental mechanisms of its precursor, namely, the shaking table. In a shaking table, the slurry is fed onto a riffled, inclined deck, and the deck is subjected to an asymmetrical motion. The asymmetric motion of the deck helps in stratifying the

particles according to density, size and shape in the longitudinal direction of the deck. Between the riffles hindered settling and consolidation trickling occur. As the velocity decreases with depth, the bottom layer of stratified material between riffles experiences more turbulence due to the asymmetrical motion of the deck and this motion of the deck also aids in transporting the heavier particles, settled between riffles, towards the heavy product end.

A great deal of literature is available describing the mechanism of separation taking place on a shaking table. The flow characteristics of a thin-film and its effectiveness in separating particles was studied to a considerable extent by Gaudin (1939), Taggart (1951) and others [17-21]. In Gaudin's analysis, the flow characteristics on the shaking table were considered to be similar to that of a laminar flow on an inclined plate. It was shown that the velocity of the streamline decreased with depth and it approached zero near the surface of the deck. In this analysis, the particle-particle interaction, roughness of the bed surface caused due to the layering of particles and non-newtonian behavior of the fluid has not been considered. In spite of these shortcomings, this analysis helps in mathematically explaining the separation process taking place on a shaking table. Sivamohan *et al.* [23-28] developed a detailed model based on first principles to explain the tabling process. Their study included evaluation of the flow characteristics of the thin film on the reciprocating and oscillating surfaces as well as the effect of the concentrating surface on slimes recovery.

### 2.3 Objectives

Given the growing interest in fine particle gravity concentrators, the development of an accurate model for simulation and scale-up purposes would be very useful. An unsuccessful effort was made to study and simulate the separation processes taking place in the MGS from a mechanistic point of view.

In this chapter, an attempt has been made to develop a model to analyze the response of the MGS to operating and feed conditions, in terms of the existing basic theories of fluid mechanics and mineral processing [29-30]. The model development is based on first principles, which makes the model ideally suited for understanding the separation phenomena taking place in the MGS. The completed model is capable of predicting coal recovery, ash rejection and pyrite rejection for a range of operating and feed conditions. Eventhough, the emphasis of the present work is coal, the model should also be applicable to other mineral systems.

## 2.4 Model Development

Feed slurry is introduced midway onto the internal surface of the drum via an accelerator feeder. It is obvious that when a slurry is introduced into the MGS, the particles in the slurry are subjected to a host of forces mainly; the pull of gravity, force exerted due to the rotation of the viscous fluid, the rub between the particle and the substrate and the push of the fluid which is opposed by the particle resistance to motion. The oscillating action of the drum imparts an additional shearing force on the particles. Thus, the velocity of the particles is dependent upon their size, density and their position in the flowing film. Moreover, the MGS is provided with a scraper mechanism, which intermittently transports the settled particles up-slope in the opposite direction to the flow of the slurry and in that process it also continually regrades the material. Thus, the relatively slow moving heavier particles are separated from the faster moving lighter ones. Hence, it is reasonable to believe that modeling this system is relatively complex in its present state. However, by making the following assumptions, the complexity of the problem is reduced to a manageable level; thereby, allowing for a reasonable prediction of the performance of the separator.

### 2.4.1 Assumptions



- a) The flow characteristics of a thin section along the axial length of the MGS were considered to be similar to that of a flow on an inclined plate. To accommodate for the higher g-forces experienced by the slurry, the gravity terms in the force balance equations were replaced by the effective gravity.
- b) The separation characteristics of only a single particle in the flowing film on an inclined smooth surface with oscillating motion were to be determined. Particle-particle contact, layering of particles on the drum surface and the surface roughness was not considered.
- c) The appearance and disappearance of the scraper was dependent only on the drum speed. Every time the particle encounters the scraper, the particle is moved up-slope about 0.9 times the pitch of the scraper.

## 2.4.2 Model Equations

### 2.4.2.1 *Computations of the flow characteristics of the thin film*

The velocity of the flowing film wetting a substratum increases gradually from zero at the bottom to a maximum at the top. The velocities ( $v_x$ ), of the different layer of the film flowing by gravity under laminar flow conditions, as if the surface is stationary [20], is

**TABLE 2.1****NOMENCLATURE**

$v_x$	=	Velocity of the fluid in $x$ -direction
$\rho_l$	=	Density of the liquid
$\rho_s$	=	Density of the solid
$g_e$	=	Effective acceleration due to gravity
$\theta$	=	Angle of tilt
$h$	=	Maximum thickness of the flowing film
$y$	=	Actual thickness of the flowing film
$\mu$	=	Viscosity of the slurry
$W$	=	Volume of the fluid flowing per unit time and unit depth
$m$	=	Mass flowrate of the slurry
$b$	=	Circumference of the drum
$Q_l$	=	Volumetric flowrate of the slurry
$m_p$	=	Mass of the particle
$v_p$	=	Velocity of the particle
$F_{ge}$	=	Force due to gravity
$F_b$	=	Force due to buoyancy
$F_d$	=	Drag Force
$r_p$	=	Diameter of the particle
$v_m$	=	Settling velocity of the particle
$v_l$	=	velocity of the liquid
$\Phi$	=	Coefficient of friction
$\Phi_1$	=	Dynamic coefficient of friction
$k$	=	Sphericity of the particle
$sw$	=	Scraper width
$N$	=	Drum speed

$$v_x = \frac{\rho_l g_e \sin \theta}{2\mu} (2h - y)y \quad [1]$$

In order to determine the velocities of the different layer using Eq. [1], the thickness of the film ( $h$ ) must be obtained. The thickness of the film ( $h$ ) is determined using Eq. [2].

$$h = \left[ \frac{3\mu W}{\rho_l g_e \sin \theta} \right]^{1/3} \quad [2]$$

where,

$$W = \frac{m}{b}$$

$$m = Q_l * \rho_l$$

$$b = \pi D$$

From Eq. [2], it was deduced that the thickness of the film was dependent on the volume of fluid flow as well as the g-forces applied. Since the MGS operates at higher g's, the thickness of the film was smaller than that observed on a conventional shaking table. The maximum film thickness of water calculated for the desired flow rates and drum speed using Eq. [2] was found to be less than 400 microns. However, it is important to note that the film thickness increases with slurry viscosity, according to Eq. [2]. The viscosity of the coal slurry used in the present investigation was found to be between 100 and 300 centipoise. Therefore, the film thickness could range between 1.2 to 2.7 mm (Figure 2.1).

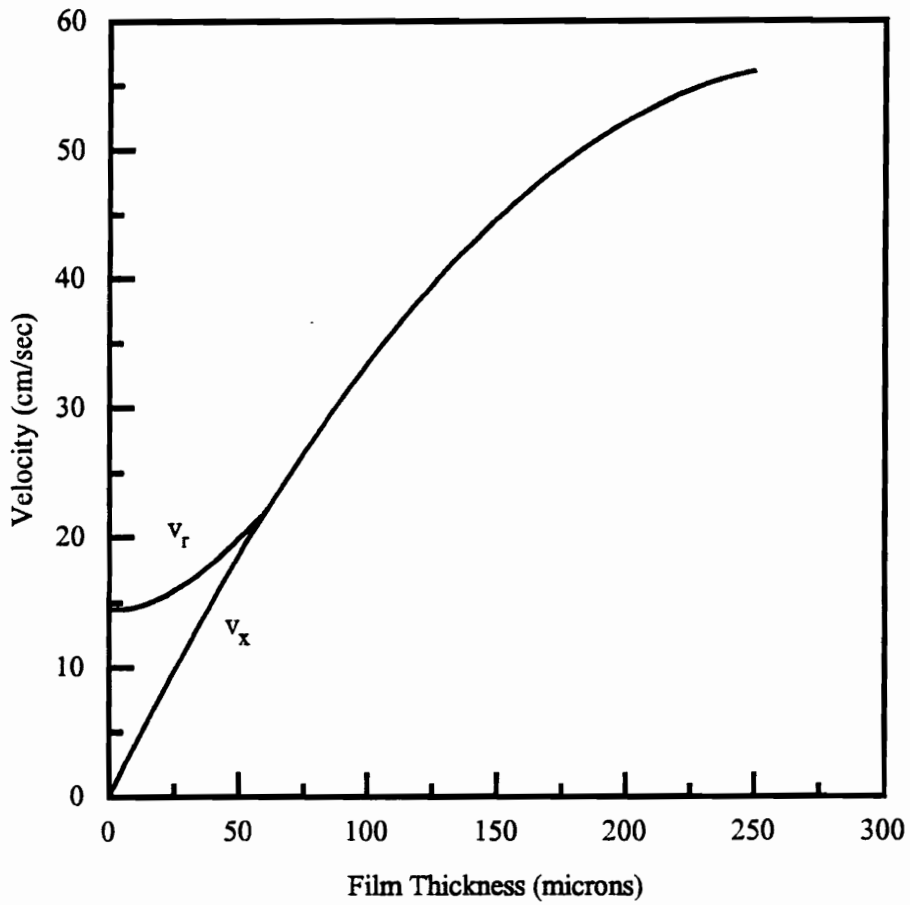


Figure 2.1. Velocity profile of the thin film flowing on an oscillating surface.

#### 2.4.2.2 Equations of motion of the particle

As shown in Figure 2.2, the particle starts settling in the flowing film and once it settles on the drum surface, it either slides or rolls depending on its mass. Therefore two sets of force balance equations have to be developed, one to describe the forces acting on the particle while it is settling and the other to describe the sliding or rolling motion of the particle on the drum surface. A schematic diagram illustrating the forces experienced by the particle, a) while it is settling and b) while it is rolling or sliding on the surface of the drum is shown in Figure 2.3.

*Forces acting on a particle settling in a flowing film:*

When a particle is settling in a thin film of liquid, the force balance equation includes both the forces acting on it while it is falling in the liquid ( negative  $y$  direction) and the streamline forces causing the fluid to push the particle in the (positive  $x$  direction).

Settling of a spherical particle ( $F_m$ ): The forces acting on a spherical particle falling in a viscous fluid can be expressed as

$$m_p \frac{dv_p}{dt} = F_{ge} - F_b - F_d \quad [3]$$

where,

$$F_{ge} = \frac{4}{3} \pi r_p^3 \rho_s g_e \quad [4]$$

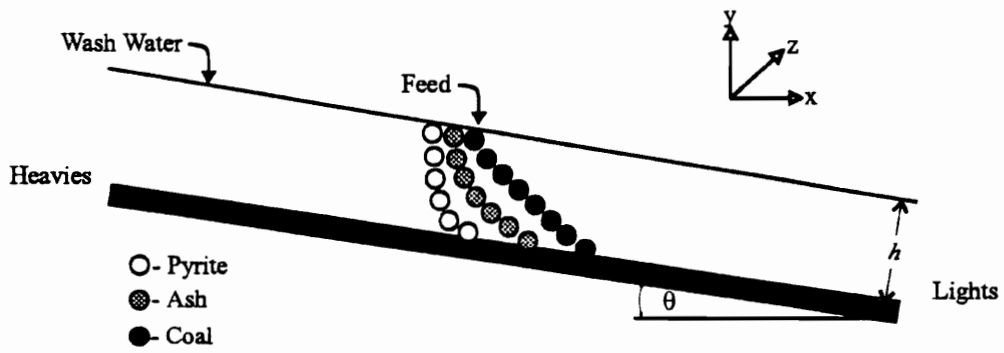


Figure 2.2. A schematic diagram of a side-view of the MGS, showing the particle trajectory in the fluid.

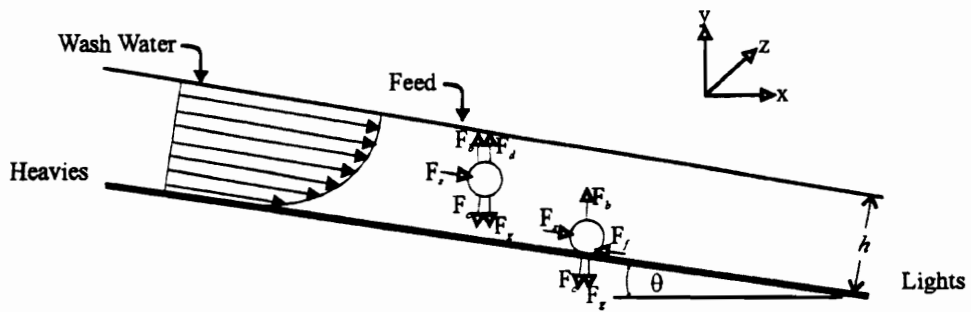


Figure 2.3. A schematic diagram illustrating the forces experienced by a particle, a) while it is settling and b) while it is rolling or sliding on the surface of the drum.

$$F_b = \frac{4}{3} \pi r_p^3 \rho_l g_e \quad [5]$$

$$F_d = 6\pi\mu r_p v_p \quad [6]$$

here,  $F_{ge}$  is the force exerted due to gravity combined with the centrifugal force acting on the particle ( $F_g + F_c$ ),  $F_b$  is the buoyant force acting on the particle and  $F_d$  is the drag force on a spherical particle deduced under Stokesian conditions.

If the particle is allowed to accelerate from rest, the velocity of the particle ( $v_p$ ), in Eq [3] will increase until  $dv/dt$  equals zero, i.e., the particle stops accelerating. This maximum velocity obtained when the particle stops accelerating is called terminal velocity, ( $v_m$ ), and is

$$v_m = \frac{2(\rho_s - \rho_l)r_p^2 g_e}{9\mu} \quad [7]$$

Push of the Fluid ( $F_s$ ): The liquid moves with a velocity that is a function of depth as determined from Eq. [1]. The particle introduced in the flowing slurry, or vice versa, offers a resistance to the motion, which is a function of the relative velocity of the fluid and the particle. In this present case, the particle and the fluid are both moving. The net resistance of the particle to the fluid or the fluid push on the particle, is proportional to the velocity and to the perimeter of the particle.



$$m_p \frac{dv_p}{dt} = 6\pi\mu r_p (v_l - v_p) \quad [8]$$

Therefore, the complete force balance equation for a particle settling in the thin liquid is the summation of the Eqs. [3] and [8].

*Forces acting on a particle situated at the bottom of a flowing film:*

There are four forces acting on a particle situated at the bottom of a flowing film. These forces are the force exerted due to gravity ( $F_{ge}$ ) combined with the centrifugal force, the frictional force ( $F_f$ ) arising out of the rub between particle and drum surface and the streamline force ( $F_s$ ) on the particle due to the liquid (Figure 2.2).

Force exerted due to gravity ( $F_{ge}$ ): For a particle of a given average radius, the gravity component along the slope (i.e., the positive x-direction) can be expressed as:

$$F_{ge} = \frac{4}{3} \pi r_p^3 \sin \theta (\rho_s - \rho_l) g_e \quad [9]$$

Frictional Force ( $F_f$ ): When the particle rubs the surface of the drum, there is a force which acts in the opposite direction of the particle movement and it is

$$F_f = -\frac{4}{3} \pi r_p^3 \Phi \cos \theta (\rho_s - \rho_l) g_e \quad [10]$$

Push of the Fluid ( $F_s$ ): As described above in Eq [8], it is the net resistance of the particle to the fluid or the fluid push on the particle and is proportional to the velocity and to the perimeter of the particle.

Therefore, the equation of motion of the particle situated at the bottom of the flowing film is

$$m_p \frac{dv}{dt} = F_{ge} + F_s - F_f \quad [11]$$

On substituting and simplifying the Eq [11], the following equation is obtained:

$$\begin{aligned} \frac{dv_p}{dt} = & \frac{(\rho_s - \rho_l)}{\rho_s} g_e (\sin \theta - \Phi \cos \theta) - \frac{9}{2} \mu k \frac{v_p}{\rho_s r_p^2} \\ & + \frac{9}{2} k \frac{\rho_l}{\rho_s} g_e \sin \theta * \frac{h}{r_p} - \frac{27}{8} \frac{\rho_l}{\rho_s} g_e \sin \theta \end{aligned} \quad [12]$$

The particle settled at the bottom of the fluid, starts to move on the surface of the drum. The particle movement is characterized by rolling or sliding motion. The coefficient of friction term in the Eq. [12], changes to a dynamic coefficient of friction. If the particle travels at low speeds, the effective friction is relatively large coefficient of dynamic sliding friction, and if it travels at high speeds, the effective friction is lower coefficient of dynamic rolling friction. As a first approximation, the dynamic coefficient of friction is assumed to be constant.

If the particle is allowed to accelerate from rest, the velocity of the particle ( $v_p$ ), in the Eq [12] will increase until  $dv/dt$  equals zero, i.e., the particle stops accelerating. This maximum velocity obtained when the particle stops accelerating is called terminal velocity of the particle ( $v_{max}$ ).

The equation for the terminal velocity of the particle ( $v_{max}$ ), obtained when a particle slides is

$$v_{max}(\text{sliding}) = r_p^2 \frac{g_e \sin \theta}{\mu} \left[ \frac{2(\rho_s - \rho_l)(1 - \Phi_D \cos \theta)}{9k} - \frac{3}{4} \rho_l \right] + r_p \frac{g_e \sin \theta}{\mu} \rho_l h \quad [13]$$

When particle rolls, the dynamic friction term in Eq. [13] may be considered to have disappeared, the terminal velocity becomes

$$v_{max}(\text{rolling}) = r_p^2 \frac{g_e \sin \theta}{\mu} \left[ \frac{2(\rho_s - \rho_l)}{9k} - \frac{3}{4} \rho_l \right] + r_p \frac{g_e \sin \theta}{\mu} \rho_l h \quad [14]$$

It is interesting to note that according to Eq. [14], the velocity of the particle increases with increase in specific gravity, which is opposite of that obtained using the Eq. [13], when particle slides. Therefore, an assumption is made that under optimum conditions for flowing-film concentration involve rolling of the lighter minerals and sliding of heavier minerals.

*Force exerted due to scraper mechanism:*

The MGS is provided with four rows of scraper rotating at a slightly higher speed than the drum. Scraper moves perpendicular to the slurry flow. Thus, when a particle comes in contact with the scraper, it is moved upstream. The velocity of the scraper with respect to the drum is

$$v_s = \omega r (1.05 * N - N) / 60 \quad [15]$$

The distance a particle is moved upstream, depends only on the relative speed of the scraper with respect to the drum.

## 2.5 Simulation Procedure

The main purpose of this model is to be able to generate partition curve for the different components of the feed, namely, lighter and heavier minerals at different size fractions, at different operating conditions.

The steps involved in the simulation are as follows:

In order to be able to generate a partition curve, it is imperative to know whether a given particle of any given size and density reports to the lights or heavies end. Therefore, this simulation involves keeping track of the position of the particle at any given time.

- a) Determination of film thickness using Eq. [2], for a given flowrate and drum speed.
- b) It is assumed that the particle introduced in the flowing film is fully submerged with the tip of the particle in contact with the topmost layer of the flowing film. The terminal velocity ( $v_m$ ) of the particle is determined by using Eq. [7], which gives the particle position in the  $y$  direction.
- c) When the particle is in suspension, the average streamline velocity ( $v_s$ ) of the fluid acting on the particle, is obtained by integrating the Eq. [1] over the entire particle diameter at any given position in the  $y$  direction. It is assumed that the particle is moving with terminal velocity in the  $x$

direction, that is, the particle velocity is equal to streamline velocity.

Hence the particle position in  $x$  direction is determined.

- d) Once the particle has settled on to the surface of the drum (i.e.,  $y$  goes to zero), the particle slides or rolls depending on its density. The velocity of the particle is calculated using Eqs [13] or [14], thus the particle position is determined.
- e) The scrapers are moving perpendicular to the flow direction, with each scraper blades positioned at 45-degree angle to the flow. Using the Eq. [15], the position of the scraper at any given time is determined.
- f) The particle keeps moving down-slope along with the fluid till it encounters a scraper. When a particle encounters the scraper, it is thrown 0.9 times the pitch in the negative  $x$  direction. A random number generator with uniform distribution is used to determine the position of particle in the  $y$  direction.
- g) The iterative procedure is continued till the particle leaves the system either from the heavies or lights end.

## 2.6 Results and Discussion

The simulation program was used to test the ‘reasonableness’ of the model, and to investigate the operating characteristics of the MGS. The simulations carried out in this investigation has been limited to the investigation of the performance of MGS on a liberated feed material. This study is intended to advance the understanding of the MGS operation and for the first time an attempt is made to develop a model for the MGS based on first principles. In spite of the major assumptions that has gone into building this model, the trend predicted using this model is in general agreement with results found in literature. The model parameters namely drum speed and feed rate are examined in detail in the following section.

### 2.6.1 Model Predictions

#### 2.6.1.1 *Effect of drum speed*

An increase in drum speed affects the operation of the MGS in two ways. An increase in the drum speed increases the g-force. It can be clearly seen from the Eq.[2], that for a given flowrate, the thickness of the film is inversely dependent on the g-force. Therefore, the film thickness reduces with increase in the g-forces, resulting in an increase in the velocity of the slurry flowing towards the lights end. Further, an increase in the drum speed, increases the settling velocity of the particle (Eq. [7]) and the inertial

mass of the mineral particles, which helps in retaining the particles closer to the bottom of the flowing film.

Simulations were carried out at different drum speeds on coal, ash-forming minerals and pyrite. The results are given in Figures 2.4 to 2.6. It is generally understood that an increase in the drum speed increases the rejection of pyrite and coarser coal. It can be seen that the effect of drum speed is more so conspicuous on coal (lighter mineral). In order to achieve a separation between the ash-forming minerals and coal, whose density difference is small, the drum speed has to be increased. But increase in the drum speed also increases the rejection of coarse coal. Therefore, the performance of the unit operation increases on a narrow size feed material.

Simulation was carried out on an monosized feed material (mean particle size of 150 microns) at different drum speeds. It is interesting to note that the cut-gravity ( $SG_{50}$ ), decreases with increase in drum speed and further the  $SG_{50}$  increases with decrease in particle size (Figure 2.7). The probable error ( $E_p$ ) is the widely used indicator to describe the separation efficiency of density-based separators. This provides a measure of the steepness of the partition curve. An ideal separation would yield an  $E_p$  value of zero. Larger  $E_p$  value reflects on the inferior performance of the unit operation. It is evident from Figure 2.8, that increase in the drum speed results in a steeper partition curve and lower  $E_p$  value. Therefore, increase in drum speed improves the separation



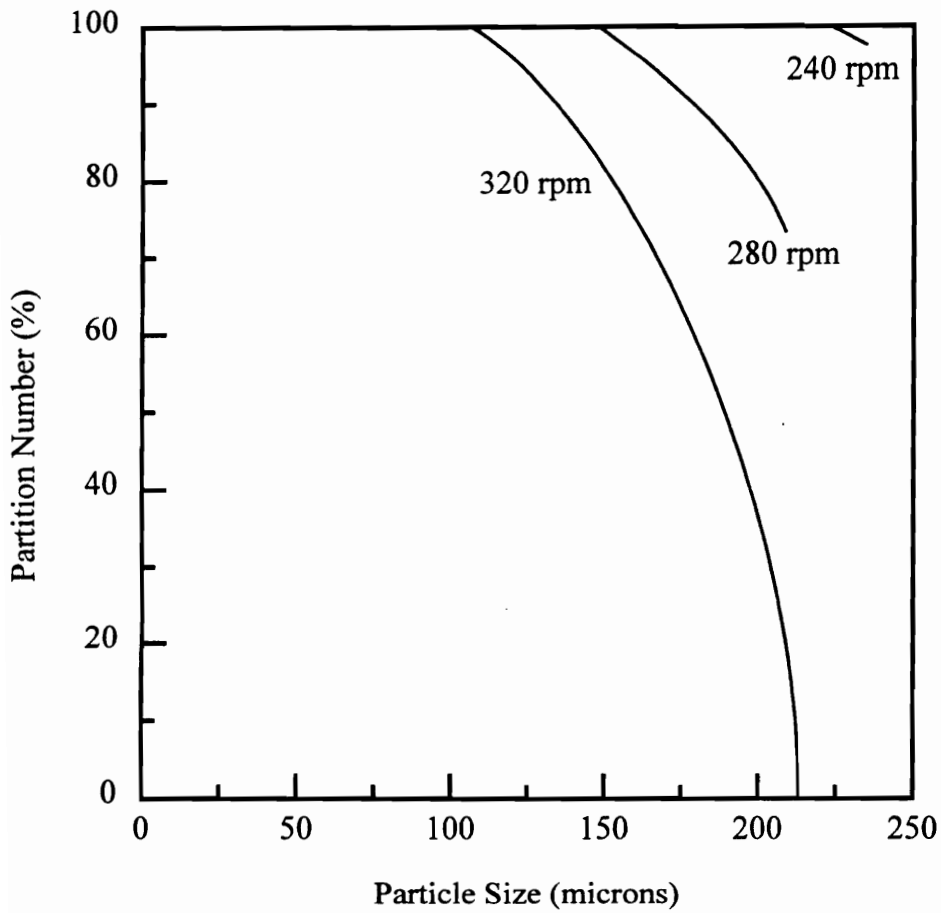


Figure 2.4. Effect of particle size on the performance of the MGS using liberated coal particles at different drum speeds.

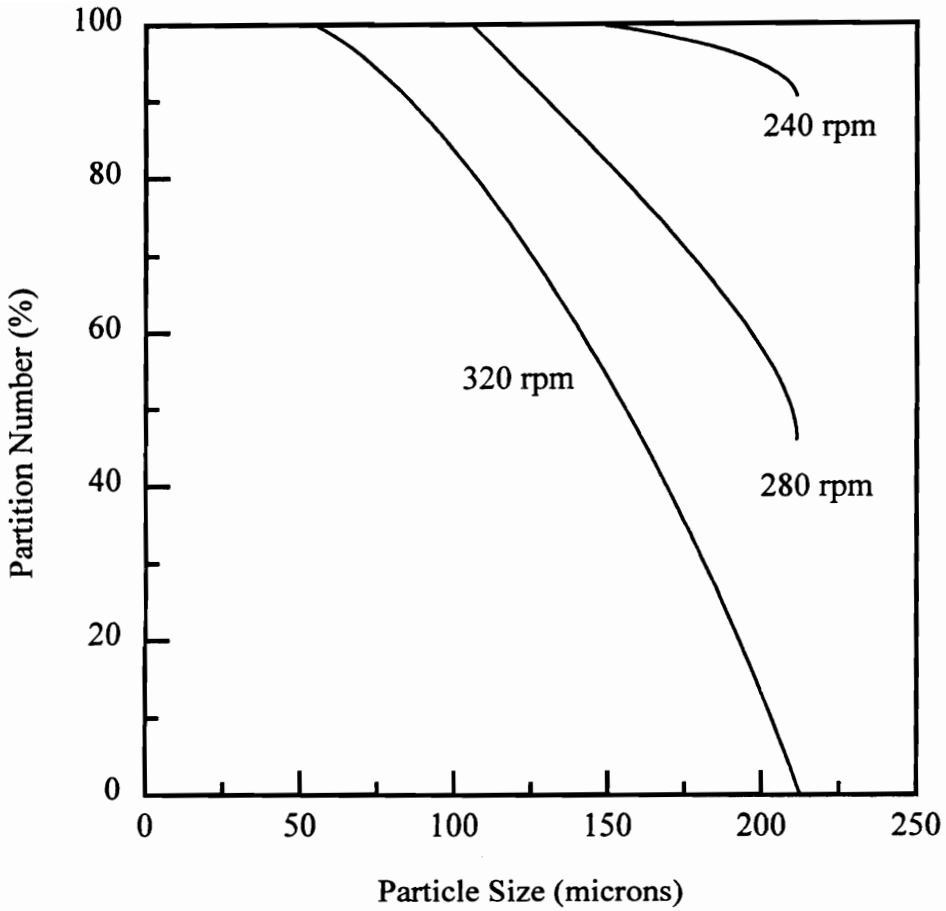


Figure 2.5. Effect of particle size on the performance of the MGS using liberated ash particles at different drum speeds.

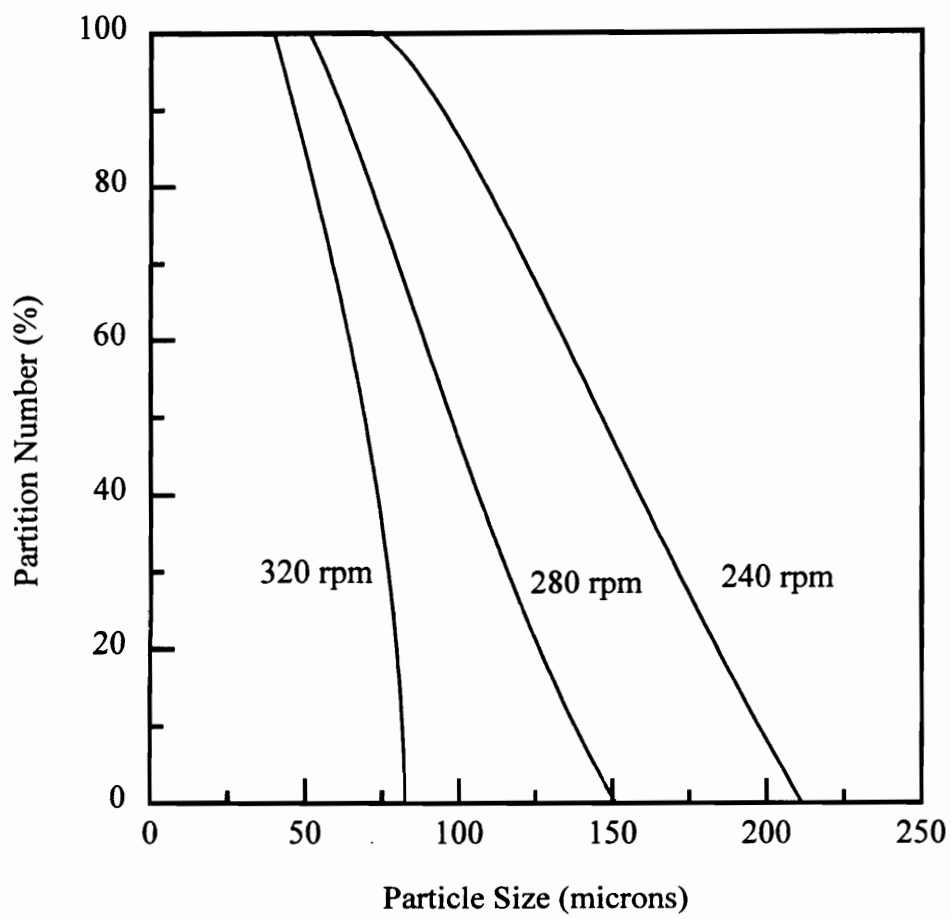


Figure 2.6. Effect of particle size on the performance of the MGS using liberated pyrite particles at different drum speeds.

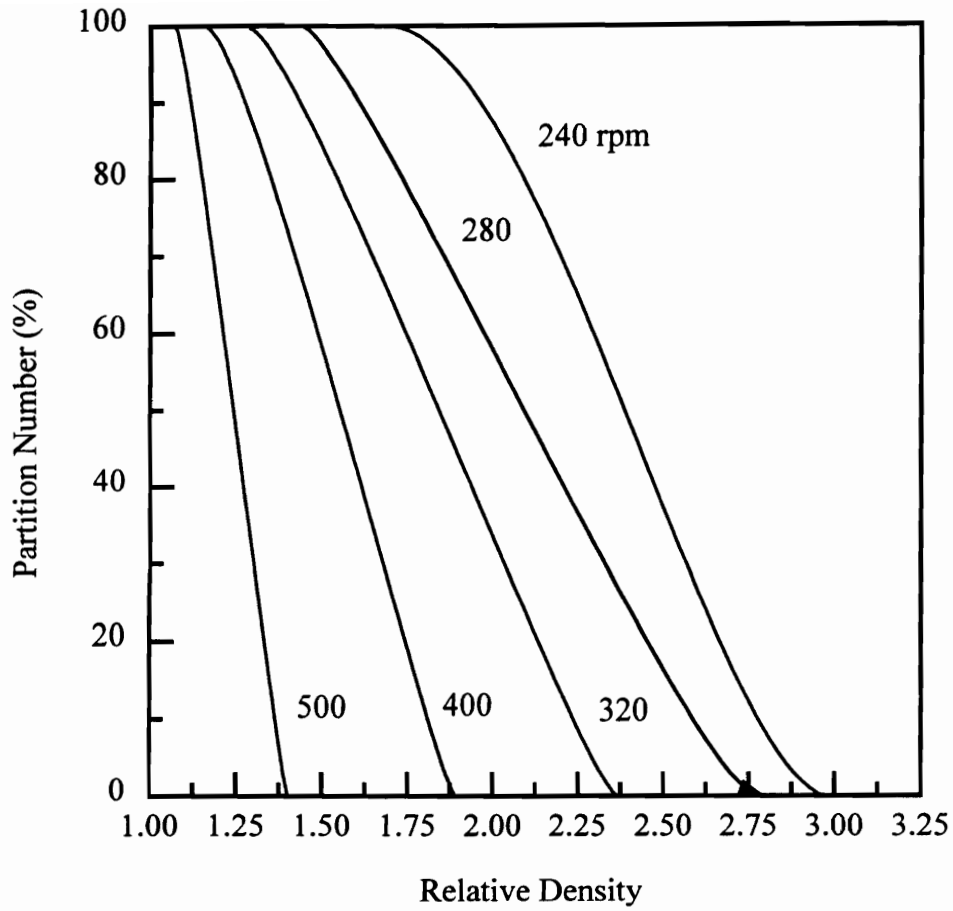


Figure 2.7. The effect of drum speed on the partition curves for the MGS.

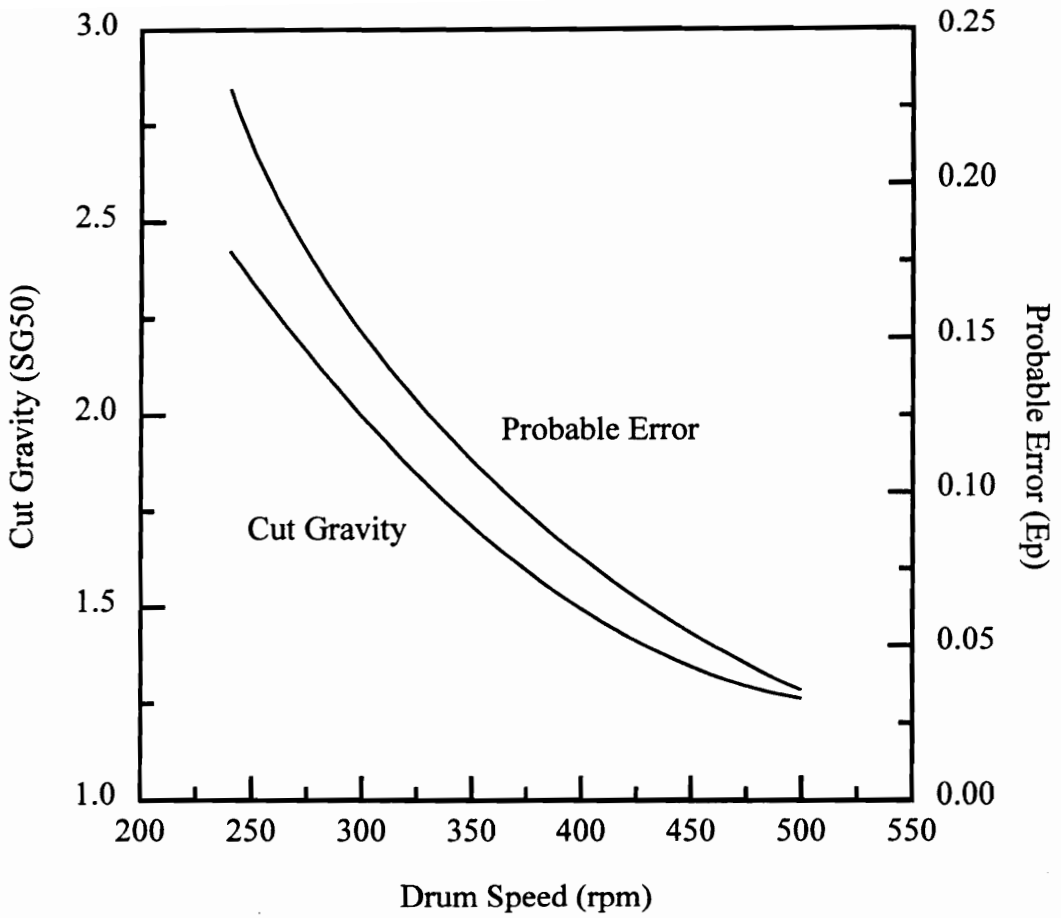


Figure 2.8. The effect of drum speed on the cut gravity and probable error in the MGS.

process.  $SG_{50}$  obtained from simulation ranges between 1.8 to 2.4 and  $E_p$  ranges between 0.12 and 0.25 as the drum speed decrease from 320 to 240 rpm. It has been reported in the literature [31] that, an  $E_p$  value of 0.20 to 0.25 is obtained on treating a similar feed material on a shaking table. Further, earlier research work has shown that increase in the percentage of -200 microns in the feed, deteriorates the performance of shaking table. This clearly indicates that increasing the g-force imparted by the rotation of drum in the MGS, increases the difference in the settling velocities between valuable and gangue minerals and also increases the inertial mass of the particles, thereby enabling it to treat finer size feed material.

#### 2.6.1.2 *Effect of particle size*

A great deal of interest has been shown lately to upgrade fine particle using gravity concentration techniques. In order to more closely examine the effect of particle size on MGS response, a series of model simulations was carried out as a function of particle size.

The simulated results shown in Figure 2.4 to 2.6, demonstrate that the separation efficiency is low at both coarser and finer size fractions. The best separation is obtained at intermediate size fraction (75 x 150 microns). These observations are in accordance with the literature available [13].

#### 2.6.1.3 *Effect of flow rate*

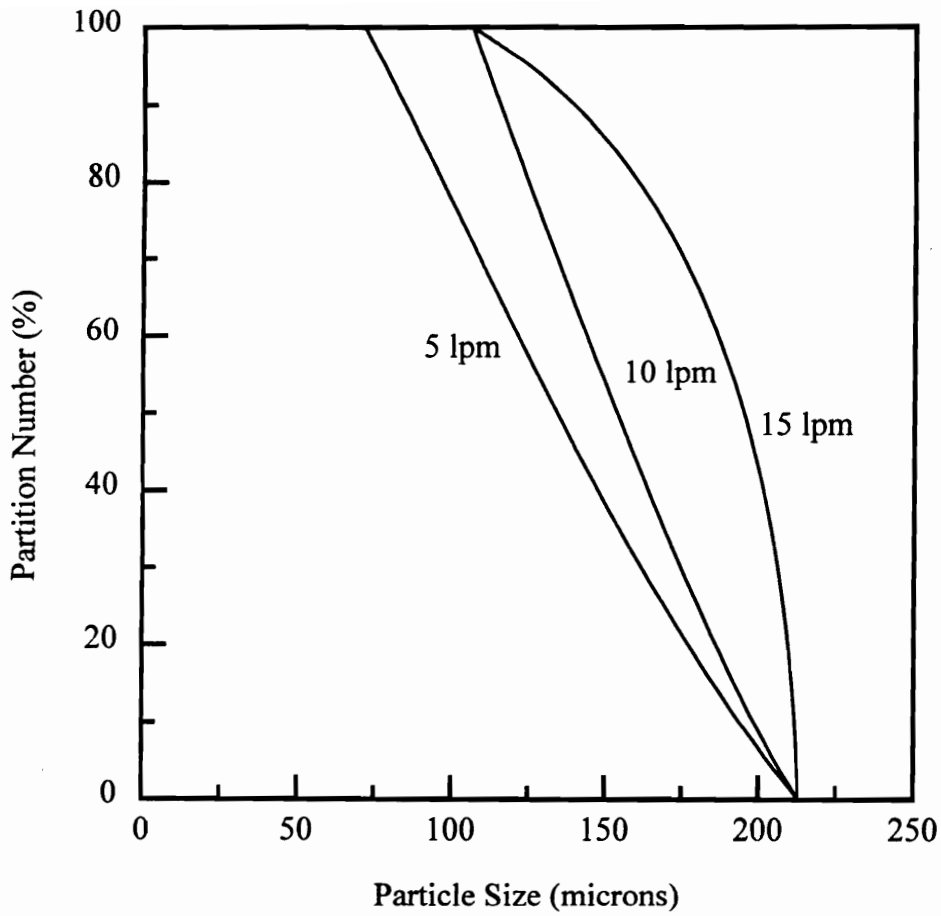


Figure 2.9. Effect of flow rate on the performance of the MGS using liberated coal particles at a drum speed of 320 rpm.

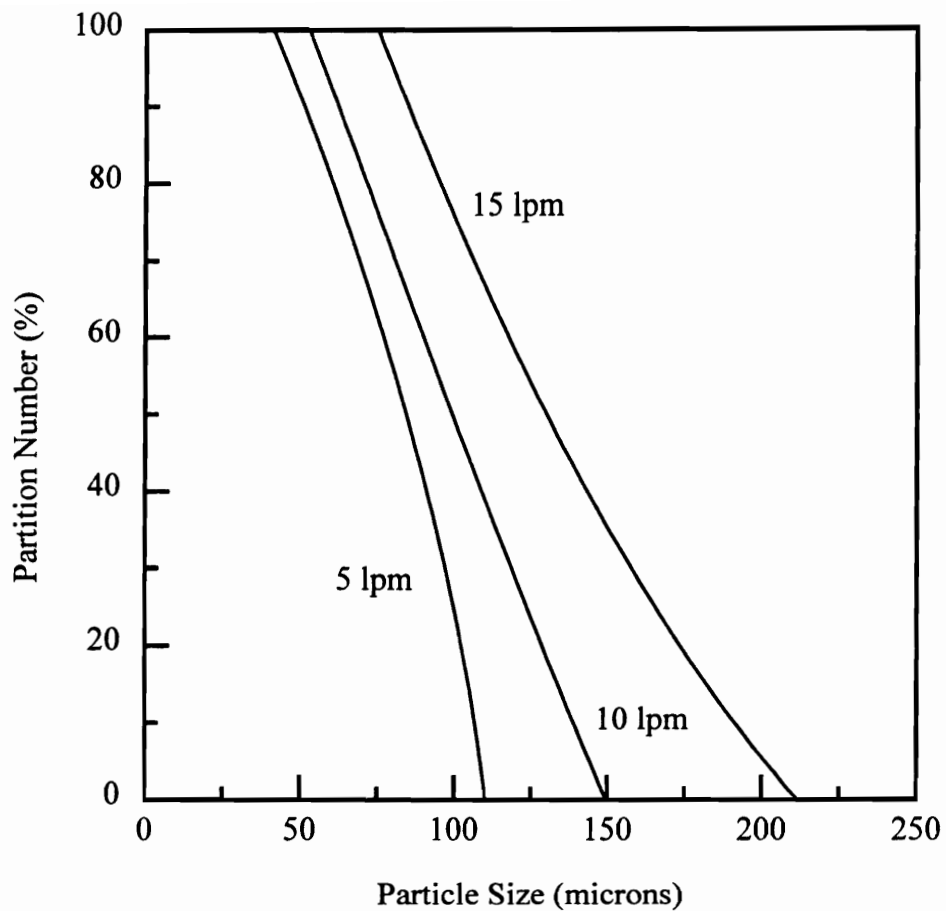


Figure 2.10. Effect of flow rate on the performance of the MGS using liberated ash particles at a drum speed of 320 rpm.



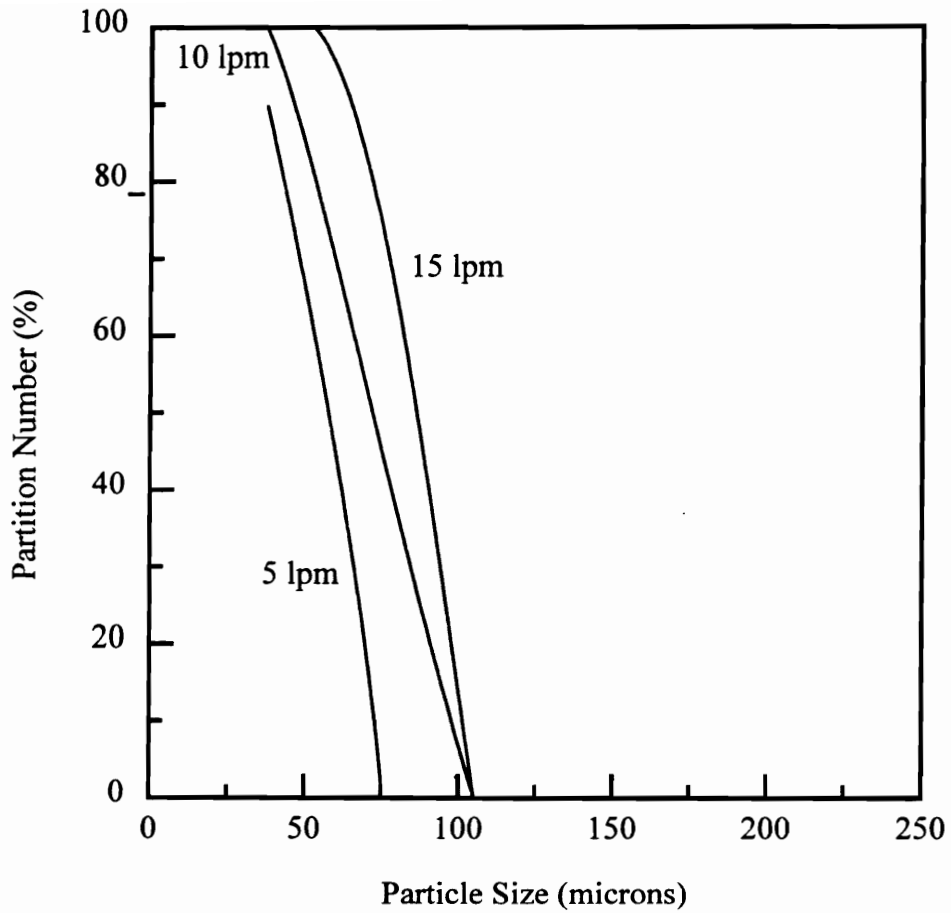


Figure 2.11. Effect of flow rate on the performance of the MGS using liberated pyrite particles at a drum speed of 320 rpm.

An increase in the flow rate for a given drum speed, increases the film thickness. Therefore, particles tend to stay in the high velocity region of the flowing film for a longer period of time, resulting in an increase in recovery to lights. As shown in Figures 2.9 to 2.11, the effect of change in the flow rate is more pronounced on less dense material, like, coal. Increase in flowrate increases the size of the particle reporting to lights. The drum speed and flowrate have complementary effect on the performance of the MGS. Therefore, it is crucial to operate MGS at a lower possible volume flow thereby increasing the retention time resulting in a better separation performance.

## 2.7 Summary and Conclusions

- a) A model based on first principles has been developed to explain the separation process taking place in the MGS. The model predictions were found to be in general agreement with the experimental results available in literature.
- b) Drum speed was found to be the most important process variable.
- c) Sharpness of separation was found to be highly dependent on drum speed. Theoretical model predicts that near perfect separation can be achieved at higher drum speed.
- d) Simulated optimum size range for the MGS was in agreement with the results published on the performance of Falcon concentrator.
- e) Performance of the MGS was found to be sensitive to changes in volumetric flow rate. Increase in volumetric flow rate resulted in an increase in recovery.

## 2.8 References

1. Yoon, R. H., Lagno, M. L., Luttrell, G. H., and Mielczarski, J. A., Proceedings, IV Int. Conf. on Proc. and Utilization of High Sulfur Coals, August, Idaho Falls, Idaho (1991).
2. Obald, H. B., SME-AIME Fall Meeting, October 16-18, Albuquerque, New Mexico (1985).
3. Paul, B. C., Honaker, R. Q., and Wang, D., Proceedings, High Efficiency Coal Preparation: An Int. Sym., SME, Littleton, Colorado (1995).
4. Adel, G. T., Wang, D., and Yoon, R. H., Proceedings of the VIII Int. Pittsburgh Coal Conference, October 14-18, Pittsburgh, Pennsylvania (1991).
5. Venkatraman, P., Luttrell, G. H., Yoon, R. H., Knoll, F. S., Kow, W. S., and Mankosa, M. J., Proceedings, High Efficiency Coal Preparation: An Int. Sym., SME, Littleton, Colorado (1995).
6. Chan, S. K., and Mozley, R. H., Sym. Minerals Engineering Viewpoint Southwest, Camborne, UK (1987).
7. Riley, D. M., and Firth, B. A., Proceedings, Coal Prep 93, X Int. Coal Prep. Exhibition and Conf., May 4-6, Lexington, Kentucky (1993).
8. Knelson, B., *Minerals Engineering*, **5**, 10-12, pp 1091-1097 (1992).

9. Laplante, A. R., and Shu, Y., XXIV Annual Meeting of the CMP, January Ottawa, Canada (1992).
10. Paul, B. C., and Honaker, R. Q., " Production of Illinois Base Compliance Coal using Enhanced Gravity Separation," *Final Technical Report*, Illinois Clean Coal Institute Project Number 93-1/5. 1B-1P (DOE Grant Number DE-FC22-92PC92521), September 1, 1993-August 31, 1994.
11. Patchejieff, B., Gaidarjiev., and Lazarov, D., *Minerals Engineering*, 7, 2-3, p. 405 (1994).
12. Yasar Ucbas., and Huseyin Ozdag., *Prog. in Min. Proc.,Technology*, (Eds. Demirel and Ersayin.) Balkema, Rotterdam (1994).
13. Traore, A., Conil, P., Houot, R., and Save, M., *Exposition on Industrial Minerals - Congress*, October 5-8., Grnoble, France (1993).
14. Wells, A., *Sym. Min. Proc. in the U.K.*, I.M.M., Leeds, UK (1989).
15. Turner, J. W. G., and Hallewell, M. P., *Minerals Engineering*, 6, 8-10, p. 817 (1993).
16. Tucker, P., Chan, S.K., Mozley, R.H., and Childs, G.J.C., *Les Techniques*, p. 45, December (1992).
17. Gaudin, A. M., *Principles of Mineral Dressing*, McGraw-Hill Book Company, New York (1939).
18. Taggart, A. F., *Handbook of Mineral Processing*, Wiley, New York (1945).

19. Kelly, E. G., and Spottiswood D. J., *Introduction to Mineral Processing*, Wiley-Interscience (1982).
20. Wang, W., Shu, H., and Jin, C., XVIII Int. Mineral Processing Cong., AusIMM, vol. 2, pp 361-368 (1993).
21. Ferrara, G., Preti, U., and Bevilacqua, P., XVIII Int. Mineral Processing Cong., AusIMM, vol. 2, pp 379-386 (1993).
22. Subasinghe, G. K. N. S., and Kelly, E. G., Control'84, pp. 87-95 (1984).
23. Sivamohan, R., and Forssberg, K. S. E., *Int. J.Mineral Processing* 15, p. 155 (1985).
24. Sivamohan, R., and Forssberg, K. S. E., *Int. J.Mineral Processing* 15, p. 281 (1985).
25. Sivamohan, R., and Forssberg, K. S. E., *Int. J.Mineral Processing* 15, p. 297 (1985).
26. Sivamohan, R., and Forssberg, K. S. E., *Production and Processing of fine Particles*, (Ed. Plumpton) pp. 387-396, CIMM (1988).
27. Sivamohan, R., and Forssberg, K. S. E., *Int. J.Mineral Processing* 28, p. 45 (1990).
28. Sivamohan, R., and Forssberg, K. S. E., *Scand. J. Metallurgy* 15 (1985).
29. Janna, W. S., *Introduction to Fluid Mechanics*, Second Edition, PWS Publishers, Boston, USA (1987).

30. White, C.M., *Proc. Roy. Soc. London, Series A*, **174** (1940).
31. Osborne, D. G., *Coal Preparation*, **2**, pp. 207-242 (1986).

## **CHAPTER 3 - EXPERIMENTAL SETUP AND PROCEDURE**

### **3.1 Introduction**

A novel fine coal-cleaning circuit was developed at the Center for Coal and Minerals Processing (CCMP). This two-stage circuit comprised of a froth flotation and an enhanced gravity separator. Preliminary results demonstrated the effectiveness of this circuit in rejecting ash forming minerals and pyrite from coal with minimal loss in recovery. Under the auspices of the U.S. Department of Energy (DOE), a bench-scale testing of the combined circuit comprising of Microcel column flotation and the Multi-Gravity Separator (MGS) was undertaken at the Coal Preparation Process Research Facility (CPPRF), Pittsburgh Energy Technology Center (PETC), Pittsburgh Pennsylvania (“Bench-scale testing of the Multi-Gravity Separator in combination with Microcel”, U.S. DOE Contract No.: DE-AC22-92PC92205).

CCMP served as the prime contractor of this project and had the overall responsibility of designing, testing and evaluating this proposed circuit. The other participants in this project were Roberts and Schaefer Company responsible for engineering design and installation of this circuit, Carpco Inc. provided technical assistance for the MGS circuit throughout this study and Consol and Kerr-McGee Coal



companies provided raw coal samples and miscellaneous technical services as required to evaluate the proposed circuit.

The primary goal of this chapter was to analyze feed sample characteristics, describe the process flowsheet and to develop a detailed test plan. A variety of laboratory characterization studies were undertaken in order to evaluate the potential cleanability of the base coal samples used in the present work, i.e., Pittsburgh No. 8 and Illinois No. 6 coal seams. Description of the process flowsheet included feed preparation, process design, circuit layout and instrumentation. A commercially available experimental design software was used to develop a detailed test plan.

## 3.2 Coal Sample Characterization

A representative 200 kg sample of each of the two coals (Pittsburgh No.8 and Illinois No.6) was collected and shipped to Virginia Tech. Upon receipt, each sample was split into eight 25-kg samples and stored in an inert atmosphere (i.e., nitrogen purge). A preliminary characterization was carried out to evaluate the overall quality of each run-of mine sample. Large pieces of coal were first hand crushed to approximately 1/2" inches and then, along with the rest of the coal, were fed to a jaw crusher and roll crusher to produce -1/4 inch particles. The crushed coals were subdivided into representative 1-kg samples and stored in a freezer to minimize oxidation.

Sample characterization included liberation studies, release analysis, washability analysis and image analysis. To determine the effects of liberation, each sample was dry pulverized using a 15 cm x 5 cm laboratory hammermill to produce two different size distributions, i.e., 28 mesh x 0 and 65 mesh x 0. In order to produce the -200 mesh sample, the crusher product was dry pulverized to -65 mesh and wet ground in a 25 cm laboratory rod mill. The rod mill was selected as opposed to a ball mill in order to minimize the production of fines.

### 3.2.1 Size Distribution

The ground coal samples were wet screened, weighed and subjected to ash and sulfur analyses. The particle size distributions and size-by-size analyses are summarized in Tables 3.1 and 3.2. The preliminary results indicate that a relatively large proportion of fines were generated by the grinding process, i.e., the proposed grinding scheme generated higher percentages of -400 mesh particles. At the 65 mesh grind, more than half of the Illinois No. 6 coal and over one-third of the Pittsburgh No. 8 was found to be finer than 400 mesh. The high production of fines is typical of an impact-type crusher, such as hammer mill. The characterization data also indicate that the Illinois No. 6 seam coal has significantly higher ash and sulfur contents than the Pittsburgh No. 8 seam coal (i.e., 45% ash and 4.6% sulfur versus 18% ash and 3.6% sulfur). For both coals, the finer size fractions tended to yield lower ash and sulfur values than did the coarser fractions. The only exception to this trend was observed for the finest size fraction, i.e., 400 mesh x 0. In this case, the higher ash content can be largely attributed to the selective grinding of ash over coal, resulting in a disproportionate amount of high-ash clay particles in the ultrafine size range.

### 3.2.2 Washability Characterization

Washability studies were conducted to estimate the degree of liberation and also as a “yardstick” against which the performance of the density-based separator (i.e., MGS) could be evaluated. The initial fine-coal washability tests were conducted using a

**Table 3.1**  
**Size-by-size ash and sulfur contents for the**  
**Pittsburgh No. 8 Seam Coal.**

Size fraction (mesh)	Individual			Cumulative		
	Wt. (%)	Ash (%)	Sulfur (%)	Wt. (%)	Ash (%)	Sulfur (%)
+28	0.00	0.00	0.00	0.00	0.00	0.00
28x35	28.06	29.71	3.64	28.06	29.71	3.64
35x48	19.17	14.07	3.47	47.23	23.36	3.57
48x65	14.34	13.33	4.13	61.57	21.03	3.70
65x100	9.91	14.10	4.07	71.48	20.07	3.75
100x150	9.09	13.93	4.03	80.57	19.37	3.78
150x200	5.25	8.99	3.52	85.82	18.74	3.77
200x270	3.85	13.73	4.96	89.67	18.52	3.82
270x400	2.71	12.93	4.40	92.38	18.36	3.84
-400	7.62	21.78	3.55	100.00	18.62	3.81

**Table 3.2****Size-by-size ash and sulfur contents for the Illinois No. 6 Seam Coal.**

Size fraction (mesh)	Individual			Cumulative		
	Wt. (%)	Ash (%)	Sulfur (%)	Wt. (%)	Ash (%)	Sulfur (%)
+28	0.71	51.72	3.25	0.71	51.72	3.25
28x35	4.91	44.70	4.91	5.62	45.59	4.70
35x48	6.16	46.75	4.00	11.78	46.20	4.33
48x65	11.64	46.50	5.77	23.42	46.35	5.05
65x100	8.18	33.79	4.36	31.60	43.10	4.87
100x150	11.02	33.88	5.01	42.62	40.71	4.91
150x200	8.62	30.64	4.85	51.24	39.02	4.90
200x270	5.62	33.20	5.75	56.86	38.44	4.98
270x400	8.24	32.80	5.84	65.10	37.73	5.09
-400	34.90	56.53	3.48	100.00	44.29	4.53

Sharples high-G centrifuge. Aqueous solutions of zinc chloride were prepared to provide a wide range of heavy liquids for the float-sink tests. Zinc chloride solutions were selected over traditional organic heavy liquids because of lower costs and reduced health risks. In each test, a small amount of fine coal was suspended in the lowest SG zinc chloride solution and passed through the centrifuge. The light fraction was collected throughout the test period, while the heavy fraction was retained inside the bowl and collected after stopping the centrifuge. The heavy fraction was resuspended in the next highest SG solution and again passed through the centrifuge. This procedure was repeated until the desired range of float-sink products were collected for each coal.

### 3.2.3 Image Analysis Characterization

Unfortunately, the fine-coal washability procedure employed in the present work proved to be unreliable. In fact, the results obtained using this procedure yielded a separation curve inferior to that obtained by flotation release analysis. This finding was considered to be highly unlikely (if not impossible), particularly for the rejection of pyritic sulfur. The main reason for this poor performance is attributed to the poor dispersion of the ultrafine-coal particles suspended in the zinc chloride solutions. Although the use of chemical dispersants appeared to improve the float-sink procedure, the data was not believed to be completely trustworthy.

For these reasons described above, the fine-coal centrifugal washability work was discontinued and an image analysis technique using a Scanning Electron Microscope Image Processing System (SEM-IPS) was employed to characterize the coal liberation. The SEM-IPS provided a particle composition analysis by area resulting in the percent of carbonaceous material, mineral matter and pyrite. An equivalent of washability by density was then calculated [1]. This technique is believed to be the most reliable method for determining fine-coal washability since it provides a direct measure of the various components contained in the coal sample and is not subject to problems related to particle dispersion.

Results of the SEM-IPS characterization tests conducted on the Pittsburgh No. 8 and Illinois No. 6 coal seams are presented in Figures 3.1-3.4. Because of the relatively high cost of the SEM-IPS work, only the 28 mesh x 0 grind was examined for each coal. In general, the image analysis data indicate that very high rejections of mineral matter and pyritic sulfur could be obtained for each of the two base coal samples. For the Illinois No. 6 seam coal, mineral matter and pyrite rejections of approximately 85-90% could be achieved while maintaining coal recoveries approaching 90%. Similar rejections in mineral matter and pyritic sulfur could also be obtained for the Pittsburgh No. 8 seam coal.

The image analysis characterization data indicate that most of the pyrite which can be liberated is freed from the coal matrix at a relatively coarse size. This

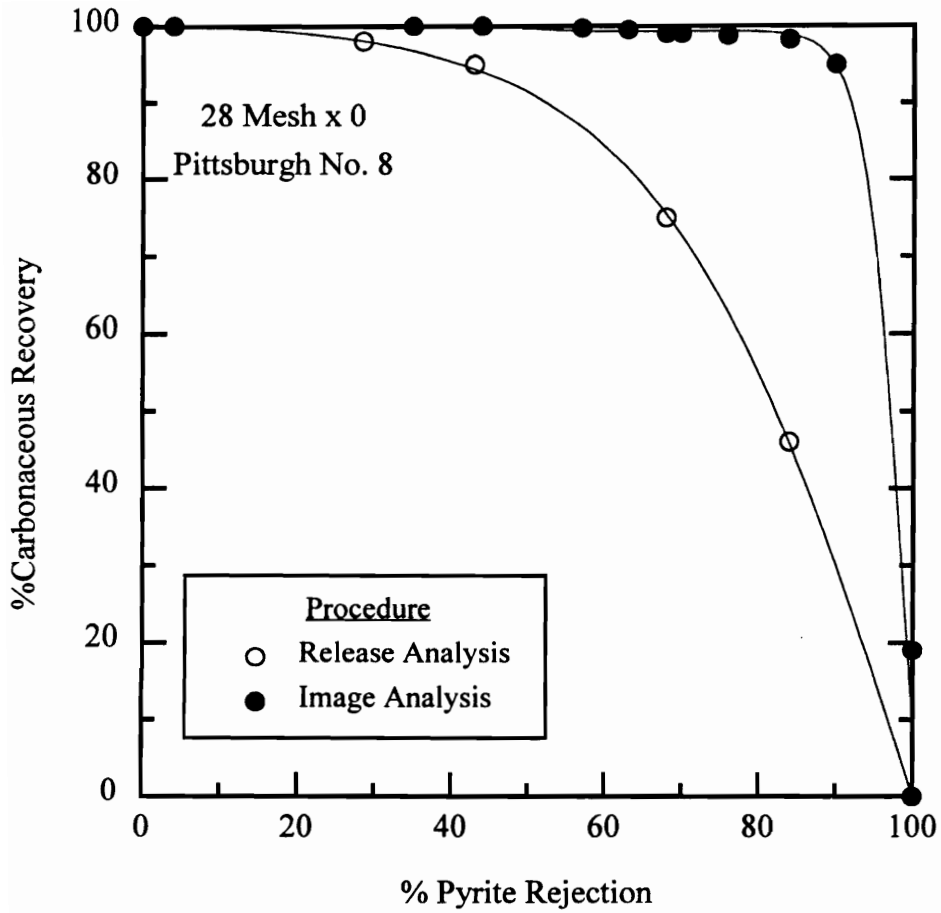


Figure 3.1. Comparison of release analysis and image analysis separation curves for pyrite obtained using a -28 mesh Pittsburgh No. 8 coal.



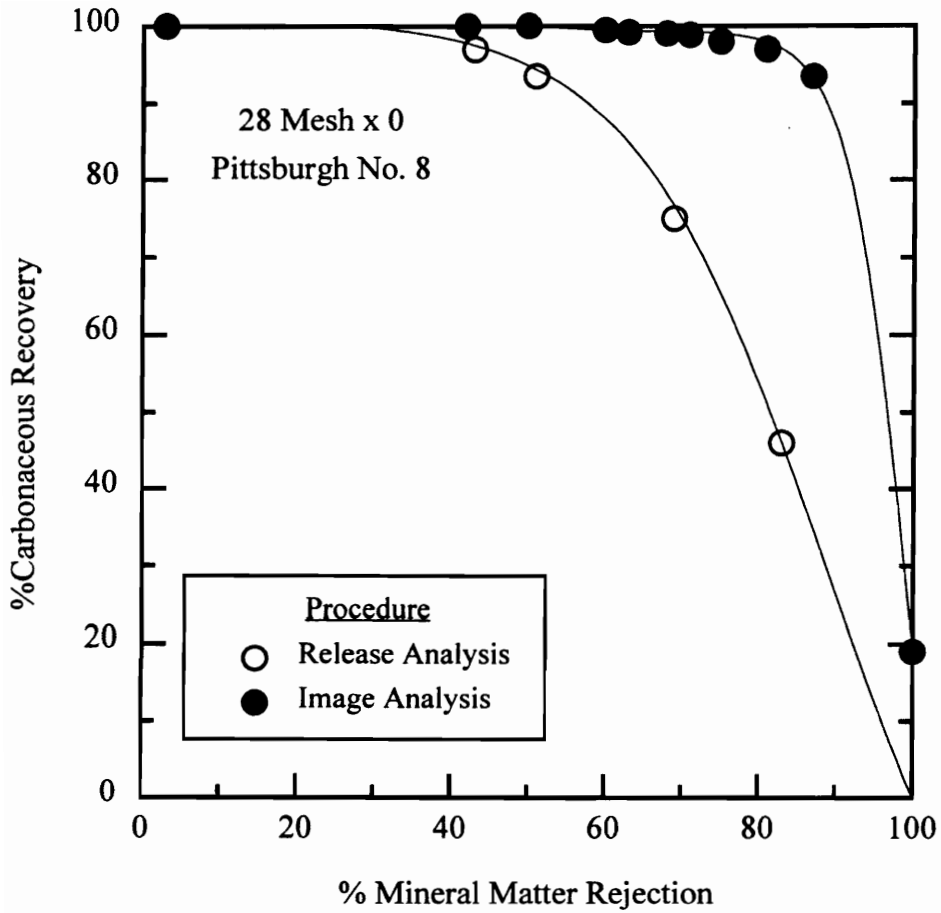


Figure 3.2. Comparison of release analysis and image analysis separation curves for mineral matter obtained using a -28 mesh Pittsburgh No. 8 coal.

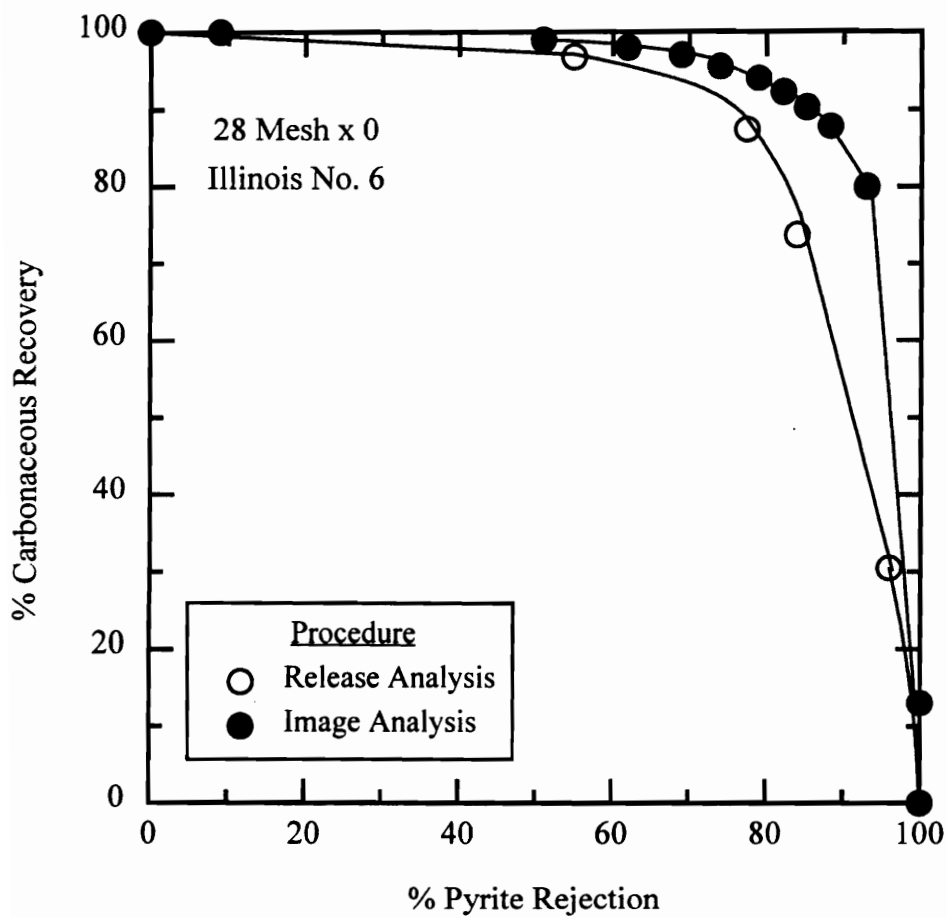


Figure 3.3. Comparison of release analysis and image analysis separation curves for pyrite obtained using a -28 mesh Illinois No. 6 coal.

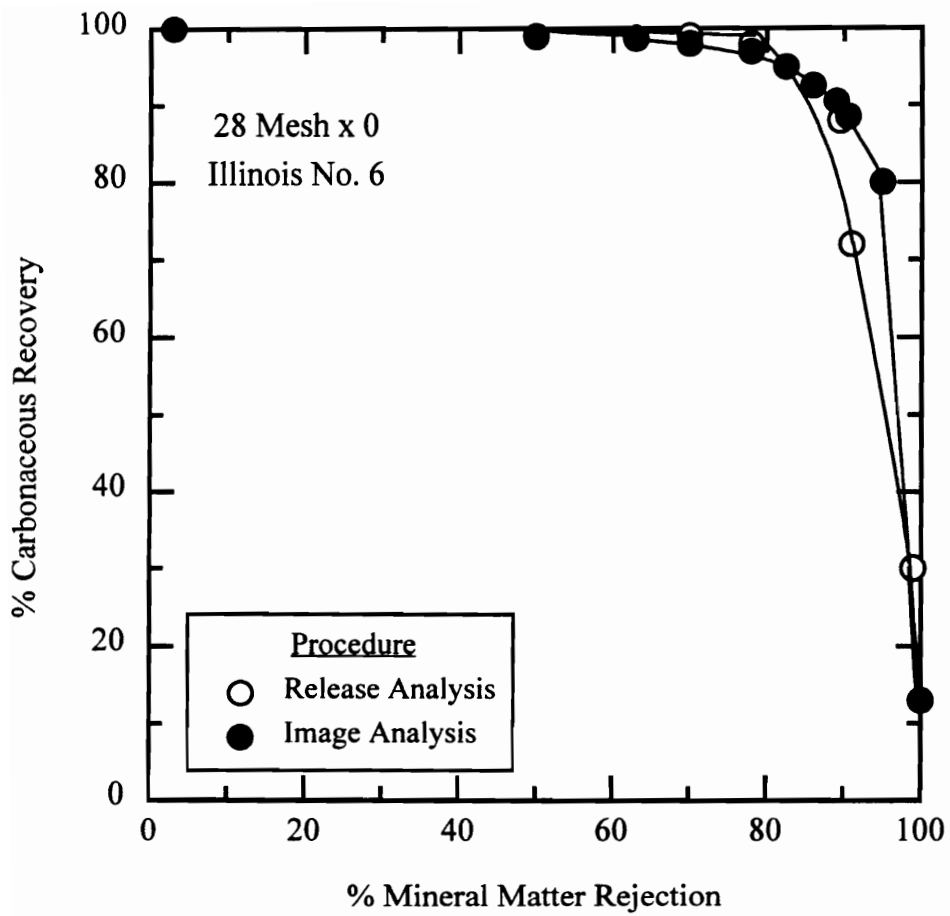


Figure 3.4. Comparison of release analysis and image analysis separation curves for mineral matter obtained using a -28 mesh Illinois No. 6 coal.

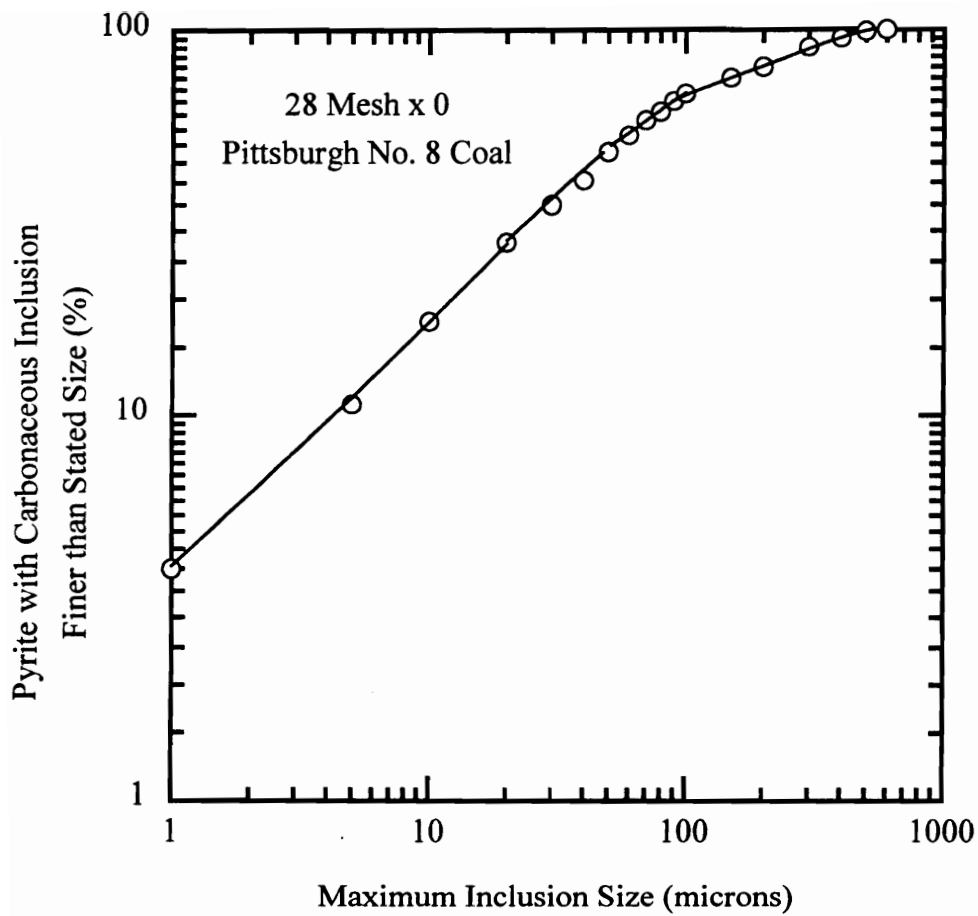


Figure 3.5. Weight percent pyrite containing carbonaceous inclusions finer than a given size obtained using a -28 mesh Pittsburgh No. 8 seam coal.

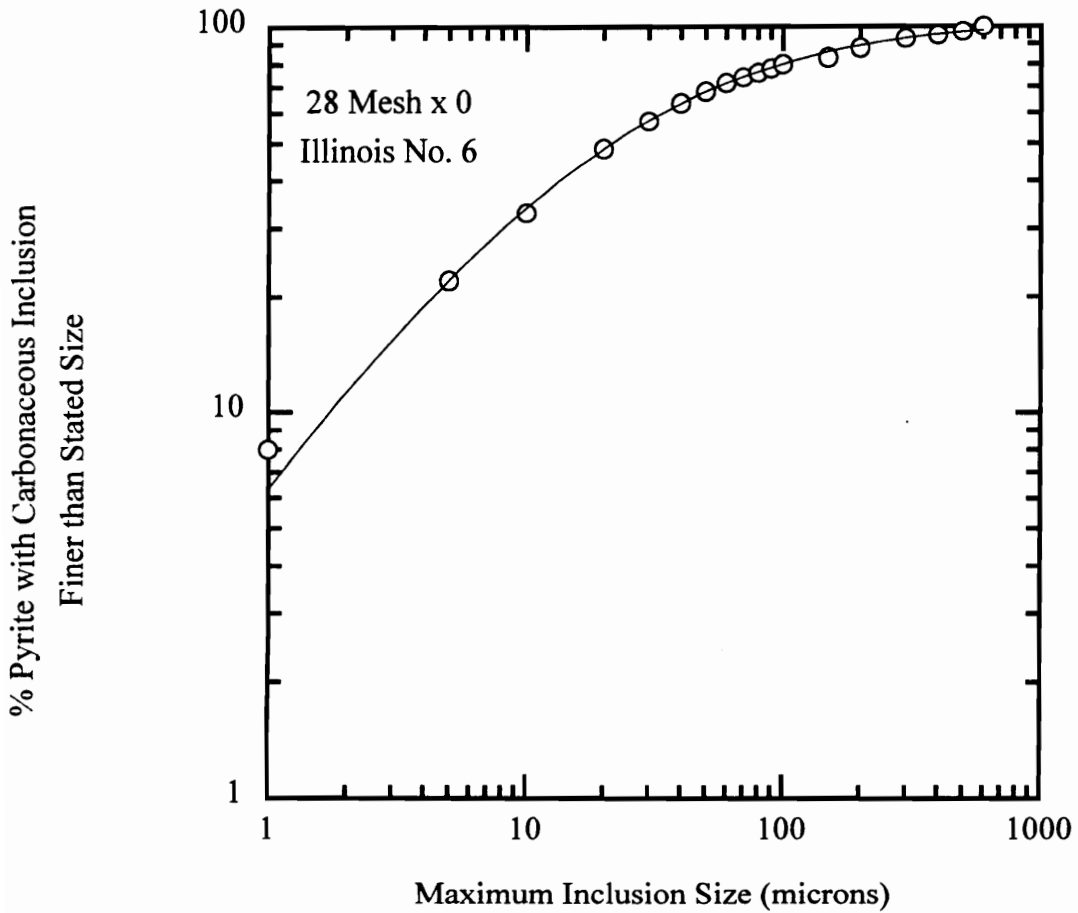


Figure 3.6. Weight percent pyrite containing carbonaceous inclusions finer than a given size obtained using a -28 mesh Illinois No. 6 coal.

phenomenon is illustrated in Figures 3.5 and 3.6, which show the weight percent of pyrite containing carbonaceous inclusions finer than a specified size for each of the two base coals. For the Illinois No. 6 seam coal, only about 30% of the pyrite contains coal inclusions smaller than 10 microns. This value falls to approximately 20% for the Pittsburgh No. 8 seam coal. The data suggest that much of the pyrite which remains locked with the coal is very finely disseminated and cannot be completely liberated even at a 400 mesh x 0 grind size.

#### 3.2.4 Release Analysis Characterization

The release analysis technique is believed to provide the optimum separation curve for a surface-based separation process such as flotation. In the present work, release analysis data provided a means by which the performance of the Microcel column could be evaluated. A Denver D-12 conventional flotation machine was used to conduct the release analysis tests. Tests were carried out on three different grind sizes using Pittsburgh No. 8 and Illinois No. 6 seam coals. Replicate tests were conducted in each case to determine the reliability of the release analysis test procedures. All products were analyzed for ash, total sulfur, pyritic sulfur and heating value.

Figures 3.7 and 3.8 shows the results of release analysis tests conducted on Pittsburgh No. 8 seam coal as a function of grind size (i.e., -28 -65 and -200 mesh). As expected, an increase in ash rejection is observed with a reduction in particle size,

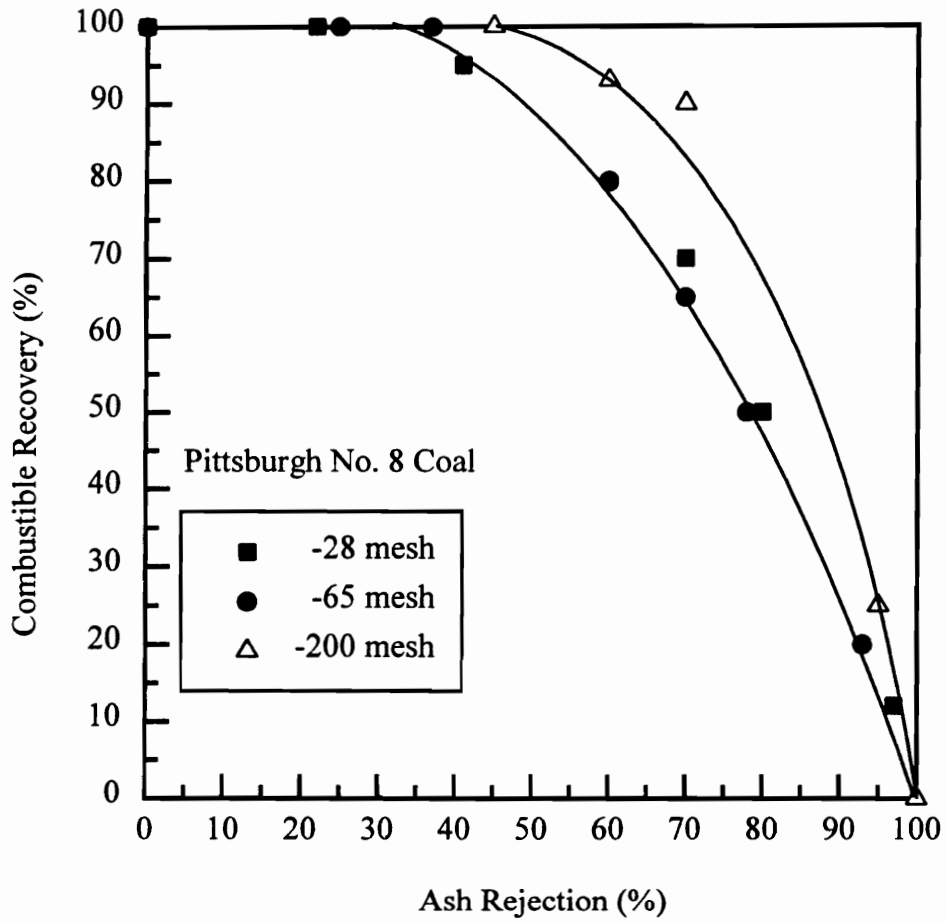


Figure 3.7. The effect of grind size on the ash release curve obtained from run-of-mine Pittsburgh No. 8 seam coal.

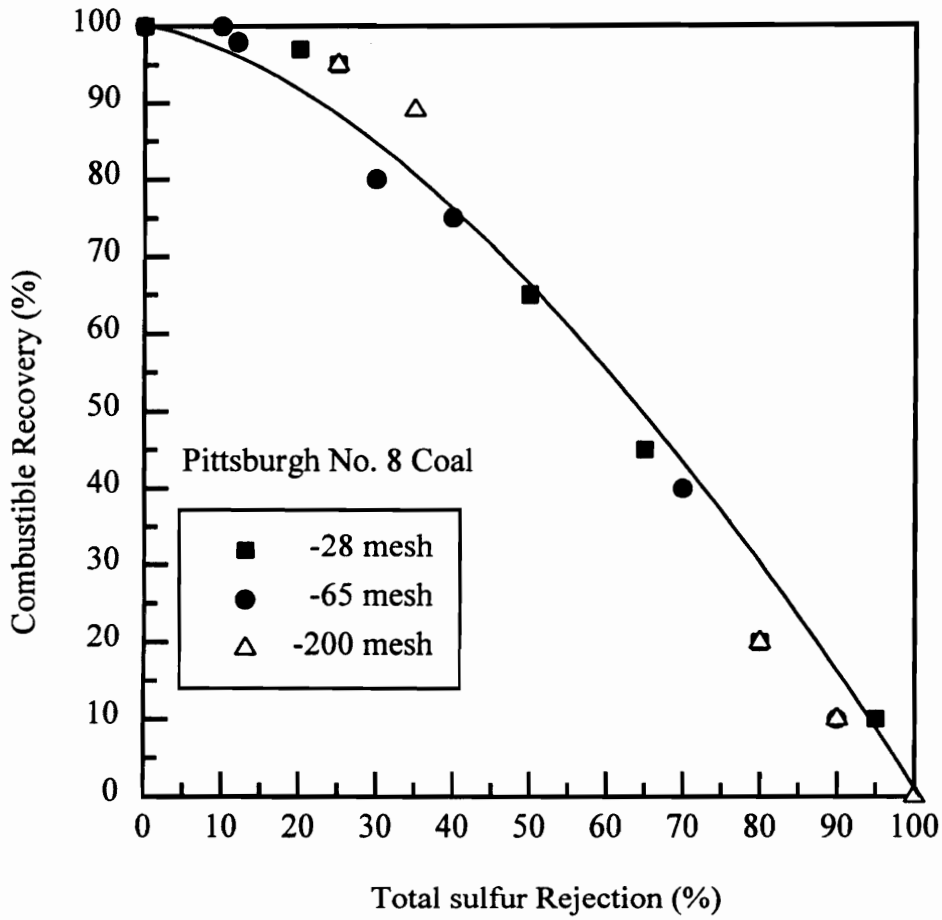


Figure 3.8. The effect of grind size on the sulfur release curve obtained from run-of-mine Pittsburgh No. 8 seam coal.



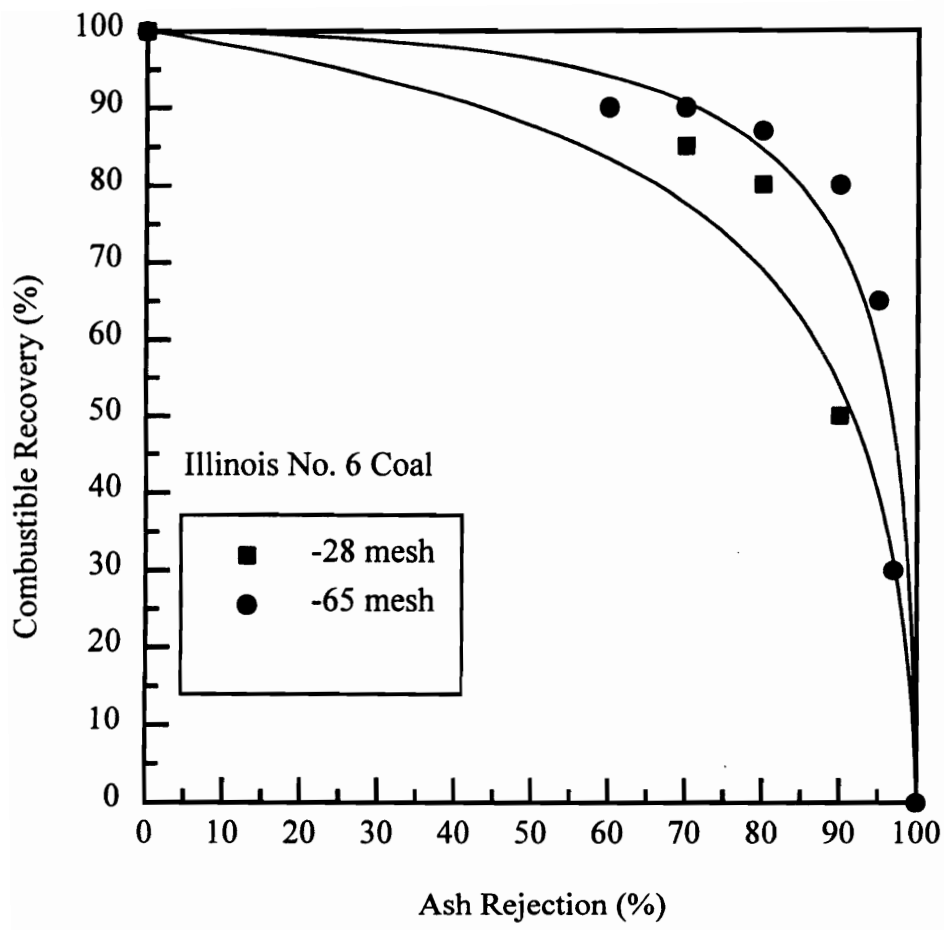


Figure 3.9. The effect of grind size on the ash release curve obtained from run-of-mine Illinois No. 6 seam coal.

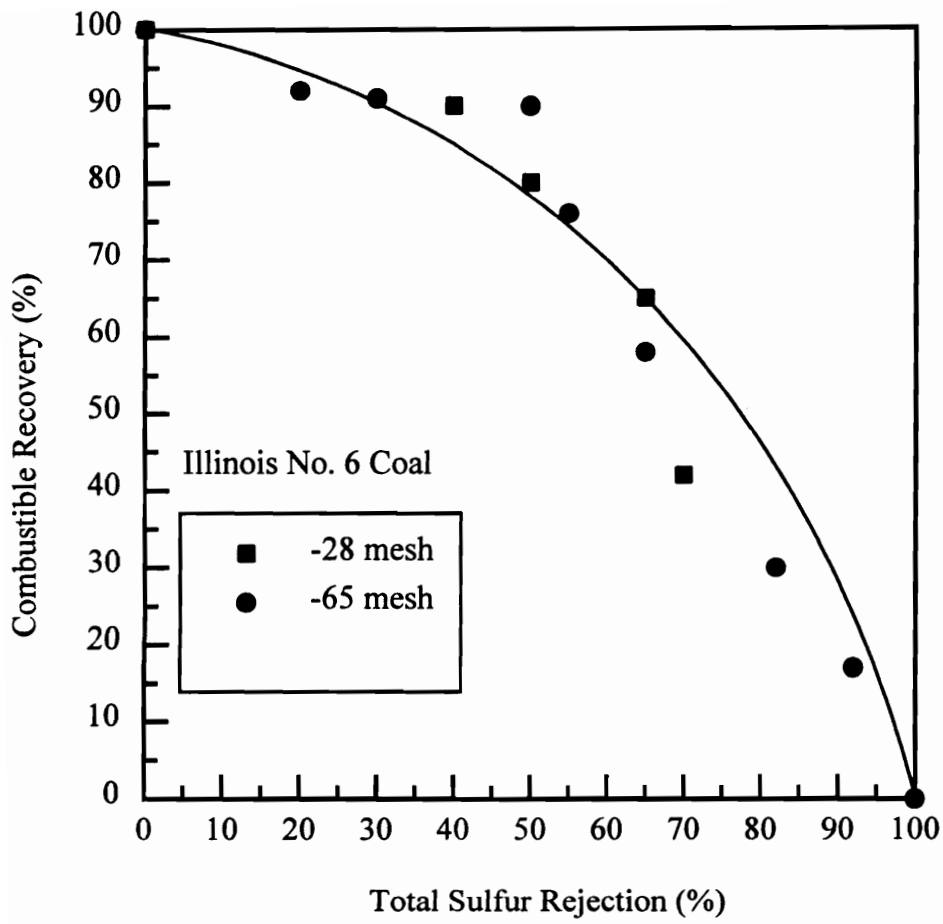


Figure 3.10. The effect of grind size on the sulfur release curve obtained from run-of-mine Illinois No. 6 seam coal.

although essentially no improvement was observed in sulfur rejection. This finding can be explained by either inadequate liberation of pyritic sulfur or the natural flotability of coal pyrite.

Figures 3.9 and 3.10 show similar results for release analysis tests conducted on Illinois No. 6 seam coal. As shown, ash rejection achieved using this coal improves with a decrease in the particle size. Furthermore, the particle size does not seem to have any significant impact on the total sulfur rejection. These findings support the conclusion that a flotation-based separation process is acceptable for the rejection of ash-bearing minerals, but is less effective for the sulfur removal. As previously stated, a density-based separation would be more effective for the rejection of pyritic sulfur due to the large difference in specific gravities of coal and pyrite.

### **3.3 Experimental Setup**

The test circuit was installed at the CPPRF, PETC in Pittsburgh, Pennsylvania. This facility is ideally suited for pilot-scale test work due to the availability of all ancillary operations for bulk solids handling, feed preparation and waste disposal.

#### **3.3.1 Preparation of Feed**

Two different coal samples (Pittsburgh No. 8 and Illinois No. 6) were used for parametric testing in the various circuit. About 75 tons of representative sample from each of the two coals was collected and stored in a nearby storage facility until required. A front-end loader was then used to thoroughly mix the samples by coning and then stored in a pile of approximately one-ton each. This material was transferred by truck in 5-ton increments and off-loaded to the coarse coal storage bins at the CPPRF. The coal from the silos are crushed to predetermined grind size using a hammermill. The crushed product from the CPPRF comminution circuit is transferred to mix tank to produce a coal slurry of desired percent solid. This feed slurry is then transported to the test circuit at a desired flow rate.

#### **3.3.2 Flowsheet Design**

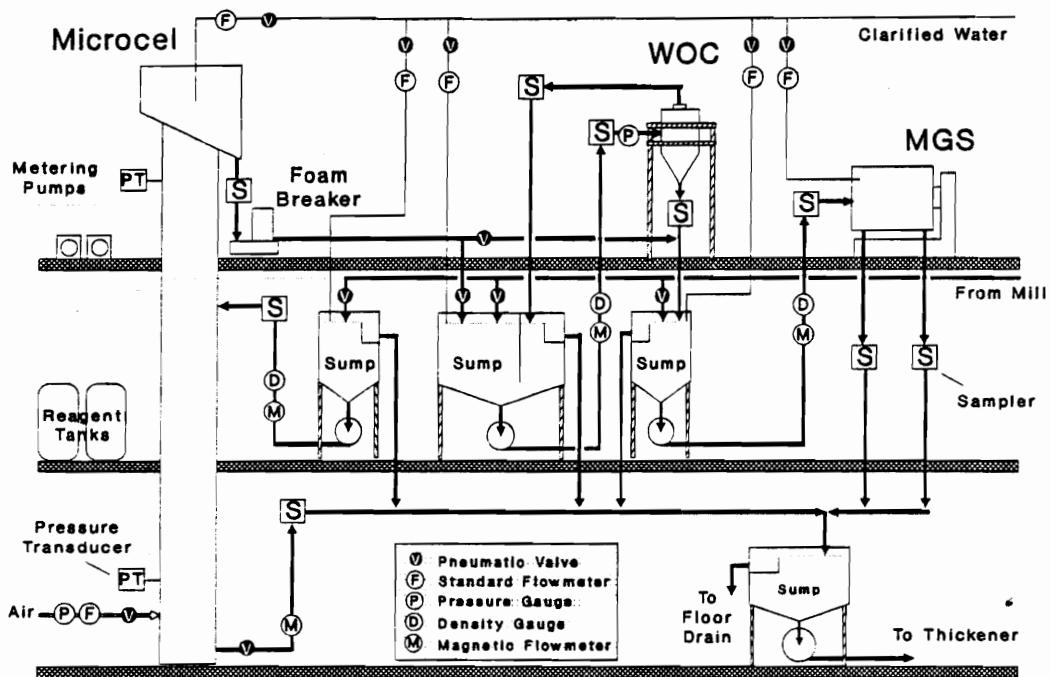


Figure 3.11 Flow diagram for the testing of the Microcel, MGS, Microcel/MGS and Microcel/WOC/MGS circuits.

A schematic of the test circuit used in the present work is shown in Figure 3.11. Equipment was selected based on a maximum capacity 500 lb/hr. As can be seen from the flowsheet, the feed slurry at a desired percent solids and flowrate enters the test circuit through a three-way automatic valve located above the CPPRF sludge tank. The automatic valve was configured to either send feed slurry to the emerging technology (ET) circuit, or by-pass it into the sludge storage tank.

The ET circuit was designed to allow for testing of a Microcel™ flotation column, Multi-Gravity Separator (MGS). The following circuit configurations were evaluated:

- Microcel only,
- Multi-Gravity Separator only, and
- Microcel/MGS in combination.

The Microcel and MGS circuits were designed to allow for independent operation of each unit. This allows a direct comparison of the performance of each device to be obtained. The Microcel/MGS circuit was used to determine the advantages of the combined processing scheme. In this circuit, the flotation product from the Microcel is de-aerated and fed directly to the MGS

The important feature of the ET circuit is its capability to independently operate the three main unit operations (i.e., Microcel and MGS ). This feature is accomplished by providing each of the unit operations with a dedicated feed sump. This feature allows each device to be evaluated without being influenced by the performance of other unit

operations. All the sumps were designed with a dish shaped bottom and were provided with side-mounted mixers to ensure that the solids would remain in a homogenous suspension.

Each process sump was provided with a variable speed (split-sheaves) pump to allow for variations in pressure and flow in each test circuit. To ensure that representative samples were obtained, each sump was provided with a slurry recirculation line. At the beginning of the test, the slurry was recirculated at relatively high velocity which helped in keeping the solids in suspension. Feed for each unit operation was bled-off the respective recirculation line through a pinch valve. The slurry density and flow rate were measured using mass flow sensors. Dilution water lines were provided in each feed sump to control percent solids. The flow rate of dilution water were controlled by pneumatic pinch valves.

Each sump/pump combination was equipped with a drain line and a constant head overflow box. These lines were directed to the ET waste sump located on ground floor. Also, a flush water line was provided on either side of the suction valve on each of the pumps. At the beginning and the end of the day, the discharge lines were flushed with fresh water, thereby keeping the pump and the discharge line free. In addition, the product and reject streams from all test circuits were discharged to the ET waste sump. Slurry from the waste sump was pumped either to the CPPRF thickener feed deaeration tank or to the sludge tank. Emergency overflow lines from the waste sump were directed

to the CPPRF's existing ground floor trenches and sent to the thickener via ground floor sump pumps.

### 3.3.3 Circuit Layout

All the process sumps were located on the ground-floor level. The base of the 20-inch column was located on the ground-floor, while the feed and the froth launders were located on the second floor. The MGS unit was also located on the second floor. The control panel and all of the reagent sumps/pumps for the flotation cell were also located on the second floor. The uniqueness of this layout was that the whole circuit was capable of being operated and monitored from the second floor.

### 3.3.4 Piping

The DOE/PETC facility provided tie-in points for the slurry, water and air lines. Since the test work was to be completed in a period of six months, schedule 80 PVC pipes were used for the slurry (instead of HDPE) and water lines. Schedule 40 steel pipes were used for the pneumatic lines. All the incoming utility lines were provided with manual shut-off valves at the tie-in points, which helped in isolating the test circuit, if necessary.

### 3.3.5 Instrumentation



A complete instrumentation package was designed and installed in order to obtain representative measurements of all process variables associated with the test circuit performance. This included gamma-nuclear density gauges on the Microcel and MGS feed sumps. The density gauge on the flotation feed line was coupled with magnetic flow meters to obtain the mass flow rates. Paddle wheel flow meters were installed on all the water addition system.

Two control loops were used to stabilize the performance of the circuit. In the first loop, a pressure reading provided by a differential pressure cell was used to control the column tailings discharge rate which, in turn, was regulated by a pneumatic pinch valve. Valve response was controlled by a stand-alone PID controller. The fractional air hold-up was determined from differential pressure measurements in the column collection zone. The second stabilizing loop was used to prevent the waste sump from overflowing or running the pump in dry condition. This was accomplished by providing the sump with a Hi/Lo sump level controller.

Several different types of remote sensors were used in the ET test circuit. A brief description of these sensors are provided in the following paragraphs.

**Density Gauges:** The Texas Nuclear E-Zcal density system was selected for density determination in the pilot plant. In this system, the coal slurry was passed through a Z-section of piping which was located between a cesium 137 and the scintillation detector head. The unit measures the bulk density of the process by passing a beam of

radiation through the material to the detector. As the density increases, the detected radiation decreases. The system automatically converts the measured radiation into a material density [2].

**Magnetic Flow Meters:** Fischer-Porter magnetic flow meters were used to measure slurry flow rates. The operation of the meter is based on Faraday's Law of Induction, which states that when a conductor is moving in a magnetic field, a voltage is induced. This voltage is proportional to the velocity of the fluid passing through the pipe [3].

**Paddle Wheel Flowmeters:** Kobold Instruments paddle wheel flowmeters were used to monitor water flow rates throughout the plant. These sensors contain small magnets in each of four paddles attached to a central rotor. As the paddle rotates, the magnets pass a coil in the sensor. The transducer generates a linear frequency output that is proportional to flow output. The operating ranges are 0.02 to 58 gpm [4].

**Control Valve:** A Red-Valve Series 5200 pneumatic control valve was used for tailings discharge control. This valve is air-to-open type of valve, where the valve actuator position is determined from a pneumatic control signal generated by a current to pressure transducer as result of a 4-20 mA input from the PID controller [5].

### 3.4 Test Plan

Prior to starting the experiments, a complete shake-down of the test circuit was completed, after which exploratory tests were conducted. During this period, density gauge and flow meters were calibrated, the PID loop in the flotation circuit was tested and finally, the integrity of the complete circuit was tested. As a part of the exploratory testing, samples were collected for a period of over one-hour, at an interval of 10-15 minutes, to determine the time taken for each of the unit operations to attain a steady-state condition. It was found that the Microcel and MGS takes about 30-45 minutes of uninterrupted operation (i.e., 2-3 slurry retention times). Detailed testing was initiated after the successful completion of the exploratory testing and calibration

The primary objective of the detailed test program was to investigate the effects of various parameters on the performance of the Microcel, MGS, combined Microcel/MGS and combined Microcel/MGS circuits. Statistically designed sets of experiments were used throughout the detailed testing program. The emphasis of the parametric testing was to characterize and optimize the performance of the MGS unit both with and without the precleaning operations (i.e., Microcel column). The numbering system used for the detailed testing program is given in Table 3.3.

**Table 3.3**

**Numbering system used for the detailed testing program.**

TEST NUMBER RANGES	CIRCUIT	COAL SEAM
201-299	MGS only	Pittsburgh #8
301-399	Microcel Conc. to MGS	Pittsburgh #8
PITT-LD	Microcel Conc. to MGS	Pittsburgh #8
501-599	MGS only	Illinois #6
601-699	Microcel Conc. to MGS	Illinois #6
ILL-LD	Microcel Conc. to MGS	Illinois #6

### 3.5 Sampling Procedure

A standard sampling procedure was followed in all tests. Once the system attained steady-state, simultaneous samples of all the product streams were collected for a predetermined time period. Feed samples were collected after the product samples, so as not to disturb the process. On completion of each test, the feed and product samples were weighed, filtered, dried and the mass of solids determined. From this, percent solids were determined. It was found that the percent solids of the feed stream were close to the density gauge display in all cases.

The dried samples were split into representative lots and subjected to several laboratory analyses, i.e., ash, total sulfur and pyritic sulfur. Earlier work showed that a good correlation existed between ash content and heating value for the two selected coals. Therefore, heating values were determined on selected samples and correlated with ash using regression analysis. This expression was used to calculate heating values from the measured ash values. On selected samples, size distribution and float-sink analysis were also conducted. Float-sink tests were carried out by a commercial laboratory (Process Technology, Inc.) that specializes in the centrifugal float-sink testing of fine coal.

### 3.6 References

1. Adel, G. T., Wang, D., and Yoon, R. H., Proceedings of the VIII Int. Pittsburgh Coal Conference, October 14-18, Pittsburgh, Pennsylvania (1991).
2. Texas Nuclear E-Zcal density system user manual.
3. "Magnetic Flow Meter", Fischer-Porter, Inc.
4. "Paddle Wheel Flowmeter", Kobold Instruments, Inc.
5. "Type A Pinch Valve", Red Valve Company, Inc.

## **CHAPTER 4 - MULTI-GRAVITY SEPARATOR PARAMETRIC STUDY**

### **4.1 Introduction**

With the depletion of high-grade ore reserves, the mining industry is increasingly resorting to mineral processing to meet the increasing global demands for raw materials [1]. Low-grade ores by nature have a higher fraction of composite particles. Therefore, in order to achieve an efficient separation, these ores need to be ground to finer sizes to improve their liberation characteristics. The need for improved liberation combined with increased mechanization has resulted in a higher production of fines [2]. Until recently, flotation has been successful in upgrading fines. However, the increased cost of processing and environmental concerns related to the use of flotation reagents have forced equipment manufacturers to look into the possibility of developing efficient gravity separators for treating fine particles [3].

Over the past decade, several continuous fine particle gravity concentrators have been developed [4,5,6]. Initial test results are very encouraging and some industrial applications, primarily in the gold and tin processing, have been extremely successful [7,8,9]. The coal industry has now begun to recognize the potential benefits of this new technology for reducing the ash and sulfur contents of their feed coals. Having realized the limitation of flotation in rejecting sulfur from coal, fine particle gravity concentrators

have become an attractive alternative. The present investigation is part of a cooperative research effort being conducted by the U. S. Department of Energy (DOE) and the coal industry to develop more efficient methods for processing fine coal.



## 4.2 Objectives

The primary goal of this investigation was to test the ability of the MGS to remove high density pyritic sulfur and ash-forming minerals, such as clay, from coal fines (28 mesh x 0). The specific objectives of this project are as follows: 1) to demonstrate the efficiency of the MGS, as a stand-alone unit, for treating fine coal, , 2) to compare the experimental results with the predictions obtained using a theoretical model developed for the MGS, 3) to determine the effects of the MGS operating parameters on the grade and recovery for the tests conducted on different coals, 4) to develop an empirical model to describe the performance of the MGS, using response surface methodology, and 5) to identify and optimize controlling operating parameters of the MGS

### 4.3 Parametric Design and Procedures

In this study, an effort is being made to understand the effect of six important operating parameters on the performance of the MGS. A Box and Behnken statistical design has been employed [10,11] to minimize the number of experiments that needed to be conducted in order to fully quantify the performance of the test unit. Literature studies show this type of incomplete factorial design to be preferred when the experimental error variance is not so large as to require a large number of observations to obtain the necessary precision. This Box-Behnken design have the advantage of having small redundancy factors, i.e., the number of runs (N) over number of constants (L)) is small. In addition, the empirical expressions obtained using this approach can provide a measure of the contribution of each parameter, as well as the joint influence of several parameters, on a given response.

Box-Behnken designs are formed by combining two-level factorial designs with incomplete block designs in a particular manner. For example, Table 4.1 shows a balanced incomplete block design for testing 4 parameters ( $k$ ) in 6 blocks ( $b$ ) of size ( $s$ ) equal to 2. The basis for a three-level design in four variables is obtained by combining this incomplete block design with the  $2^2$  factorial given in Table 4.2. The two asterisk (\*) in every row of the incomplete block design are replaced by the  $s = 2$  columns of the  $2^2$  design. Wherever an asterisk doesn't appear, a column of zeroes are inserted. The design

**Table 4.1**

**A balanced incomplete block design for four variables in six blocks [11].**

	$x_1$	$x_2$	$x_3$	$x_4$
1	*	*		
2			*	*
3	*			*
4		*	*	
5		*		*
6	*		*	

**Table 4.2**

**A  $2^2$  factorial design [11].**

	$x_i$	$x_j$	
[	-1	-1	]
	1	-1	
	-1	1	
	1	1	

is completed by the addition of a number of center points (i.e., 0, 0, 0, 0), with about three center points being desirable with the present arrangement. The resultant design is a rotatable second order design suitable for studying four variables in 27 tests. The design is capable of being blocked in three sets of nine tests as shown in Table 4.3. Similarly, design for studying 5 parameters involves 46 tests with 3 replicate tests.

The effectiveness of an experimental design depends on the proper selection of high, low and optimum values for each parameters. Therefore, the first step was to conduct exploratory tests to understand the process. In Tables 4.4 and 4.5, test conditions for each of the two coals to be tested are given. Tests were performed in random order to minimize external bias. Replicate tests conducted are useful in determining the variance in the feed coal characteristics and assay techniques during the course of the test program.

**Table 4.3**

**A three-level design for four variables in three blocks [11].**

$\pm 1$	$\pm 1$	0	0
0	0	$\pm 1$	$\pm 1$
0	0	0	0
-----			
$\pm 1$	0	0	$\pm 1$
0	$\pm 1$	$\pm 1$	
0	0	0	0
-----			
$\pm 1$	0	$\pm 1$	0
0	$\pm 1$	0	$\pm 1$
0	0	0	0

**Table 4.4**  
**Parametric test matrix used to investigate the performance**  
**of the MGS unit for the Pittsburgh No. 8 coal seam.**  
**MGS Conditions Held Constant**  
 Shake Amplitude (mm):15; Shake Frequency (cps):5;Tilt Angle  
 (degrees):6  
**MGS Variables**

Test Number	Grind Size (microns)	Drum Speed (rpm)	Wash Water (lpm)	Percent Feed Solids	Feed Rate (lbs/hr)
201	200	280	1.02	35	110
202	200	280	1.02	35	235
203	200	241	1.48	26	169
204	200	280	0.53	25	273
205	200	240	0.53	25	159
206	200	280	0.53	25	100
207	200	280	0.95	26	200
208	200	321	1.10	15	173
209	300	280	0.91	16	261
210	300	281	0.95	35	216
211	300	280	0.98	25	260
212	300	280	1.51	26	215
213	300	280	0.91	25	110
214	300	321	0.95	25	217
215	300	280	0.45	26	215
216	300	241	1.02	25	217
217	200	280	1.02	14	239
218	200	282	0.49	35	210
219	200	280	1.51	35	216
220	200	320	0.98	25	334
221	200	240	0.98	24	347
222	200	280	0.98	26	164
223	200	240	0.98	26	137
224	200	281	1.51	25	313
225	200	281	1.48	16	200
226	200	242	0.94	15	212
227	100	284	0.98	36	197
228	100	282	0.91	25	100
229	100	280	0.98	26	321
230	100	320	0.98	26	198
231	100	280	0.49	25	204
232	100	240	0.98	25	208
233	100	280	1.48	26	200
234	100	280	0.98	15	205
235	200	320	0.95	35	208
236	200	241	0.95	35	223
237	200	320	0.98	35	128
238	200	280	0.98	25	176
239	200	321	0.53	26	186

**Table 4.5**

**Parametric test matrix used to investigate the performance of the MGS unit for the Illinois No. 6 seam coal.**

**MGS Conditions Held Constant**

Shake Amplitude: 15 mm; Shake Frequency: 5 cps;  
Tilt Angle: 6 degrees; Grind Size (d80): 200 microns;

**MGS Variables**

Test Number	Drum Speed (rpm)	Wash Water (lpm)	Percent Feed Solids (w/w)	Feed Rate (lbs/hr)
501	280	0.76	30.71	345
502	280	0.76	24.16	199
503	281	1.63	34.63	200
504	321	1.51	25.81	212
505	280	0.00	18.95	234
506	280	0.76	17.14	306
507	281	0.80	29.60	242
508	283	1.51	24.46	272
509	280	0.00	26.32	293
510	281	0.83	33.89	141
511	283	0.68	25.56	210
512	320	0.83	17.06	207
513	241	1.55	26.40	216
514	320	0.76	28.13	141
515	320	0.80	37.77	230
516	240	0.76	24.36	267
517	280	0.00	30.11	155
518	241	0.80	37.18	225
519	320	0.76	25.38	279
520	281	0.83	18.24	136
521	280	1.59	28.63	148
522	240	0.80	29.61	153
523	241	0.83	17.22	209
524	281	1.59	17.30	214
525	322	0.00	25.72	217
526	241	0.00	26.20	227
527	281	0.00	37.75	260



## 4.4 Results

### 4.4.1 Pilot-Plant MGS Testing

In order to determine the feasibility of the MGS for processing run-of-mine coals, a series of tests were conducted on both the Pittsburgh No. 8 and Illinois No. 6 coals. Tables 4.4 and 4.5 summarize the operating conditions used for the MGS during the course of this test work. After setting the operating parameters at predetermined levels established by the test plan, the MGS was allowed to operate for a period of time sufficient to reach steady-state conditions. Once the system attained steady-state (generally 45-60 minutes), timed samples of the feed and product streams were collected and assayed for ash, sulfur, pyritic sulfur and heating values as described previously in Chapter 3.

The assay values of feed, clean coal and tailings streams, for each experiment, were evaluated using a commercially available mass-balancing software package (BILMAT) [12]. This program adjusts all the assay values to produce a self-consistent set of experimental data. Assay values which did not balance well were considered to be unreliable and were eliminated from the data set. Figure 4.1 shows the measured and adjusted values for tests carried out using Pittsburgh No. 8 coal. It can be seen that there is a very good agreement between measured and adjusted data.

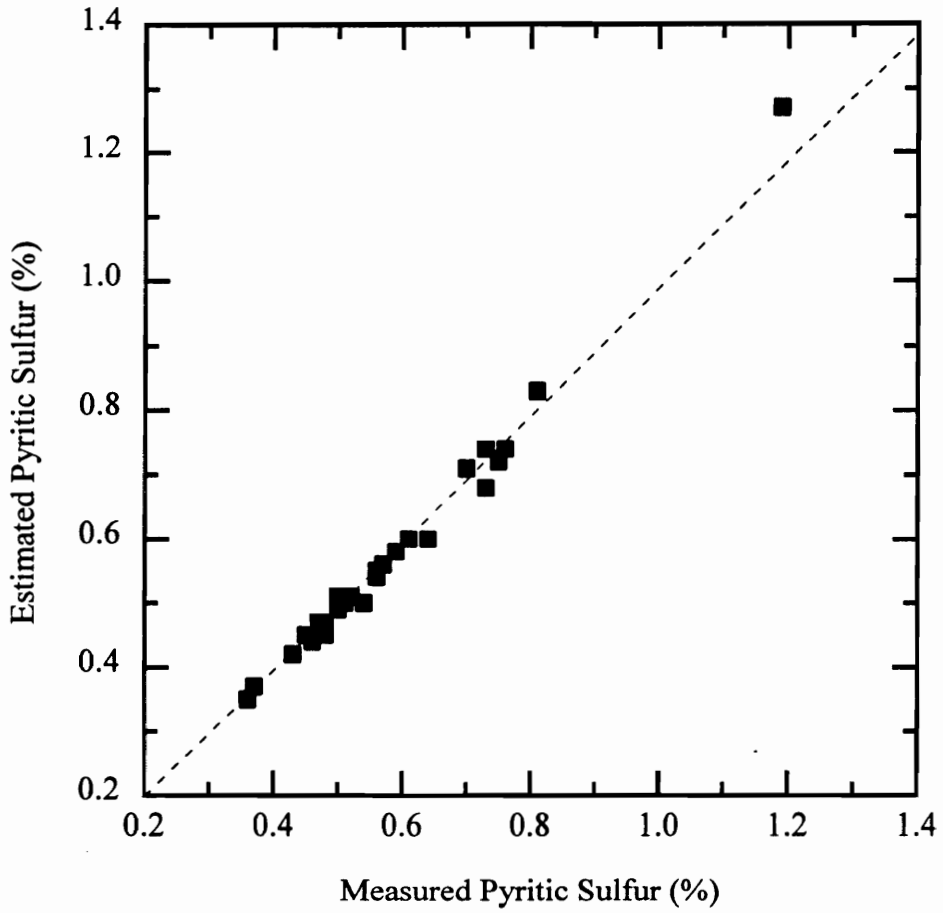


Figure 4.1. Measured pyritic sulfur data versus estimated data from the material balance for the tests conducted on the MGS using Pittsburgh No. 8 seam coal.

## 4.5 Discussion

### 4.5.1 Separation Performance

Performance curves of the type presented in Figure 4.2 are commonly used to describe the performance of the process over a wide range of operating parameters. It is interesting to note that although the MGS tests were conducted over a wide range of operating conditions, most of the experimental data points were found to fall along single grade-recovery curves. Therefore, the grade-recovery relationship appears to be primarily determined by the characteristic nature of the feed coal sample, i.e., degree of liberation. It is also important to note that any point on the curve can be obtained by more than one combination of operating variables.

Figures 4.3 show the product recoveries as a function of ash, total sulfur and pyritic sulfur rejections obtained for each test run using Pittsburgh No. 8 coal. The dashed lines in each figure represent the result that would have been obtained if the separation were entirely non-selective. It is clear from these results that the MGS is capable of rejecting mineral matter from coal even at a finer grind size. Data obtained using the Pittsburgh No. 8 coal indicate that the MGS could achieve an ash rejection of 40% , total sulfur rejection of 50% and pyritic sulfur rejection of 70% at a combustible recovery approaching 90%. Similar rejections of ash, total sulfur and pyritic sulfur were

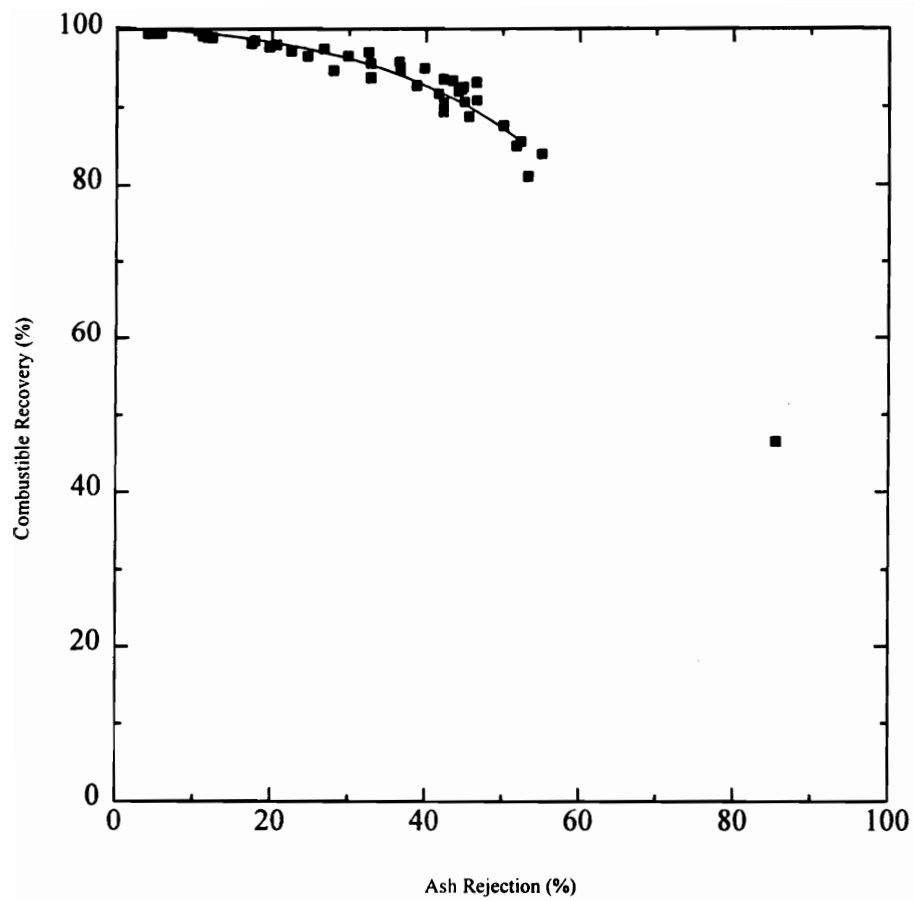


Figure 4.2. Combustible recovery as a function of feed ash rejection obtained using Pittsburgh No. 8 seam coal.

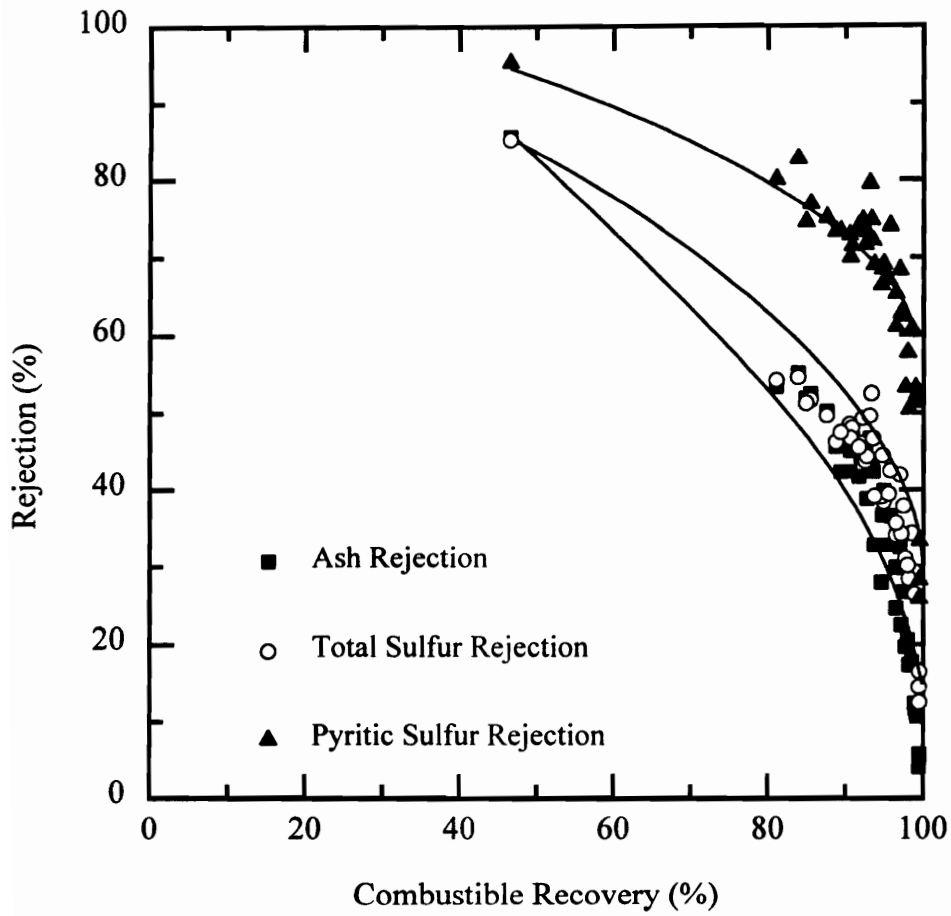


Figure 4.3. Combustible recovery versus rejection plots obtained during the parametric testing of the MGS using the Pittsburgh No. 8 Coal.

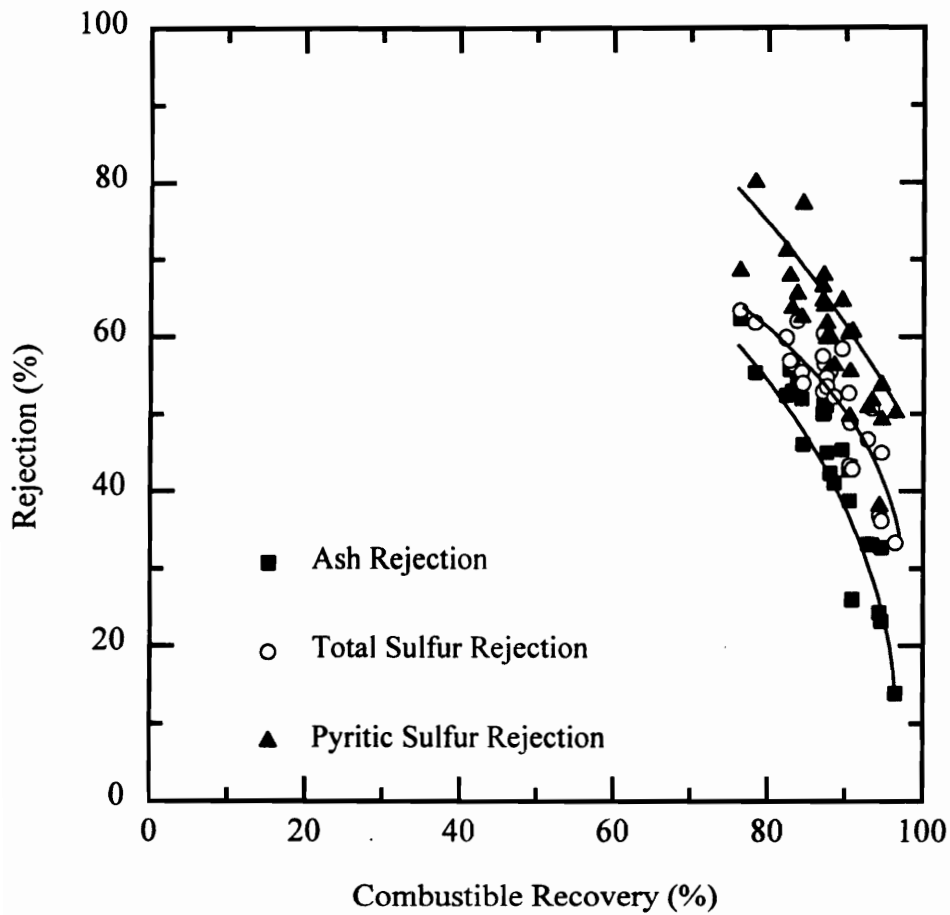


Figure 4.4. Combustible recovery versus rejection plots obtained during the parametric testing of the MGS using the Illinois No. 6 Coal.

obtained for the Illinois No. 6 coal, but at a slightly lower combustible recovery of 85% (see Figures 4.4).

The contribution of various operating parameters on the performance of the MGS using Pittsburgh No. 8 coal is better illustrated in Figure 4.5. As shown, most of the data points are grouped along distinct parabolic curves. In each case, the same maximum separation efficiency could be obtained at an ash rejection of 40%, total sulfur rejection of 50% and pyritic sulfur rejection of 70%. It is interesting to note that these levels of rejection correspond to the “elbow” in the respective grade-recovery curves (Figure 4.3). Therefore, it can be concluded that the maximum separation efficiency for a given coal occurs at the point just before the large deterioration in yield and grade. The maximum separation efficiency for the Illinois No. 6 coal was obtained at the same rejection level as that of Pittsburgh No. 8 coal, but at a slightly lower combustible recovery. This is reflected in the lower separation efficiency value shown in Figure 4.6. These findings suggest that the relationship between separation efficiency and mineral matter rejection is primarily determined by the nature of the feed coal.

The test data clearly show that the MGS is very effective in separating high-density pyrite from low-density coal. On the other hand, the MGS appears to be less effective in removing ash-forming mineral matter from coal. The relatively poor ash rejections obtained with the run-of-mine coals can be largely attributed to the presence of clay minerals in the feed to the MGS. Because of their ultrafine size, these particles lack

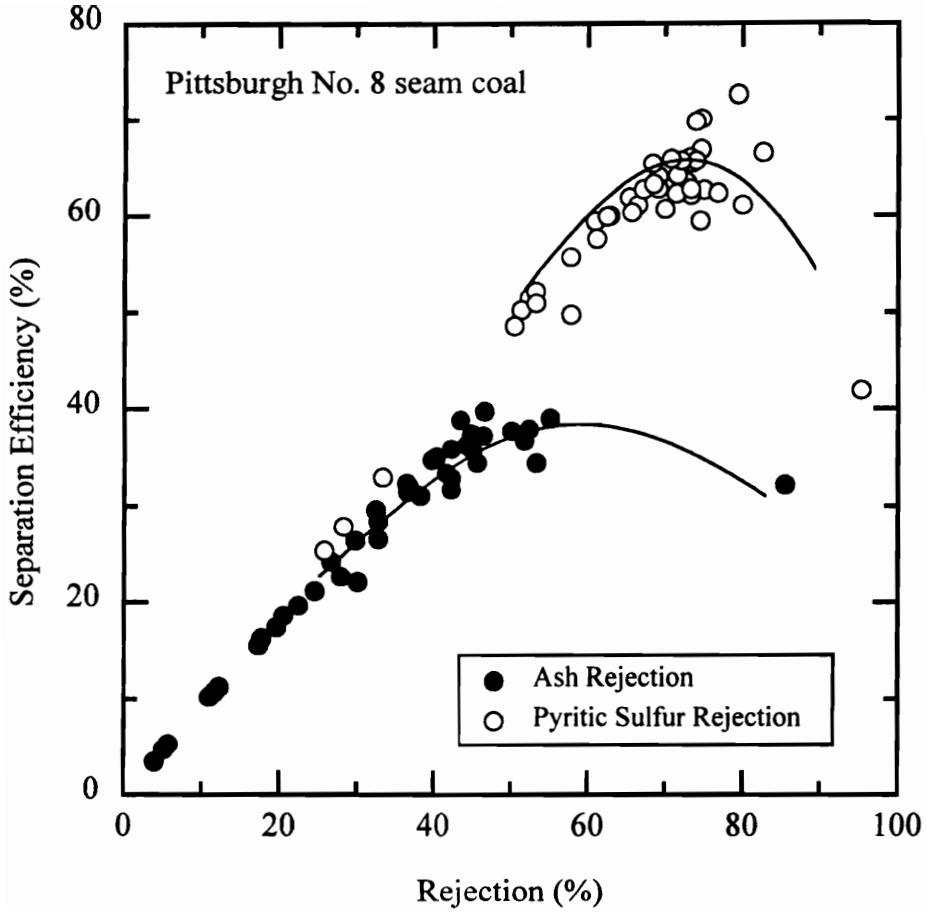


Figure 4.5. Separation efficiency as a function of ash and pyritic sulfur for Pittsburgh No. 8 seam coal.



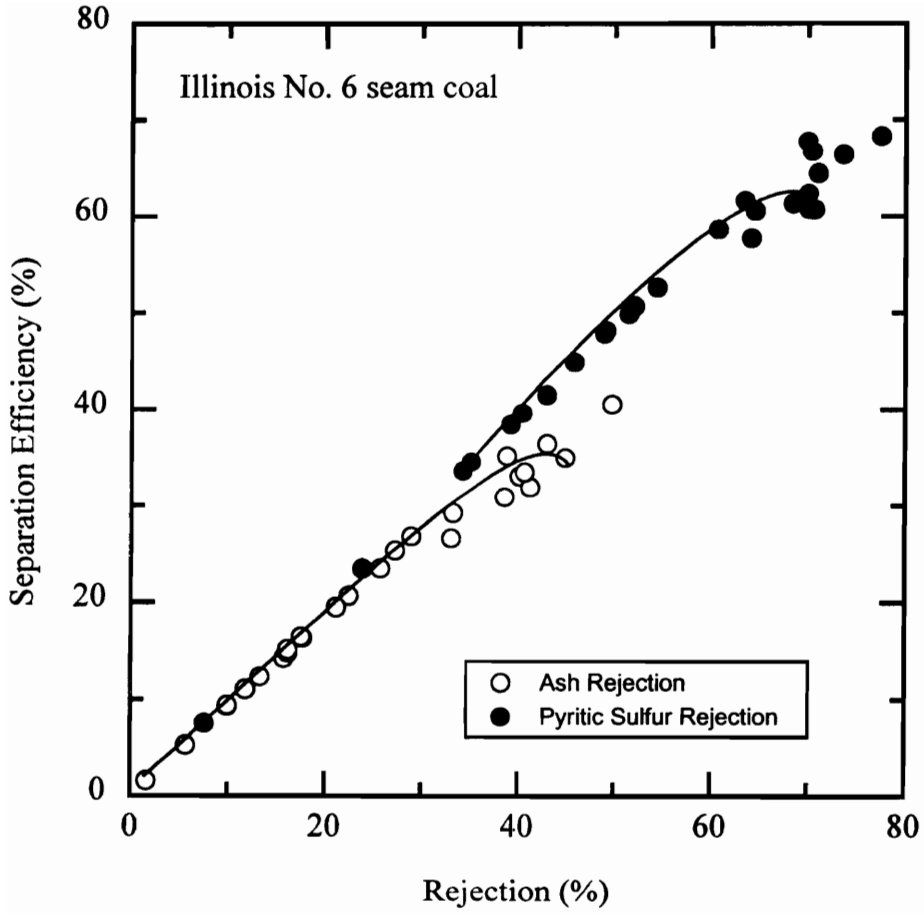


Figure 4.6. Separation efficiency as a function of ash and pyritic sulfur for Illinois No. 6 seam coal.

sufficient mass to be pinned to the drum surface and are readily entrained with the flowing film into the clean coal.

#### 4.5.2 Effect of Particle Size

The parametric study illustrates the effectiveness of the MGS for separating high-density pyrite from low-density coal. On the other hand, the unit appears to be less efficient in rejecting ash-forming mineral matter. The poor ash rejection can be largely attributed to ultrafine clay slimes which are too small to be pinned to the drum wall and report to the clean-coal product entrainment in the process water. To test this hypothesis, tests were also conducted on flotation feed samples obtained from an operating preparation plant. This series of tests utilized a slightly coarser grind-size than that previously employed for the parametric tests. The size-by-size test results, which are summarized in Table 4.6 and Figure 4.7, show that the best overall separation was obtained for particles in the 100 x 325 mesh size class. In this size range, ash and pyritic rejections of 75-80% were obtained at a combustible recovery of 85%. As expected, the finest size fraction (i.e., 325 mesh x 0) gave the worst results in terms of ash rejection, although the rejection of pyritic sulfur was still good (i.e., 72.6%). It is also interesting to note that the performance of the MGS also drops when treating particles larger than 48 mesh. Particles in this size range have sufficient mass to be pinned to the drum, but the physical size of the particles places them in the high-velocity region of the flowing film. As a result, the pinning force is incapable of preventing larger particles from being

**Table 4.6****Performance data for the MGS**

Particle Size (mesh)	Pittsburgh No. 8 Seam Coal		Illinois No. 6 Seam Coal	
	SG <sub>50</sub>	E <sub>p</sub>	SG <sub>50</sub>	E <sub>p</sub>
+100	2.28	0.156	2.00	0.110
100 x 200	1.90	0.126	1.95	0.085
200 x 400	1.94	0.155	2.19	0.087
-400	1.97	0.205	2.71	0.155

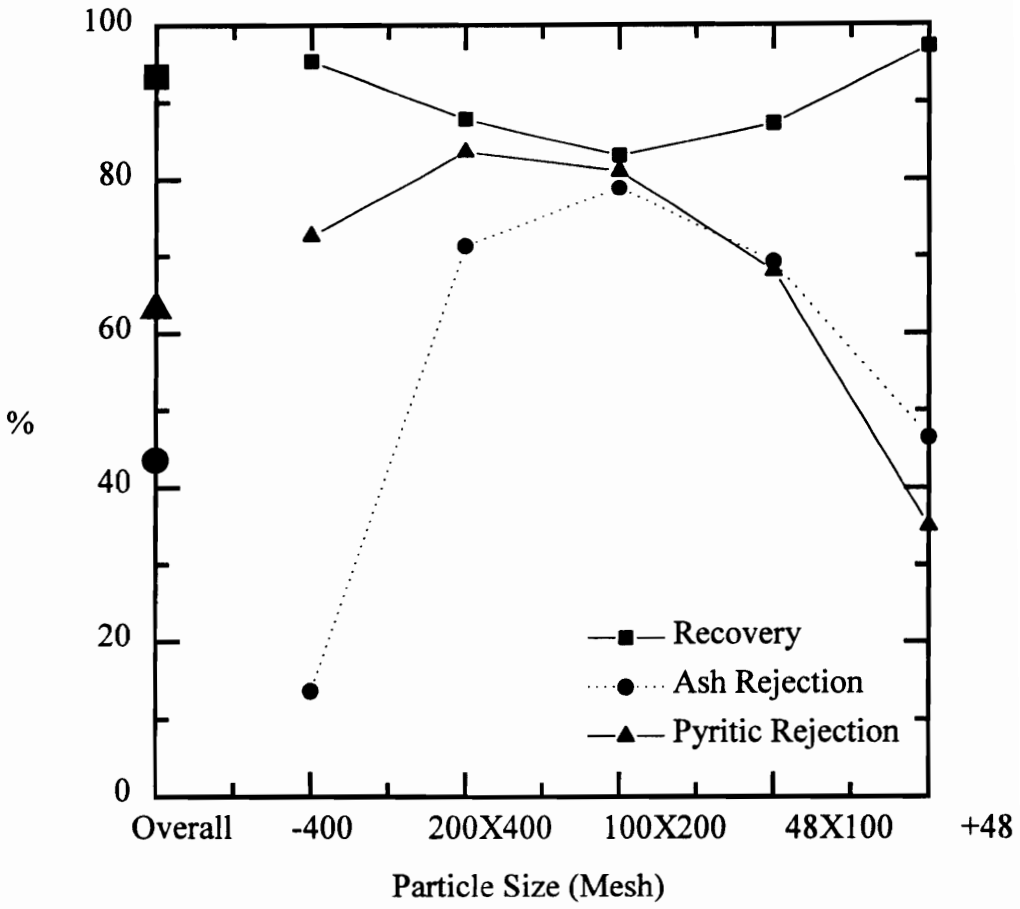


Figure 4.7. Effect of particle size on the performance of the MGS.

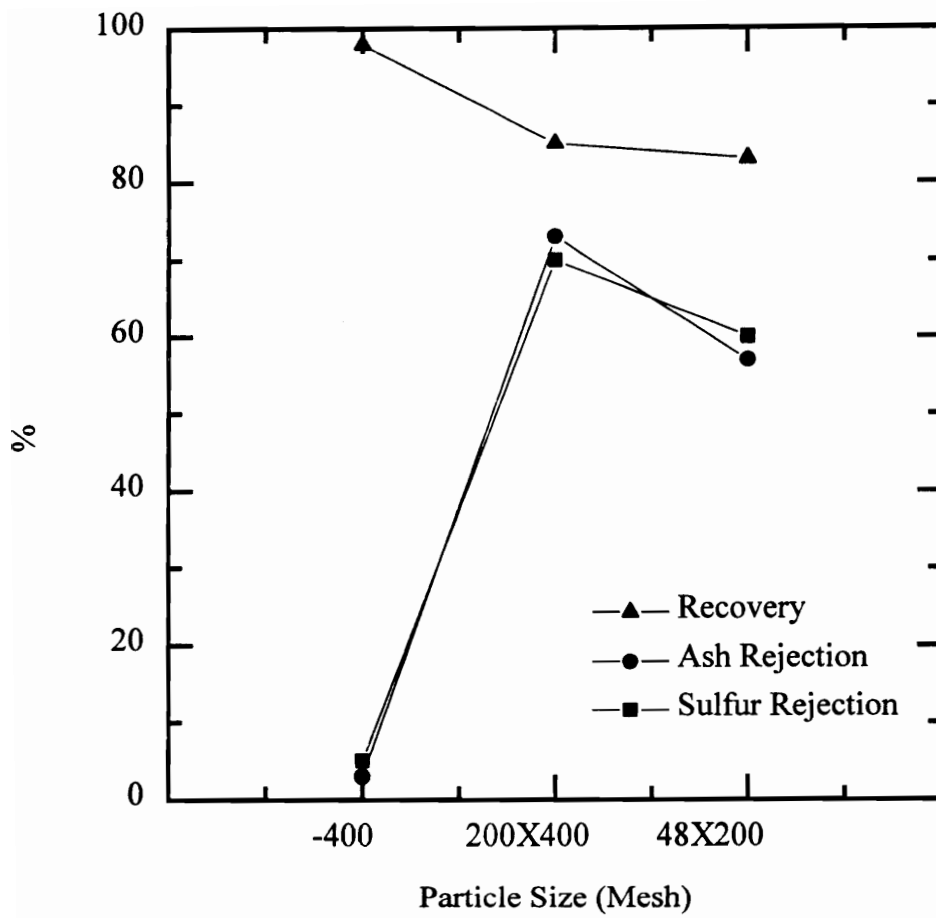


Figure 4.8. Effect of particle size on the performance of the Falcon concentrator [13].

carried along with the flowing-film into the clean coal product. Research work conducted using other enhanced gravity concentrators also showed similar trends (see Figure 4.8) [13]. As shown, the best separation performance was achieved on the 100 x 325 mesh fraction. The minus 325 mesh size fraction is also not effectively de-ashed by the enhanced gravity concentrators. Therefore, desliming the feed is very important to produce acceptable clean coal products from these unit operations.

### 4.5.3 Partition Curves

#### 4.5.3.1 *Variation in separation density ( $SG_{50}$ ) and Probable Error ( $E_p$ ) with particle size*

Partition curves of the type presented in Figures 4.9-4.10 for the MGS are commonly used to describe the efficiency of density-based separators and their separation efficiency. From these performance curves, it is obvious that the separation is dependent on the particle size. Table 4.6 summarizes the specific gravity of separation ( $SG_{50}$ ) and probable error ( $E_p$ ) for the tests carried out using Pittsburgh No. 8 and Illinois No. 6 coals. As expected, the 100 x 400 mesh fraction displays best separation efficiency. The separation efficiency decreases substantially in the finer size range.

The specific gravity of separation ( $SG_{50}$ ) was found to increase with decrease in particle size for Illinois No. 6 coal. The  $SG_{50}$  ranged from 1.95-2.19 for plus 100 mesh and 100 x 400 mesh fractions, while the  $SG_{50}$  of minus 400 mesh fraction was found to

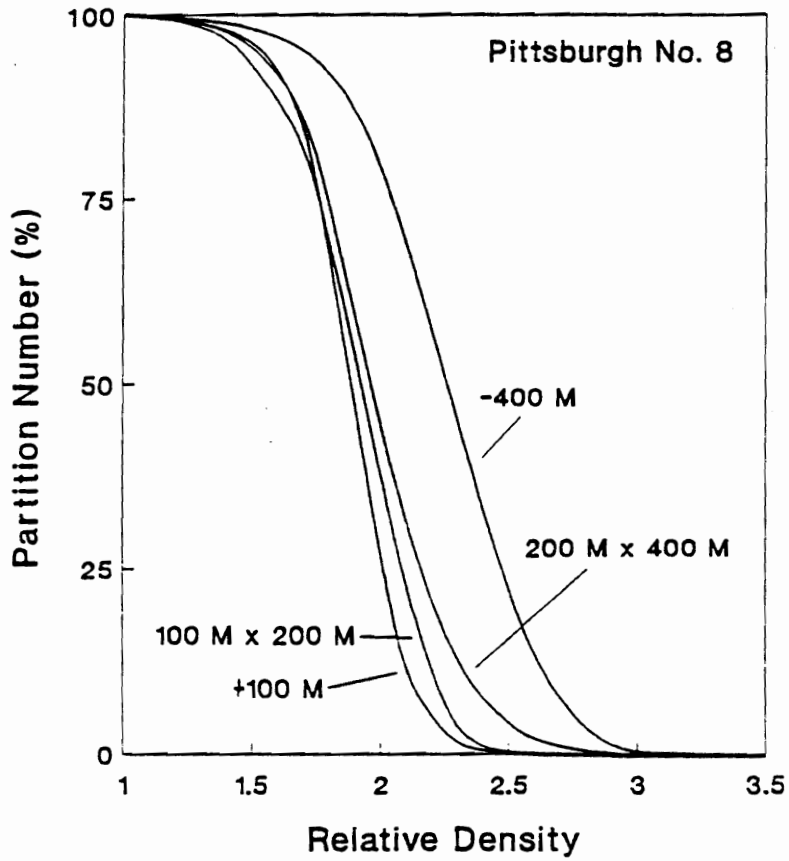


Figure 4.9 Effect of particle size on the partition curves for the MGS unit obtained during the long-duration testing of the Pittsburgh No. 8 seam coal.

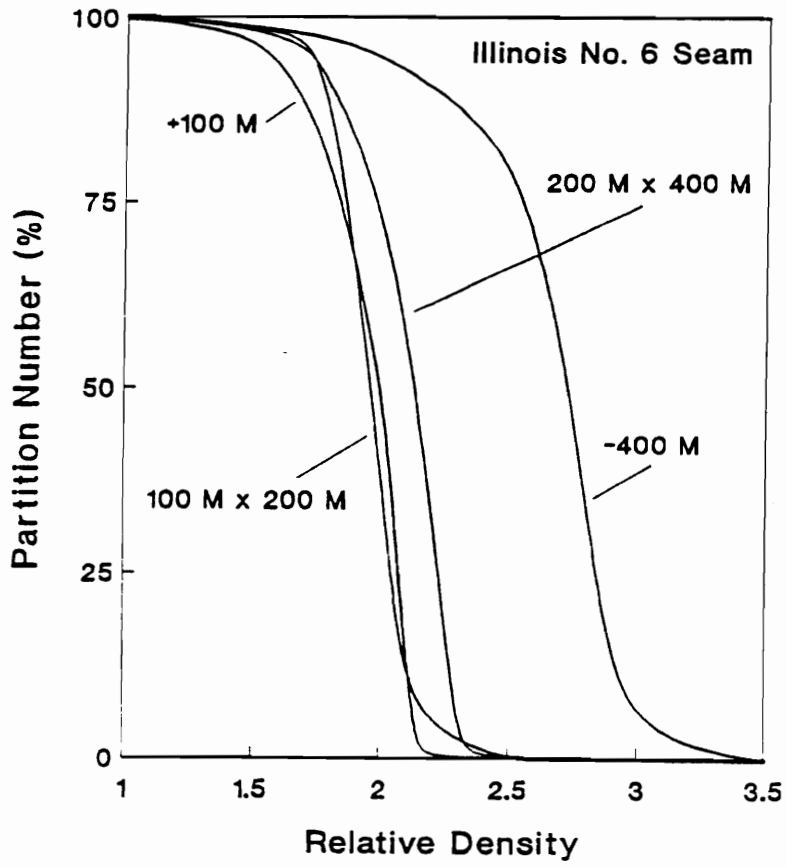


Figure 4.10 Effect of particle size on the partition curves for the MGS unit obtained during the long-duration testing of the Illinois No. 6 seam coal.



be 2.71. This higher  $SG_{50}$  value could be due to the entrainment of minus 400 mesh pyrite reporting to the clean coal. Similar observations can be made for the MGS performance using Pittsburgh No. 8 coal. However, there was no significant difference in  $SG_{50}$  for minus 400 mesh fraction. A plausible reason for this difference could be less pyrite is concentrated in the finer fractions of the Pittsburgh No. 8 coal than the Illinois No. 6 coal. Figure 4.11 shows the effect of particle size on the  $SG_{50}$  [14,15,16]. This data also suggests that the  $SG_{50}$  increases with a decrease in particle size, this phenomenon is common amongst density-based separation processes. It is important to note that the separation density decreases at higher bowl speed for Falcon concentrator. Simulation results, from the theoretical model developed in chapter 2, also indicate that the sharpness of separation increases with increase in the applied centrifugal force (see Figure 2.7 and 2.8).

Probable Error ( $E_p$ ) is a widely used performance estimator for density-based concentrators. In an ideal separation, all material lighter than the relative density of separation would report to the clean coal product, while heavier material would report to the refuse. Under this condition, a perfect separation would be achieved and the  $E_p$  value would be zero. Unfortunately, since no unit operation yields a perfect separation, nonzero values of  $E_p$  are to be expected in practice. It is interesting to note that the probable error ( $E_p$ ) values ranged from 0.110 for the plus 100 mesh size fraction to 0.155 for the minus 400 mesh size fraction for tests conducted using the Illinois No. 6 coal.

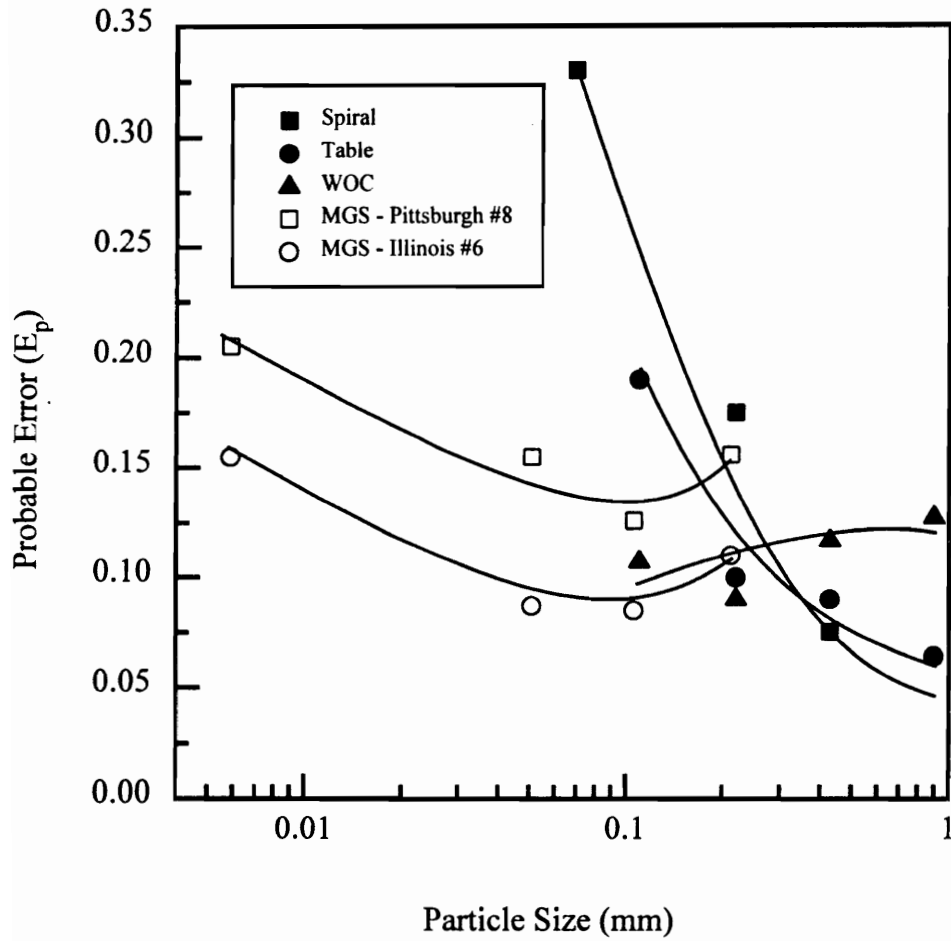


Figure 4.11. Effect of the particle size on reduced probable error for commonly used separators treating fine coal [15,16].

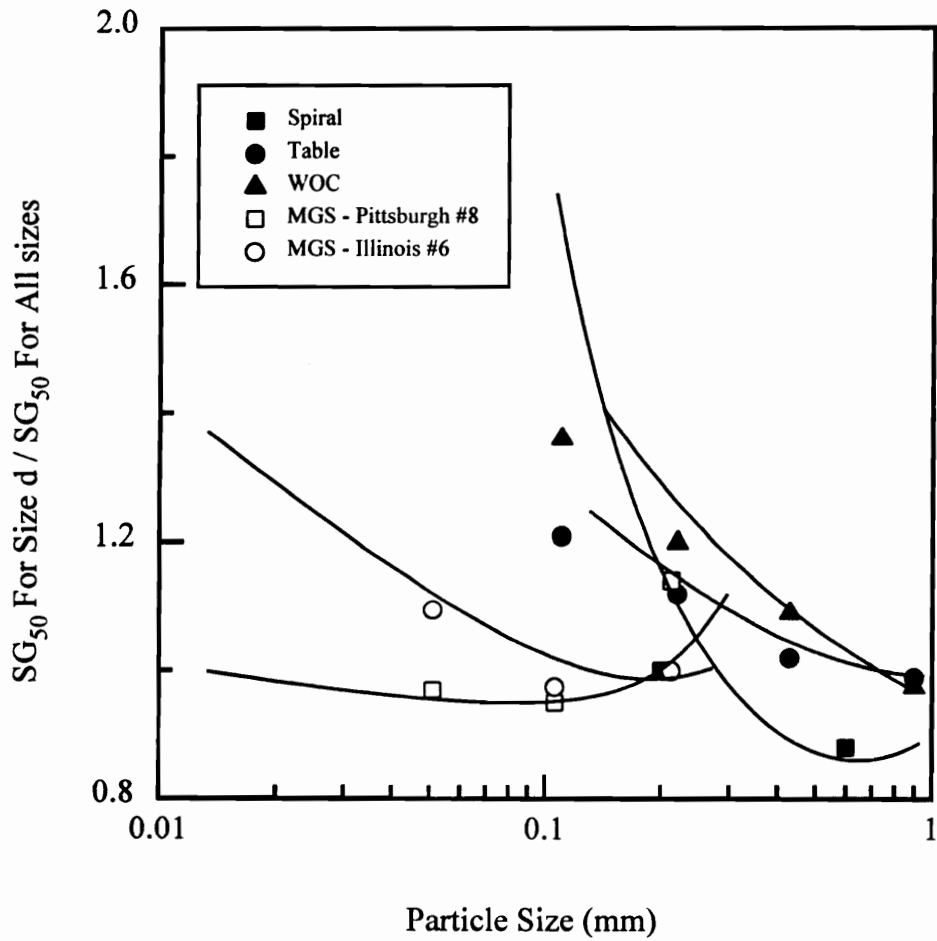


Figure 4.12. Effect of the particle size on relative cut specific gravity for commonly used separators treating fine coal [15,16].

The sharpest separations were achieved between 100 mesh and 400 mesh, in which  $E_p$  values of approximately 0.085-0.087 were achieved. On the other hand, test data obtained using the Pittsburgh No. 8 seam indicated a poorer level of performance. The  $E_p$  values varied from 0.156 to 0.205 for the plus 100 mesh and minus 400 mesh fractions, respectively. The sharpest separations were again achieved at intermediate sizes (100 x 400 mesh) which gave  $E_p$  values in the range of 0.125 to 0.155. It is worthwhile to mention that the simulation results on a 150 micron particle (using the model developed in Chapter 2) have  $E_p$  values ranging between 0.12 to 0.18. For comparison, the average  $E_p$  values obtained with the MGS are also plotted along with those reported in the literature for conventional coal cleaning processes in Figure 4.12 [15,16]. This plot illustrates that the MGS is capable of significantly extending the particle size range over which density-based separations are effective.

#### 4.5.4 Statistical Analyses of the Parametric Data

This section deals with statistical data analysis, empirical model development and interpretation of the modeling parameters. Statistical data analysis was carried out using a commercially available software package known as DESIGN-EXPERT (developed by Stat-Ease, Inc., Minneapolis, Minnesota) [17]. As discussed earlier, this package is capable of creating the required test matrix and performing all required statistical

computations and regression analyses. The overall objective of this effort is to develop an empirical relationship between various operating parameters (drum speed, feed rate, feed percent solids, etc.) and a variety of response variables (combustible recovery, rejections, separation efficiency etc.).

#### 4.5.4.1 *Model development*

Experiments were conducted according to the parameter settings specified in the test matrix developed using DESIGN-EXPERT. Test results obtained were entered into the DESIGN-EXPERT software package. The first step in the model development was to fit the data using linear, quadratic and cubic models. It is well understood that simpler model is preferred over complex ones, provided that the simpler models predicted well. Therefore, in the present work, all the data were fit using linear or quadratic models. Several statistical routines were conducted to determine the goodness-of-fit for each model.

#### 4.5.4.2 *Interpretation of the statistical analyses*

To determine the reliability of the empirical models developed using the DESIGN-EXPERT software, the predicted results were compared with experimental results in Figure 4.13. As shown, there is a good correlation between the predicted and experimental results. Once the model was determined to be reliable, it was important to

evaluate the contributions from the different operating parameters. This relative contributions were quantified using the net effect (E) which is given by:

$$E = \frac{1}{n} \left[ \sum_{i=1}^n (R+)_{i} - \sum_{i=1}^n (R-)_{i} \right] \quad [18]$$

where  $n$  is the total number of responses carried out at the high level and  $(R+)_{i}$  and  $(R-)_{i}$  are the values of the responses at the high and low levels, respectively. It is important to note that larger E values indicate that the given operating parameter has a significant influence on the response under consideration. The correlation matrix describing the influence of the various operating parameters on the response of the process are provided in Tables 4.7-4.8.

#### *Effect of Drum Speed*

Statistical analyses on all four sets of data clearly indicate drum speed to be the most important operating parameter. For the Pittsburgh No. 8 coal, an increase in drum speed resulted in a lower combustible recovery, while the rejections of ash, total sulfur and pyritic sulfur increased. Similar trends were observed in tests carried out using the other three coals. As explained in Chapter 2, an increase in drum speed affects the operation of MGS in two ways. First, an increase in drum speed results in an increase in the inertial mass of the particles, increasing their tendency to pin to the drum wall and form a solid layer. These particles are moved towards the high-density discharge end of the drum by the scraping mechanism. Test results clearly indicate a decrease in combustible recovery at higher drum speed. Secondly, an increase in drum speed

**Table 4.7****Correlation matrix for the testing of the Pittsburgh No. 8 seam coal using the MGS**

Process Response	Process Variable				
	Increasing Grind size	Increasing Feed Rate	Increasing Drum Speed	Increasing Wash Water	Increasing Feed Solids
Comb. Rec.	S↓	S↓	L↓	S↑	M↓
Energy Rec.	S↓	S↓	L↓	S↑	M↓
Ash Rejection	S↑	S↑	L↑	S↓	M↑
Sulfur Rej.	S↑	S↑	L↑	S↓	L↑
Pyritic Rej.	S↓	S↑	L↑	S↓	M↑
Efficiency	S↓	M↓	L↑	S↓	L↑
lb SO <sub>2</sub> /MM Btu	M↑	S↑	L↓	S↑	L↓

Correlation: L=Large, M=Medium, S=Small

**Table 4.8**

**Correlation matrix for the testing of the Illinois No. 6 seam coal using the MGS**

Process Response	Process Variable			
	Increasing Drum Speed	Increasing Feed Solids	Increasing Wash Water	Increasing Feed Rate
Comb. Rec.	L↓	M↓	L↑	M↑
Energy Rec.	L↓	M↓	L↑	M↑
Ash Rejection	L↑	M↑	S↓	M↓
Sulfur Rej.	L↑	L↑	M↓	L↓
Pyritic Rej.	L↑	L↑	L↓	L↓
Efficiency	M↑	L↑	M↓	L↓
lb SO <sub>2</sub> /MM Btu	L↓	M↓	S↑	S↓

Correlation: L=Large, M=Medium, S=Small



increases the flow rate of the slurry in an axial direction towards the low-density end of the drum. However, this effect only becomes dominant when the volumetric flow rate is very high and solids content is very low. Under these conditions, the recovery increased considerably, but the product had a higher ash and sulfur content.

#### *Effect of Feed Solids Content*

In general, the MGS is believed to have a lower capacity compared with other enhanced gravity separators. Based on the theoretical studies on MGS, it was also found that higher volumetric flow rates were detrimental to achieving high separation efficiencies. Therefore, in an effort to increase the feed capacity, test runs were conducted at higher feed percent solids. Increasing the feed percent solids tended to increase the throughput capacity for the same volumetric flow. This also tended to reduce the coal recovery and improve the rejection of mineral matter. However, as discussed in the following paragraphs, the low recovery values obtained at higher percent solids can be overcome by increasing wash water addition rate to the MGS.

#### *Effect of Feed Rate*

An increase in feed rate affects both the mass loading and retention time within the MGS. In most continuous processes, an increase in feed rate would increase the mass loading and decrease the retention time. The lower retention time would result in a lower recovery. Therefore, as expected, an increase in feed rate resulted in small loss in recovery when processing the Pittsburgh No. 8 coal by the MGS. However, tests

conducted using the Illinois No. 6 coal showed an increase in the coal recovery as the feed rate increased. A possible explanation for this unexpected finding could be due to the feed characteristics of the Illinois No. 6 coal. As described in Chapter 3, the Illinois No. 6 coal has a higher percentage of middlings and disproportionately higher percentage of fines than the Pittsburgh No. 8 coal. These fines, with their smaller mass, may remain suspended in the high velocity regime of the flowing film and report with the clean coal to the low-density end of the MGS. This conclusion is supported by the tests conducted using the “precleaned” Illinois No. 6 coal which showed a lower recovery at higher feed rate (which is in general agreement with most of the findings in literature). A small increase in recovery at higher feed rates was observed for tests carried out with “precleaned” Pittsburgh No. 8 coal, although this anomaly was attributed to changes in the percentage of middlings particles reporting to clean-coal or reject streams.

#### *Effect of Wash Water*

Wash water is added close to the high-density discharge end of the MGS drum. The wash water cleans the high-density product by carrying away light particles which are released by the ploughing action of the scraper mechanism. Statistical analyses demonstrate the importance of wash water in maintaining acceptable levels of separation performance. In general, an increase in the wash water flow rate resulted in an increase in coal recovery. It is interesting to note that wash water had a very significant impact on the tests results obtained using the Illinois No. 6 coal. This could be due to two main

reasons: (i) the wider range of wash water flow rates (i.e., 0 - 1.5 liters/min) used in these tests and (ii) the higher percentage of fines (-400 mesh) in this particular coal sample. Also, the wash water addition rate is directly related to feed percent solids. All the analyses indicate that increase in feed percent solids should be accompanied by higher wash water addition rate to achieve desired recovery and grade.

#### *Effect of Grind Size*

Tests were conducted using the Pittsburgh No. 8 coal at different grind sizes. The statistical analyses suggest that the grind size has only a small influence on process performance. An increase in the grind size resulted in a loss of coal recovery, while the rejections of ash and total sulfur increased. This is similar to the observations made with changes in the other operating parameters. Whenever a change in an operating parameter was made, it resulted in an increase in recovery with a corresponding decrease in the rejection of mineral matter. However, one notable exception to this rule was found for the effect of grind size on pyritic rejection. In this case, both the coal recovery and pyritic sulfur rejection decreased when coarser feeds were processed. This phenomenon can be explained by incomplete liberation of the pyrite at the coarser grind sizes.

#### *Effect of Shake Amplitude*

Studies conducted in the present work suggest that the shake amplitude has a relatively small impact on the process responses. An increase in the shake amplitude resulted in a small increase in coal recovery and slight reduction in the rejection of mineral matter.

Although the shake amplitude had a smaller impact than most of the other operating parameters, this variable may still have played an important role in enhancing the stratification of the particles in flowing film. The stratification is due to the Bagnold force which creates a reverse classification of particles in the flowing film, i.e., coarser low-density particles on top and finer high-density particles at the bottom. This phenomenon is said to be vital for treating multi-layer particles on a flowing film separator, thus increasing the capacity of the unit without sacrificing performance.

#### 4.5.4.3 *Parametric testing summary*

The parametric studies carried out in the present work have provided a wealth of information regarding the performance of the Multi-Gravity Separator (MGS). Drum speed was found to be the most important operating parameter. This variable was found to impact both the separation performance of the unit as well as its throughput capacity. In general, an increase in the drum speed increased the inertial mass of particles, thereby extending the capability of the unit to treat very fine particles. Conventional gravity separators are only effective in treating particles up to approximately 0.5 mm because of the small difference in settling rate of fine particles (see previous discussion in Chapter 1). However, an increase in the g-force helps to increase the settling velocity of particles as small as a few microns, thereby extending the domain of the enhanced gravity concentrations into treating even ultrafine particles. In addition, an increase in drum speed reduces the thickness of the flowing film and increases the net velocity of particles

towards the low-density discharge end of the unit. Since the density differential is small between coal (SG  $\approx$ 1.5) and associated gangue minerals such as clay (SG $\approx$ 2.3) or shale (SG  $\approx$ 2.5), higher 'g' forces are required to achieve a selective separation. Therefore, the MGS should be operated at higher drum speeds to maximize the separation efficiency.

Higher drum speeds also enhanced the throughput capacity of the MGS. In fact, feed percent solids was found to be second most important operating parameter for the unit. In general, an increase in percent solids of the feed stream for a given volumetric flow significantly increased the capacity in terms of solids throughput. This was found to be beneficial in improving the rejections of ash, total sulfur and pyritic sulfur. Also, an increase in feed solids content decreased the coal recovery by reducing the velocity of the flowing film which carries particles into the clean coal product. In addition, the flow rate of wash water was found to be highly interrelated with feed solids content. The wash water addition rate was found to be necessary to prevent entrapped coal particles from reporting to high-density discharge end. At higher feed solids contents, the additional of the wash water helped to increase coal recovery as well as improve the rejection of mineral matter. The statistical analyses indicate that the grind size and shake amplitude have only a small influence on the performance of the MGS.

#### 4.6 Summary and Conclusions

- a) A detailed Box-Behnken parametric study was conducted to evaluate the performance of the Multi-Gravity Separator (MGS) for fine coal cleaning applications. This enhanced flowing-film concentrator was designed to overcome problems normally encountered with surface-based separation processes such as froth flotation and oil agglomeration.
- b) Test results obtained in the present work indicate that MGS is very effective in rejecting particles containing high-density components such as pyrite. Therefore, the MGS is well-suited for coal desulfurization.
- c) Clay minerals were found to be rejected less efficiently by the MGS due to their ultrafine size. Therefore, in order to obtain high rejections of ash, these particles must be removed from the feed coal by desliming and/or other separation techniques prior to MGS processing.
- d) Test data obtained in the present work shows that the MGS is capable of rejecting approximately 75-85% of the pyritic sulfur from the Pittsburgh No. 8 seam coal at a combustible recovery of 90%. Similar rejections of ash and pyritic sulfur were obtained using the Illinois No. 6 coal, but at a slightly lower combustible recovery of 85%.

- e) The ability of the MGS to separate particles on the basis of specific gravity was found to be highly dependent on particle size. The separation was found to be most selective for the 100 x 325 mesh size fraction. The MGS was less efficient in treating the minus 325 mesh fraction. The poor performance was attributed to the presence of ultrafine particles (particularly clay particles) which are too small to be effectively pinned to the drum surface. Test results clearly indicate that high percentage of the “slimes” from this size fraction report with the clean coal by entrainment. It is also interesting to note that the performance of the MGS drops when treating particles larger than approximately 48 mesh. Particles in this size range have sufficient mass to be pinned to the drum, but the physical size of the particles places it in the high-velocity region of the flowing film. As a result, the pinning force is incapable of preventing the particle from being carried along with the flowing-film into the clean coal product.
- f) The specific gravity of separation obtained using the MGS ranged from 1.7 to 2.7 depending on the specific coal sample and size fraction being examined. The lowest specific gravity of separation was obtained for 100 x 325 mesh fractions, while the highest was obtained for the minus 325 mesh fractions.
- g) Size-by-size partition curves were constructed to evaluate the separation performance of the MGS.  $E_p$  values ranged of 0.15 to 0.20, with the lowest  $E_p$  values being obtained for the 100 x 325 mesh size fraction.

- h) Statistical analyses identified drum speed as the most important MGS operating parameter. An increase in the drum speed improved the rejection of mineral matter, but resulted in significant losses of low-density clean coal to the reject stream. Feed rate, feed solids content and wash water addition rate were found to have moderate impact on process performance.
- i) The data obtained from the experimental testing of the MGS were found to be in good agreement with the simulation results conducted using model developed in Chapter 2. This finding suggests that the theoretical model is valid for the range of test conditions examined in the present work.



#### 4.7 References

1. Leonard, J.W., and Mitchell, D.R., Coal Preparation, 5th Edition, (1991).
2. Miller, F.G., Trans. AIME, Vol. 229, (1964).
3. Burt, R.O., Prod. and Process. of Fine Particles, Plumpton(Ed.), CIMM, (1988).
4. Forssberg, E., and Nordquist, T., Minl. and Metall. Process., May, (1987).
5. Knelson, B., Minerals Engg., Vol. 5, No. 10-12, (1992).
6. Honaker, R.H., Proc. SME, February, 14 - 17, (1994).
7. Houot, R., and Joussemet, R., Les Techniques de l'Ingenieur, A5191, (1991).
8. Chan, B.S., Mozley, R.H., and Childs, G.J.C., Minerals Engg., Vol. 4, (1991).
9. Burt, R.O., and Mills, C., CIM Bull., (1985).
10. Box, G.E.P., and Behnken, D.W., Technometrics, Vol. 2, (1960).
11. Box, G.E.P., and Draper, N.R., Jour. Amer. Stat. Assoc., Vol. 54, (1959).
12. BILMAT, CANMET Development Manual, (1990).
13. Luttrell, G.H., Honaker, R.Q., and Phillips, D.I., 12th Intl. Coal Prep. Exhibition and Conf., May 2-4, (1995).
14. Deurbrouck, A.W., and Hardy, J., USBM, DOE, RI No. 7673, (1972).
15. Pillai, K.J., Mathematical Modelling of Water-Only Cyclone, Ph. D., Dissertation, Colarado School of Mines, (1988).
16. Osborne, D.G., Coal Preparation Technology, Vol. 1, (1988).

17. DESIGN-EXPERT, Stat-Ease, Inc., Minnesota, USA, (1993).

## **CHAPTER 5 - TESTING OF COMBINED FLOTATION/DENSITY CIRCUITS**

### **5.1 Introduction**

The 1990 Clean Air Act Amendment (CAAA) mandates stricter emission standards for coal-fired utilities in the United States. As a result, many utilities will be forced to switch to higher quality coals or resort to flue-gas scrubbing. Many of the Central Appalachian coal producers, particularly those mining high sulfur coal, could be adversely affected by this mandate [1].

Several studies conducted by U.S. Department of Energy (DOE) and research institutes across the nation have identified that improvements in fine coal cleaning could produce increased supplies of compliance coal [2,3]. At present, froth flotation is the most widely used technique for fine coal cleaning. This process is highly effective in rejecting ash-forming minerals, but is less efficient in removing pyrite. The main reasons for the poor pyrite rejection are (i) pyrite can become hydrophobic when superficially oxidized and (ii) composite particles containing small inclusions of carbonaceous material are readily floatable. In an effort to overcome these shortcomings, several research institutes are presently evaluating the potential of several enhanced gravity separators, like Multi-Gravity Separator and Falcon Concentrator, for fine coal cleaning [4,5]. As discussed in Chapter 4, these fine gravity separators are highly selective in

rejecting pyrite from coal. However, the capability of these units to reject ash-forming minerals (particularly clay) is far inferior to that of flotation. The main reason for the inferior performance is that ultrafine clay particles do not have sufficient mass to prevent them from being entrained in the flowing film along with the lower density coal particles. One method of improving the performance would be to deslime the feed coal prior to feeding to the fine particle gravity concentrators. Recent test work conducted using the Falcon concentrator at Southern Illinois University at Carbondale supports this hypothesis. However, this approach could have some practical problems including the high costs of desliming and large losses of valuable coal. An attractive alternative to desliming was proposed at the Center for Coal and Minerals Processing (CCMP) at Virginia Tech. In this approach, froth flotation was used to remove fine mineral matter from the coal prior to processing by the enhanced gravity concentrator. This processing scheme is believed to be capable of higher rejections of mineral matter and improved coal recoveries as compared to desliming.

## 5.2 Objectives

Earlier research work conducted at the Center for Coal and Minerals Processing (CCMP) has dealt in detail about the advantages of Microcel column flotation over conventional flotation in terms of fines recovery and ash rejection. In addition, extensive studies have been conducted at this institution to identify the mechanisms responsible for the relatively poor rejection of pyritic sulfur by surface-based processes such as froth flotation [7]. In Chapter 4, extensive test work on the MGS clearly demonstrated the advantages of enhanced gravity separators for fine coal desulfurization. Unfortunately, the MGS performed poorly in rejecting ultrafine ash-forming particles. To overcome the shortcomings associated with surface- and density-based separation methods, a new processing scheme to upgrade fine coal was developed at CCMP. In this process, fine coal is first treated by column flotation where hydrophobic coal is separated from hydrophilic ash-forming minerals. The column concentrate is then treated using an enhanced fine particle gravity concentrator which effectively exploits the large density difference between coal ( $SG \approx 1.5$ ) and pyrite ( $SG \approx 4.8$ ).

In the present work, bench-scale tests were conducted using the combined froth flotation-enhanced gravity separation circuit proposed by CCMP. The primary objective of this effort was to conduct a performance evaluation of the combined circuit and to determine its potential for near-term application in the coal industry.

## 5.3 Results and Discussion

The effects of several key operating parameters were evaluated using the combined flotation-gravity separation circuit. These included Microcel feed rate, MGS feed rate, MGS drum speed, MGS shake amplitude and MGS wash water addition rate. Although previous test work indicated that the MGS feed percent solids was an important operating parameter, it was not included in this study because the feed to the MGS from the column cell was fixed by the solids content of the flotation concentrate. The feed percent solids of flotation product seldom increased above 25%, and in most cases ranged between 15-20%. The test levels for the various operating parameters and test matrix for both the Pittsburgh No. 8 and Illinois No. 6 coals are provided in Tables 5.1 and 5.2.

In each series of test runs, material-balanced data sets were used to calculate the performance indicators for the column, MGS and the overall combined column/MGS circuit. The performance curves obtained for the combined circuit are shown in Figures 5.1 - 5.10.

### 5.3.1 Separation Performance

In the combined Microcel/MGS circuit, the run-of-mine coal is fed to Microcel and the Microcel concentrate becomes the feed to the MGS. The low-density product obtained from the MGS is the final clean coal product.

Therefore, samples collected from this two-stage circuit can provide useful performance information related to the Microcel, MGS and the combined Microcel/MGS circuit. Figures 5.1-5.3 show the recovery-rejections plots for the Microcel, MGS and combined Microcel/MGS obtained using Pittsburgh No. 8 coal. The test data indicate that the Microcel is capable of rejecting more than 70% of the ash forming minerals at a 90% combustible recovery, while the MGS was better in rejecting pyritic sulfur. However, the combined Microcel/MGS circuit was able to reject more than 75% of the ash and pyritic sulfur at a combustible recovery of approximately 90%. This clearly indicates that combining flotation and the MGS into one circuit provides higher rejections of mineral matter while maintaining a high recovery of coal. Tests conducted using the Illinois No. 6 coal show similar trends (Figures 5.4-5.6). In this case, the column alone was capable of rejecting approximately 85% of the ash-forming material, while the MGS was capable of rejecting 75% of the pyritic sulfur at a combustible recovery of 90%. The combined Microcel/MGS circuit was able to achieve a rejection of about 80% of both ash and pyritic sulfur at a combustible recovery of 85%.

The data obtained in this study suggest that the Microcel and MGS technologies each possess unique characteristics that allow them to reject different types of mineral impurities from coal. These capabilities are best illustrated in Figures 5.7 and 5.8. These plots show the sulfur and ash contents of the clean coal products obtained during the

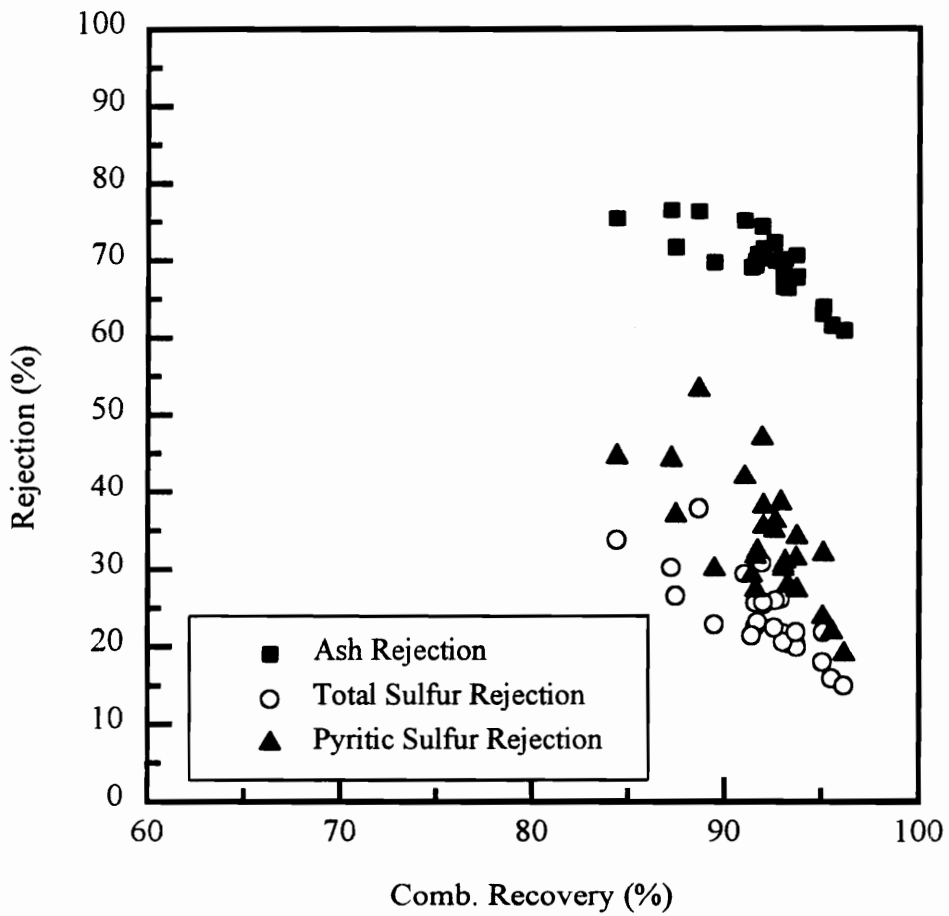


Figure 5.1 Combustible recovery versus rejection plots obtained for the Microcel unit during the parametric testing of the combined Microcel/MGS using the Pittsburgh No. 8 seam coal.



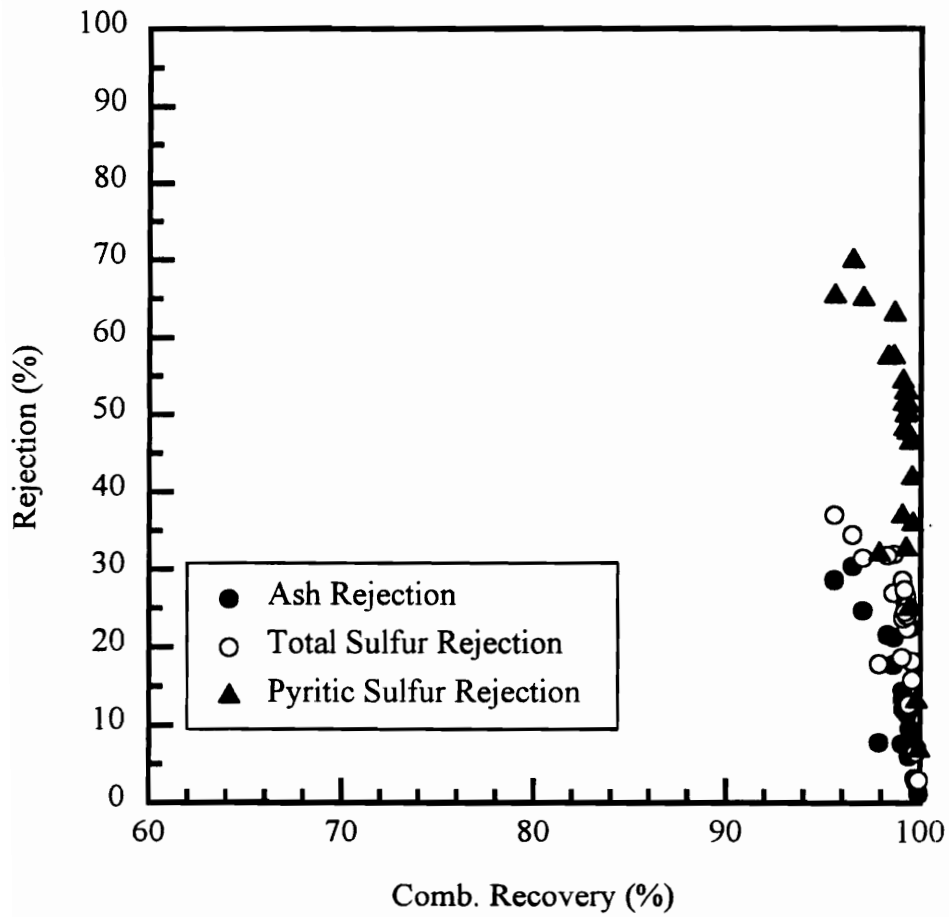


Figure 5.2 Combustible recovery versus rejection plots obtained for the MGS unit during the parametric testing of the combined Microcel/MGS using the Pittsburgh No. 8 seam coal.

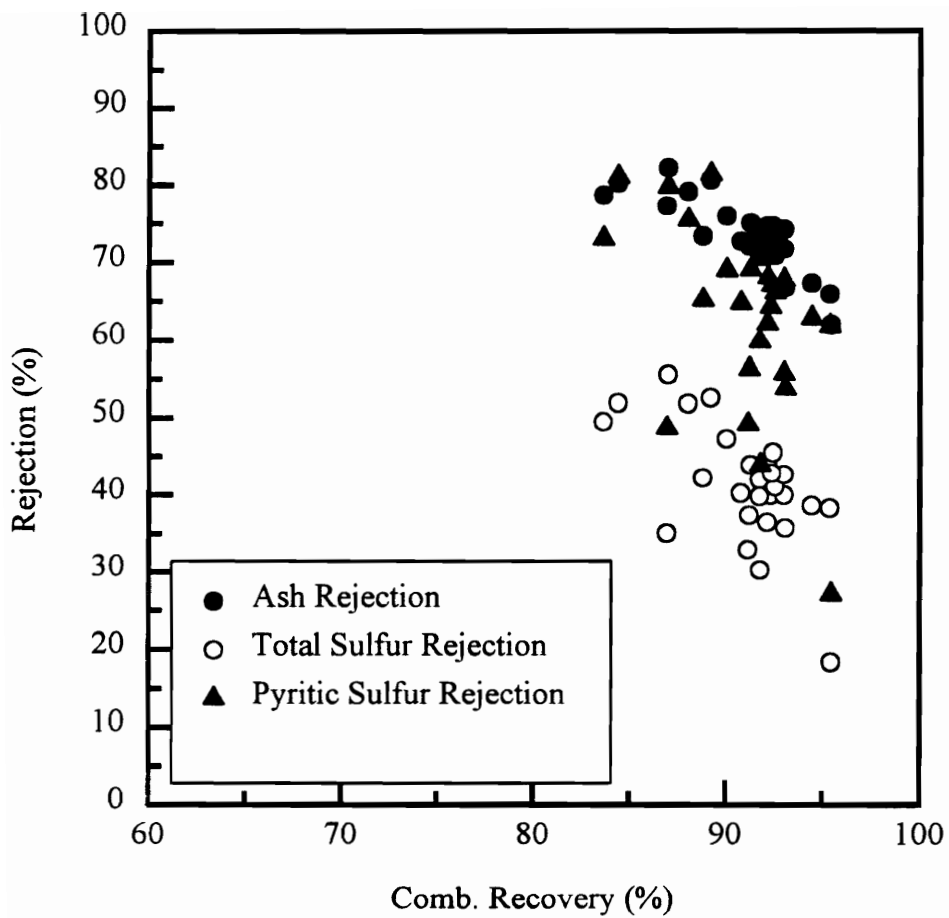


Figure 5.3 Combustible recovery versus rejection plots obtained during the parametric testing of the combined Microcel/MGS using the Pittsburgh No. 8 seam coal.

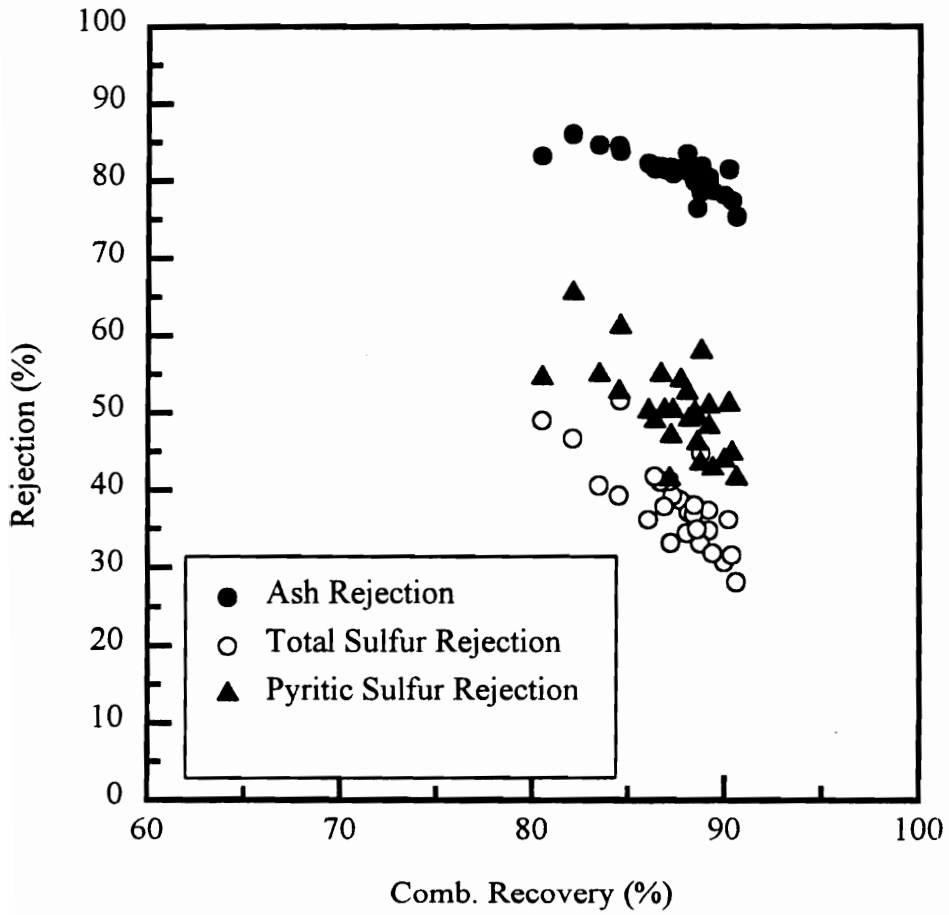


Figure 5.4 Combustible recovery versus rejection plots obtained for the Microcel during the parametric testing of the combined Microcel/MGS using the Illinois No. 6 seam coal.

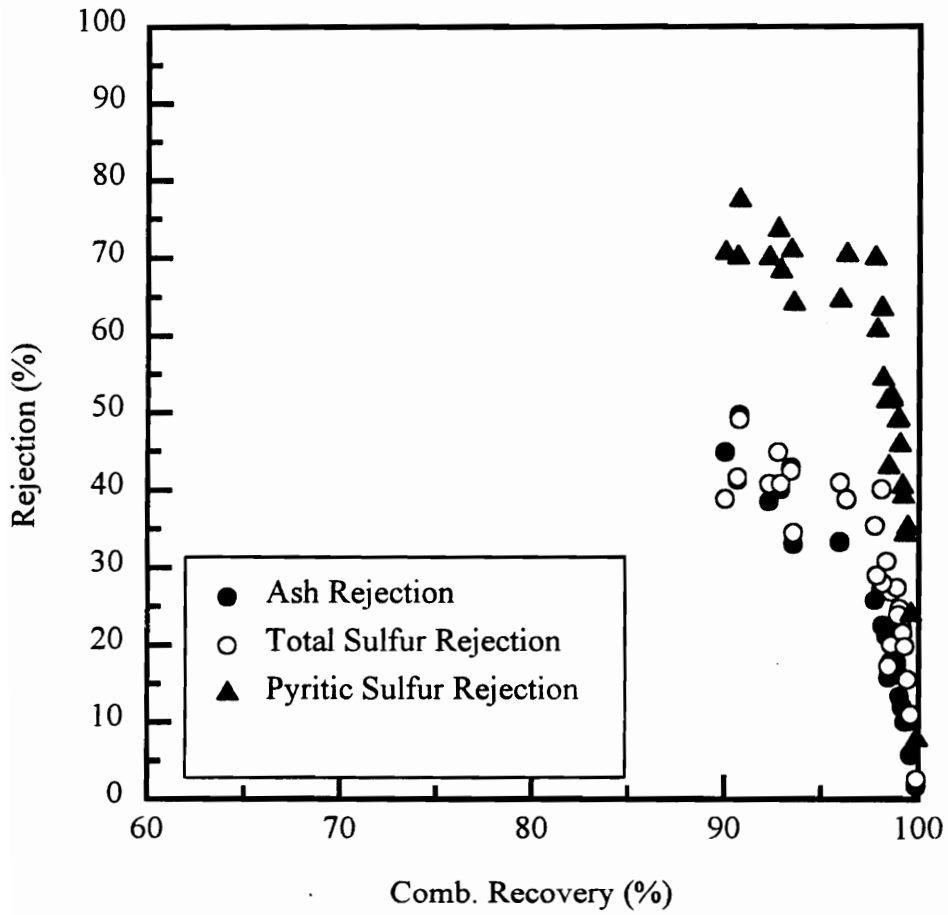


Figure 5.5 Combustible recovery versus rejection plots obtained for the MGS during the parametric testing of the combined Microcel/MGS using the Illinois No. 6 seam coal.

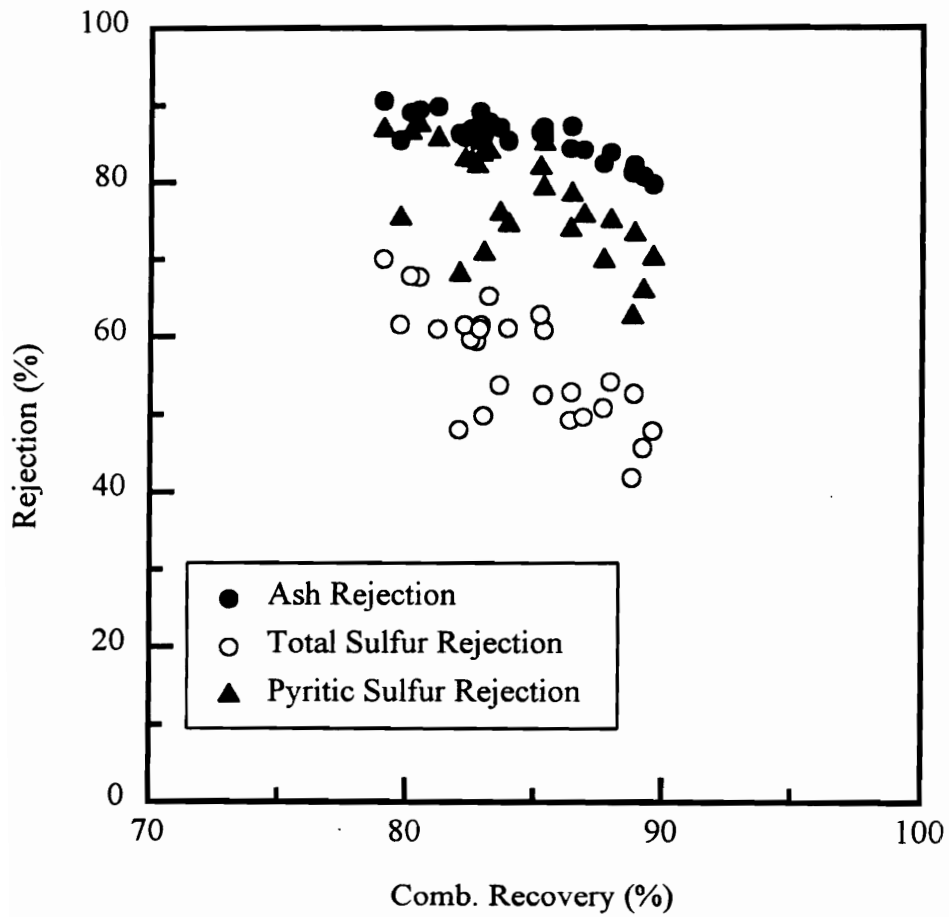


Figure 5.6 Combustible recovery versus rejection plots obtained during the parametric testing of the combined Microcel/MGS using the Illinois No. 6 seam coal.

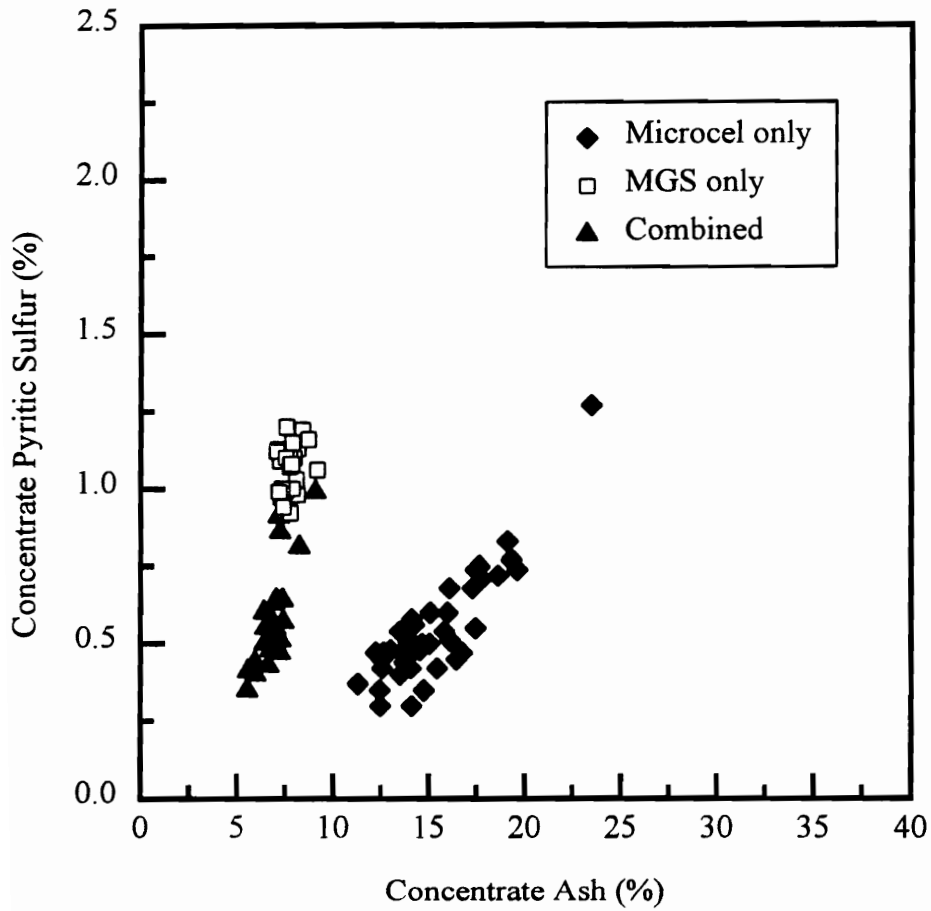


Figure 5.7 Concentrate sulfur versus ash content obtained during the parametric testing of the Pittsburgh No. 8 coal.

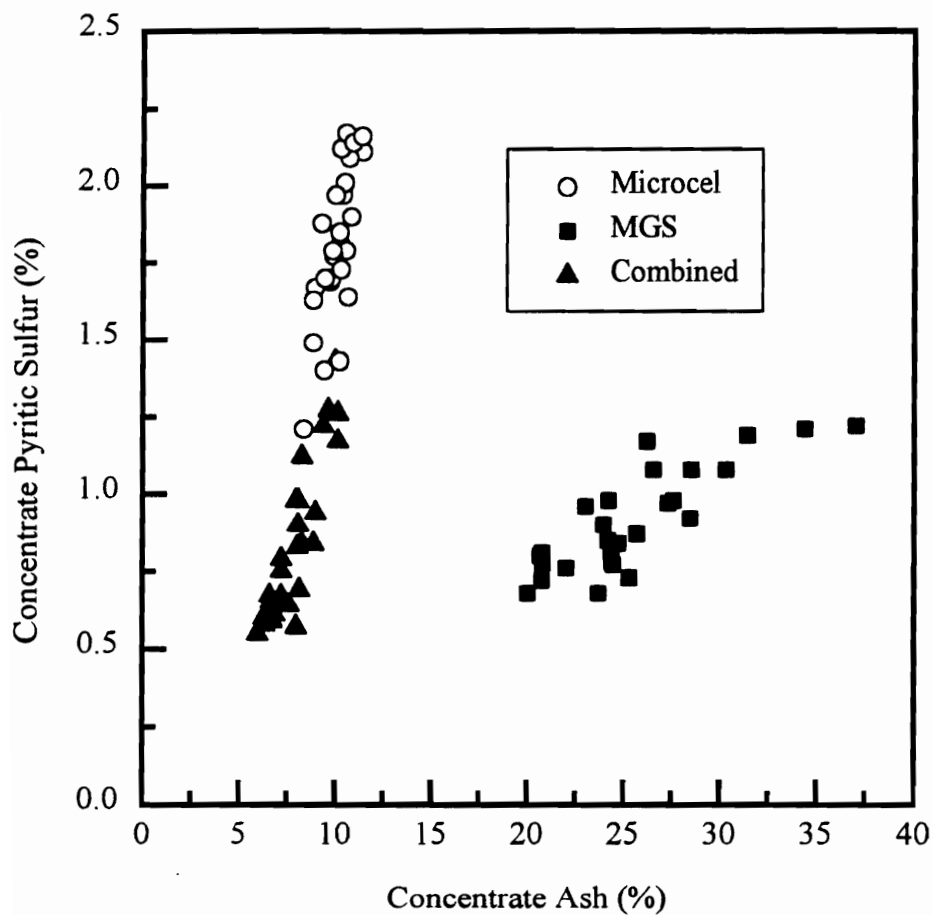


Figure 5.8 Concentrate sulfur versus ash content obtained during the parametric testing of the Illinois No. 6 coal.

parametric test programs conducted using the various circuit configurations. As shown, the Microcel test data fall in the low-ash/high-sulfur region of the plot. This indicates a preferential removal of ash-forming minerals using the surface-based technique. On the other hand, the data obtained using the density-based process (i.e., the MGS) fall in high-ash/low-sulfur region of the plots. The combined Microcel/MGS circuit takes advantage of the benefits of both the surface- and density-based processes and provides a low-ash and low-sulfur product. The major advantage of this approach is that it can achieve high rejections of ash and sulfur on a 28 mesh x 0 size fraction.

### 5.3.2 Long-Duration Testing

The combined Microcel/MGS circuit is capable of achieving high rejections of ash and pyritic sulfur (about 70%) at a combustible recovery of 90%. These capabilities make this processing scheme an attractive option for treating high-sulfur Central Appalachian coals. In an effort to demonstrate the potential near-term applicability of this approach, and also to establish the steady-state variability and operability of this circuit, tests were conducted for over a period of at least 10 hours of continuous operation. The parametric studies conducted on each coal helped to identify the best operating conditions to conduct the long duration tests.

The recovery-rejection curves obtained from long-duration testing of the Pittsburgh No. 8 coal are shown in Figures 5.9. The data were found to be in good



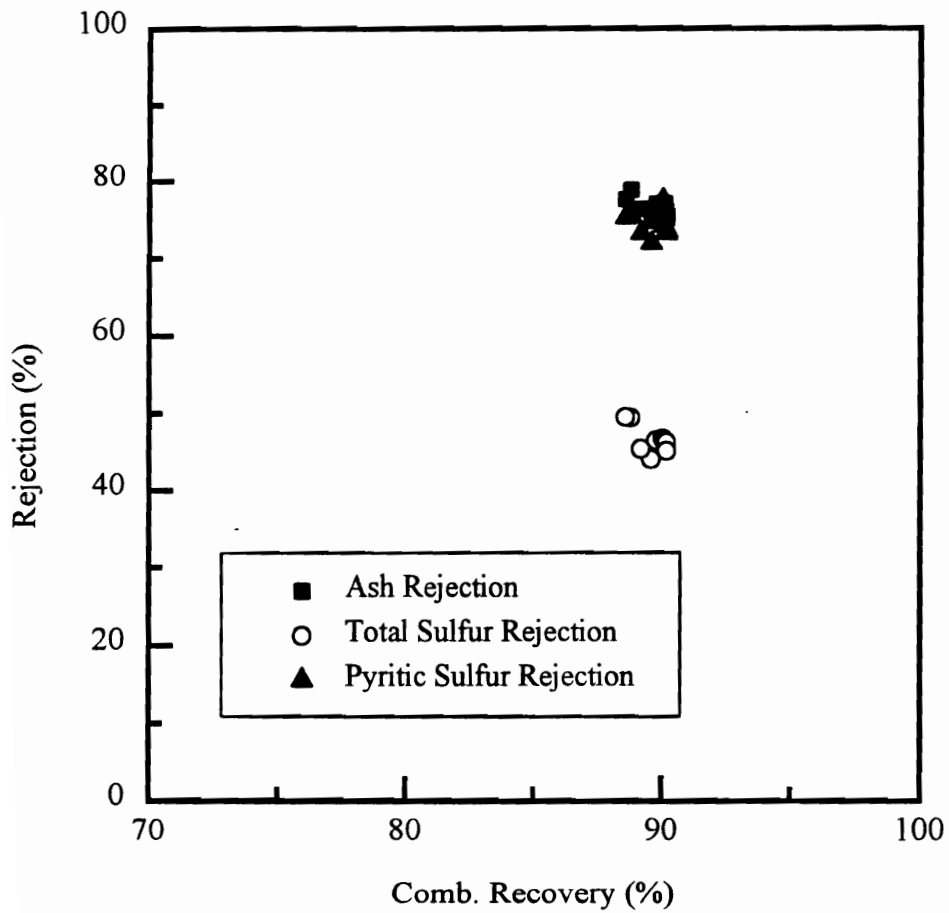


Figure 5.9 Combustible recovery versus rejection plots obtained during the long-duration testing of the combined Microcel/MGS using the Pittsburgh No. 8 coal.

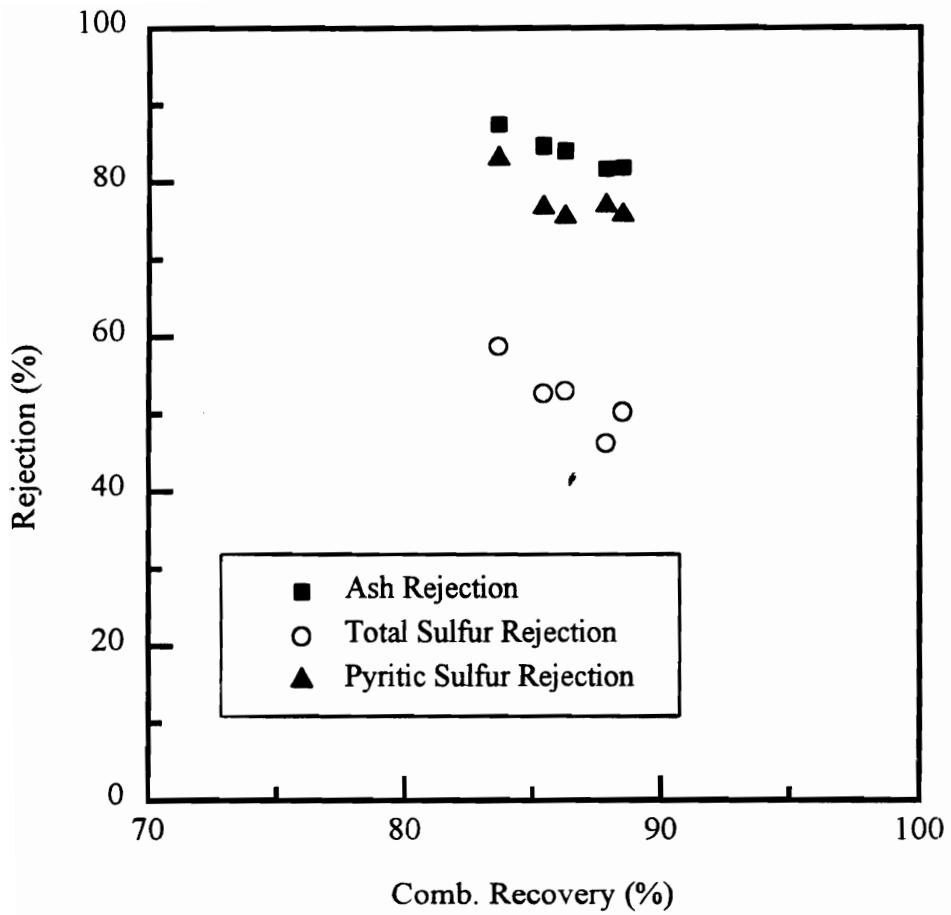


Figure 5.10 Combustible recovery versus rejection plots obtained during the long-duration testing of the combined Microcel/MGS using the Illinois No. 6 coal.

agreement with those obtained during the parametric testing programs described previously. In average, rejections of ash and pyritic sulfur were over 75% at a combustible recovery between 85-90%. Similar rejections were obtained at a slightly lower recovery (80-85%) for test conducted on Illinois No. 6 coal (Figure 5.10). Figures 5.9-5.10 also illustrate the consistency of the performance of all the unit operations in the combined flotation/MGS circuit. Test results clearly indicate that (i) the two-stage circuit is mechanically sound and able to operate continuously for a period of over 10 hours and (ii) the circuit is capable of accommodating feed fluctuations without minimal impacts on the product grade.

### 5.3.3 Economic Evaluation

The combined Microcel/MGS circuit has proved highly effective in improving the performance of fine coal cleaning. The preliminary cost-benefit analysis conducted on the Central Appalachian coal indicates the economic feasibility of this circuit [8].

Table 5.3 summarizes the cost-benefit analysis for the Pittsburgh No. 8 seam coal. As shown, the MGS had the lowest overall costs in terms of cost per ton of ash and SO<sub>2</sub> removed (i.e., \$15.26 and \$44.23, respectively). Unfortunately, the ash content of the MGS product was higher (i.e., 14.1%) than that normally desired by electric utilities. On the other hand, Microcel concentrate had lower ash (6.98%) and it was reasonably good at reducing the sulfur content of this particular coal. Hence, for this coal, the

Microcel process provided the best overall return on the capital investment. Although the combined Microcel/MGS circuit produced a superior quality product with 6% ash and 0.55% sulfur, this circuit arrangement had the lowest overall return on investment due to the high capital costs associated with the installation of two-stage circuit.

**Table 5.1**

**Parametric test matrix used to investigate the performance of the Combined Microcel/MGS circuit for the Pittsburgh No. 8 seam coal.**

**Microcel Conditions Held Constant**

Wash Water: 40 lpm; Percent Solids: 15; Air Flow Rate: 8.89 SCFM;  
Diesel Dosage: 1 lbs/t; Frother Dosage: 0.5 lbs/t;

**MGS Conditions Held Constant**

Shake Amplitude: 15 mm; Shake Frequency: 5 cps; Percent Solids: 20;  
Tilt Angle: 6 degrees; Grind Size (d80): 200 microns;

**Combined Variables**

Test Number	Column Feed (lbs/hr)	Drum Speed (rpm)	Wash Water (lpm)	MGS Feed (lbs/hr)
301	514	282	0.51	249
302	527	283	1.02	378
303	415	241	1.51	259
304	392	242	0.98	373
305	414	280	0.49	381
306	427	282	1.06	260
307	420	322	1.50	241
308	414	242	0.98	124
309	415	320	0.98	351
310	391	280	0.49	135
311	397	280	1.51	393
312	410	280	1.55	134
313	458	280	0.95	259
314	302	280	0.98	160
315	333	241	1.00	267
316	529	281	0.98	141
317	474	241	0.98	276
318	491	320	0.98	267
319	491	282	1.55	285
320	444	242	0.49	326
321	383	280	0.95	313
322	427	320	0.51	297
323	393	320	0.97	170
324	311	280	0.51	268
325	318	281	1.55	285
326	294	281	0.95	474
327	324	320	0.98	328

**Table 5.2**

**Parametric test matrix used to investigate the performance of the Combined Microcel/MGS circuit for the Illinois No. 6 seam coal.**

**Microcel Conditions Held Constant**

Wash Water: 40 lpm; Percent Solids: 11; Air Flow Rate: 8.89 SCFM;  
Diesel Dosage: 1 lbs/t; Frother Dosage: 0.5 lbs/t; Feed Rate: 550 lbs/hr;

**MGS Conditions Held Constant**

Shake Amplitude: 15 mm; Shake Frequency: 5 cps; Percent Solids: 22;  
Tilt Angle: 6 degrees; Grind Size (d80): 200 microns;

**Combined Variables**

Test Number	Drum Speed (rpm)	Wash Water (lpm)	Shake Amplitude (mm)	MGS Feed (lbs/hr)
601	283	1.51	10	269
602	283	0.95	15	269
603	280	0.47	20	257
604	239	1.06	15	342
605	239	0.95	20	276
606	280	0.95	15	268
607	240	1.51	15	273
608	280	1.51	15	161
609	323	1.10	10	306
610	239	0.45	15	259
611	322	0.91	20	282
612	322	0.98	15	148
613	280	1.59	20	241
614	282	0.95	15	300
615	280	0.45	15	148
616	321	1.06	15	343
617	282	0.45	15	357
618	282	0.93	20	378
619	240	0.96	15	163
620	282	1.51	15	353
621	283	0.53	10	281
622	241	1.06	10	219
623	322	1.55	15	238
624	281	1.10	10	160
625	320	0.53	15	305
626	280	0.98	20	135
627	281	1.10	10	377

**Table 5.3**

**Cost-benefit analysis for the Pittsburgh No. 8 seam coal**

Cost Indicator	Microcel Only	MGS Only	Microcel/MGS Combined
Production Cost: (\$/ton clean coal)	\$4.04	\$1.88	\$5.15
Removal Cost: (\$/ton ash)	\$22.50	\$15.26	\$24.88
(\$/ton sulfur)	\$517.95	\$88.46	\$407.87
(\$/ton SO <sub>2</sub> )	\$259.97	\$44.23	\$158.16
Economic Indicators:			
Rate of Return	77.0%	55.1%	50.2%
Payback Period	1.37 yrs	1.95 yrs	2.16 yrs

**Table 5.4**

**Cost-benefit analysis for the Illinois No. 6 seam coal**

Cost Indicator	Microcel Only	MGS Only	Microcel/MGS Combined
Production Cost: (\$/ton clean coal)	\$4.97	\$2.14	\$6.61
Removal Cost: (\$/ton ash)	\$11.56	\$9.92	\$12.66
(\$/ton sulfur)	\$161.51	\$73.08	\$153.64
(\$/ton SO <sub>2</sub> )	\$80.76	\$36.54	\$76.82
Economic Indicators:			
Rate of Return	36.7%	NA	29.9%
Payback Period	3.03 yrs	NA	3.78 yrs



Table 5.4 summarizes the results of a similar economic feasibility study conducted for the Illinois No. 6 coal. Despite the fact that the MGS has the lowest cost of sulfur removal, it was inefficient in reducing the ash content of the final product to below 25%. Therefore, it was not technically feasible to operate the MGS as a stand-alone unit for this particular coal. Of the remaining two alternatives, Microcel was found to be more attractive over the combined Microcel/MGS circuit because of its lower cost of installation.

A comparative study between the various coal cleaning technologies on the basis of cost per ton of SO<sub>2</sub> removed is illustrated in Figure 5.11. It is very obvious that coarse coal cleaning devices such as jigs and dense-medium separators show the lowest costs of sulfur removal. However, the pyrite rejections obtained using these conventional technologies are only in the range of 50-55%. Advanced coal cleaning processes show significantly improved pyrite rejections over the conventional processes; however, the costs of desulfurization are in the range of \$243-327/ton of SO<sub>2</sub> removed. It is worthwhile to mention that these costs are comparable to those for flue-gas scrubbing, which are reported to be in the \$250-350/ton range.

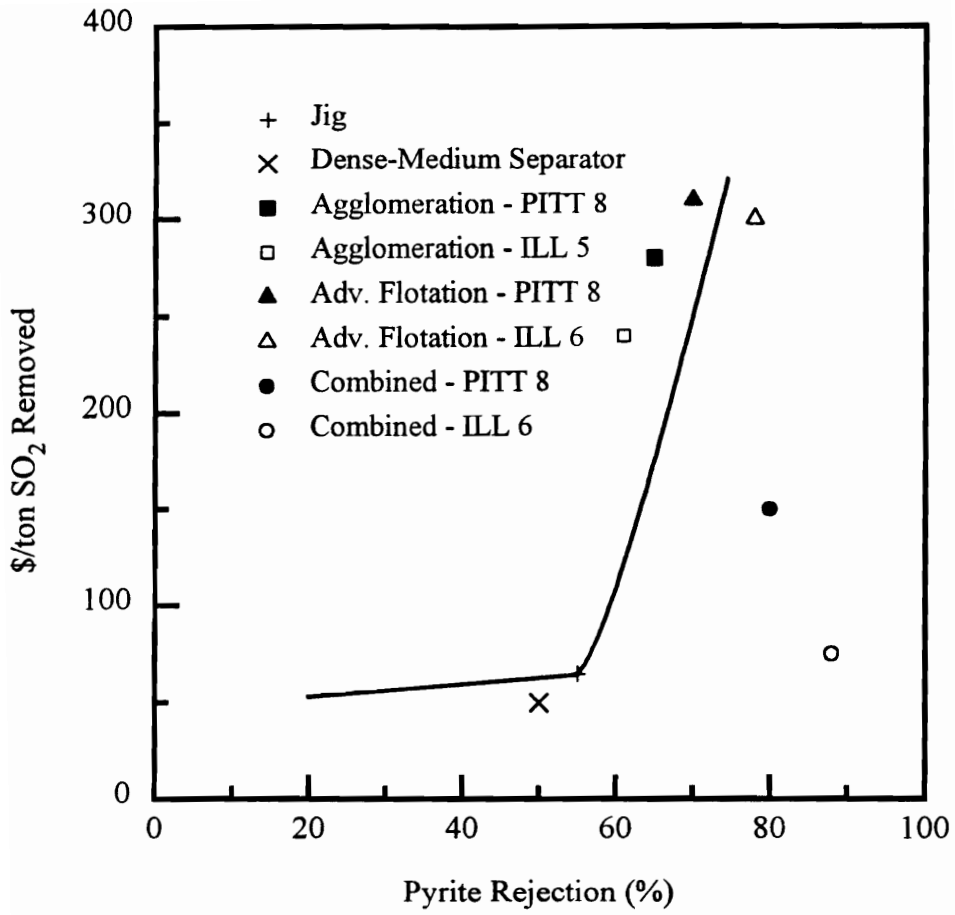


Figure 5.11 Cost of SO<sub>2</sub> removed versus pyrite rejection for several traditional and advanced circuits.

#### **5.4 Summary and Conclusions**

- a) A pilot-scale test program was carried out to evaluate the performance of a novel fine coal cleaning circuit developed at Virginia Tech. This two-stage circuit combines an advanced flotation column known as Microcel with an enhanced gravity concentrator called a Multi-Gravity Separator (MGS). This circuit has been capable of overcoming problems normally encountered with single-stage surface- and density-based coal cleaning processes.
- b) Test results indicate that surface-based processes such as the Microcel column was very efficient in removing hydrophilic clay minerals, while density-based processes such as the MGS was highly effective in rejecting middlings containing high-density pyrite. Combining these processes into a single fine coal cleaning circuit allowed highly efficient separations to be achieved.
- c) Test data obtained in the present work indicate that the combined Microcel/MGS circuit was capable of rejecting approximately 75-85% of the ash and pyritic sulfur from the Pittsburgh No. 8 coal at an energy recovery approaching 95%. Similar rejections were obtained at slightly lower energy recovery of 90% for the Illinois No. 6 coal. These results demonstrate the capabilities of this novel approach for producing higher quality coal fuels from moderate-to-high sulfur coals.

- d) One of the major advantages of the combined Microcel/MGS circuit was that it allows high levels of mineral matter rejection to be achieved without ultrafine grinding.

## 5.5 References

1. Hower, J.C., and Parekh, B.K., Coal Preparation, Leonard, J.W. (Ed.), 5th Edition (1991).
2. Paul, B., Illinois Clean Coal Institute, Quarterly Report, February, (1994).
3. Honaker, R., Illinois Clean Coal Institute, Quarterly Report, February, (1994).
4. Tucker, P., Appl. Math. Modeling, Vol. 9, (1985).
5. Honaker, R.H., Proc. SME, February, 14 - 17, (1994).
6. Venkatraman, P., Luttrell, G.H., Yoon, R.H., Knoll, F.S., Kow, W.S., and Mankosa, M.J., Proc., High Efficiency Coal Preparation: An Int. Sym., SME, Littleton, Colorado (1995).
7. Yoon, R.H., Adel, G.T., and Luttrell, G.H., Proc. 2nd Intl. Conf. on Process. and Utilization of High Sulfur Coals, Carbondale, Illinois, Sept. 27 - Oct. 1, (1987).
8. Luttrell, G.H., Venkatraman, P., Phillips, D.I., and Yoon, R.H., DOE Final Report, Contract No.: DE-AC22-92PC92205.

## CHAPTER 6 - CONCLUSIONS

The results of the present investigation may be summarized as follows:

- a) A simple model based on first principles has been developed to explain the separation process taking place in the MGS. The model predictions are in general agreement with the experimental data available in the literature. Drum speed was found to be the important controlling parameter. The model predicts an improvement in the sharpness of separation at higher drum speed.
- b) A detailed parametric study was conducted on the MGS to evaluate its potential in treating fine coal (28 mesh x 0). Test results indicate that the MGS was very effective in rejecting high density components such as pyrite, while it was less efficient in rejecting ultrafine clay “slimes”. Hence, the MGS is well-suited for coal desulfurization.
- c) The MGS performance was found to be highly dependent on particle size. The best separation efficiencies was obtained on size fractions between 100 x 325 mesh fraction. Preliminary tests results also indicate that the performance of the MGS on a deslimed feed is comparable with or better than flotation, however, this needs further investigation.
- d) Statistical analyses identified drum speed as the most important process parameter. Feed rate, feed solids content, wash water addition rate etc., were

found to have moderate impact on the process. These findings corroborate the theoretical model predictions.

- e) An advanced fine coal cleaning circuit developed at Center for Coal and Minerals Processing (CCMP), Virginia Tech by combining surface-based process (Microcel column flotation) and density-based process (MGS) was evaluated in this study. Test results clearly demonstrates the capability of this circuit to achieve higher rejections with minimal loss in recovery without ultrafine grinding. And also, it was found that this circuit was capable of rejecting most of the hazardous air pollutants (HAPs) commonly found in coal. Therefore, this circuit is ideally suited for treating high sulfur eastern U.S. coals.

## CHAPTER 7 - RECOMMENDATIONS FOR FURTHER STUDY

Based upon the experience and information obtained during the course of this investigation, additional research in the following areas is suggested.

- a) Test results of this investigation demonstrate the effectiveness of the Microcel/MGS circuit to produce compliance coal from high ash and high sulfur coal fines (28 mesh x 0). Of the two unit operations tested, Microcel has several successful commercial installations in the coal industry, while the MGS, although performing efficiently in the mineral industries, is a new-comer to the coal industry. In spite of its superior performance in terms of sulfur rejection, the low-capacity and high-cost of the MGS could delay its near-term commercialization in the coal industry. More systematic investigations are needed to evaluate the potential of other enhanced gravity separators, like Falcon concentrator, to improve the economic viability of the proposed circuit.
- b) Test results indicate the superior performance of the MGS on a de-slimed feed. Additional test work is required to determine the optimum size-range that can be effectively treated by the MGS.
- c) In order to improve the capacity of the proposed circuit, it was envisaged to develop an improvised Water-only cyclone (WOC). Unfortunately, this effort could not be completed in the stipulated time period. Therefore, it will be



interesting to investigate the possibility of including a WOC in this circuit, between flotation and enhanced gravity separator.

- d) In the present work, a simple model has been developed to understand the fundamental operating principle of the MGS. This model predicts the trend of the separation phenomenon taking place in the MGS. Drum speed has been identified as the most important operating parameter. However, additional studies are needed to quantify the flow characteristics of the slurry on the rotating drum surface of the MGS and the effect of the scraping mechanism in the separation process. This information would be required to design, optimize and scale-up the MGS based on first principles. In particular, the influence of drum speed, feed percent solids, scraping rate, etc., on the motion of particles within the MGS would be beneficial.
- e) Preliminary studies conducted in this investigation show the trace element removal capabilities achieved using this circuit. An elaborate study is needed to evaluate and improve the rejection of trace elements from different coals.

## VITAE

Parthasarathy Venkatraman was born in Tirunelveli, a medium-sized town in the southern part of India. After his education in Madras, he obtained degree in Mineral Engineering from Indian School of Mines, Dhanbad, India. Then he worked for Steel Authority of India Limited for about three years before enrolling in Ph.D., program at Virginia Tech in 1992. Presently he is working at Carpc, Inc., Jacksonville, Florida.

*v. Par Venkat*

---